El uso de la teledetección de alta resolución como herramienta para realizar un manejo eficiente del riego en viñedos

Autor: Joaquim Bellvert Rios

Directores: Elías Fereres Castiel

Pablo Zarco-Tejada

Córdoba, Enero 2014

TITULO: *El uso de la teledetección de alta resolución como herramienta para realizar un manejo eficiente del riego en viñedos*

AUTOR: *Joaquim Bellver Rios*

DEPARTAMENTO DE AGRONOMÍA

TESIS DOCTORAL

El uso de la teledetección de alta resolución como herramienta para realizar un manejo eficiente del riego en viñedos

Autor: Joaquim Bellvert Rios

Directores: Elías Fereres Castiel

Pablo J. Zarco-Tejada

Córdoba, Enero 2014

TÍTULO DE LA TESIS:

EL USO DE LA TELEDETECCIÓN DE ALTA RESOLUCIÓN COMO HERRAMIENTA PARA REALIZAR UN MANEJO EFICIENTE DEL RIEGO EN VIÑEDOS

DOCTORANDO/A:

JOAQUIM BELLVERT RIOS

INFORME RAZONADO DEL/DE LOS DIRECTOR/ES DE LA TESIS
(se hará mención a la evolución y desarrollo de la tesis, así como a trabajos y publicaciones derivados de la misma).

El doctorando ha realizado un trabajo encomiable, incorporando disciplinas distintas a aquellas en las que se basa su formación y ha demostrado ampliamente la capacidad e independencia en el trabajo que se debe requerir a todo egresado con el grado de doctor y que a veces se echa en falta. Sus investigaciones han sido parcialmente evaluadas por expertos anónimos de las revistas con censores donde se han publicado parte de sus investigaciones, lo cual también avala el trabajo realizado. En resumen, se trata de una tesis doctoral de muy buena calidad, innovadora y que sin duda ha de tener un impacto en el sector

Por todo ello, se autoriza la presentación de la tesis doctoral.

Córdoba, 15 de noviembre de 2013

Firma del/de los director/es

Fdo.: Elías Fereres Castiel   Fdo.: Pablo Zarco Tejada

Agradecimientos

Muchas son las colaboraciones que debo agradecer en la presente tesis, en la que he tenido la suerte de contar con un excepcional grupo de trabajo, sin cuya ayuda nada de esto hubiera sido posible.

En primer lugar me gustaría agradecer especialmente al Dr. Joan Girona la posibilidad de poder realizar esta tesis doctoral en colaboración con el programa del Uso eficiente del agua del IRTA y también con el laboratorio Quantalab del IAS-CSIC de Córdoba. Mucho ha sido el avance desde las primeras medidas de potencial hídrico foliar de la P15 de Raïmat, con el objetivo de obtener un mapa de la variabilidad del estado hídrico, hasta donde hemos llegado actualmente. Gracias Joan.

También agradecer el apoyo prestado durante todo este tiempo a todos los compañeros del IRTA, a Xavier Vallverdú, Jaume Casadesús, Gerardo López, Germán Estudillos, Mercè Mata, Carles Paris, Jesús del Campo, Núria Bonastre, Núria Civit, Joan Ventura, Gerard Pinyol, Jordi Pujades y Jordi Oliver; y especialmente al Dr. Jordi Marsal, quién me ha aconsejado y ayudado en todo momento en cada una de las dudas, correcciones que he tenido en el transcurso de esta tesis. Él es quien me ha introducido al mundo de la investigación y ayudado a avanzar científicamente.

Un sincero agradecimiento a mis tutores, a Elías Fereres y Pablo Zarco-Tejada. Gracias por darme la oportunidad de hacer esta tesis doctoral con vosotros.

Agradecer también a todo el equipo maravilloso del Quantalab, especialmente a Rafa Romero, Alberto Hornero y Victoria González. Alberto, gracias por todo el tiempo dedicado durante los primeros años, poniendo el sensor térmico a punto. Y a ti Rafa, muchísimas gracias por todas las horas dedicadas, tu eficiencia y rapidez en el procesado de imágenes.

Y sobretodo quiero agradecer y dedicar esta tesis a mis padres y hermanos, quienes me han apoyado en todo momento. Finalmente, agradecerle el apoyo a mi pareja, Núria: El camí ha estat llarg, però sense tú donant-me suport en els moments difícils no hauria arribat a entregar mai aquesta tesis. Gràcies.

Índice

Introducción

Capítulo 1

Identifying irrigation zones across a 7.5-ha 'Pinot noir' vineyard based on the variability of vine water status and multispectral images

Capítulo 2

Mapping crop water stress index in a `Pinot-noir´ vineyard: comparing ground measurements with thermal remote sensing imagery from an unmanned aerial vehicle

Capítulo 3

Seasonal evolution of crop water stress index in grapevine varieties determined with high resolution remote sensing thermal imagery

Índice de Figuras

Introducción

Capítulo 1

Capítulo 2

Capítulo 3

Índice de Tablas

Capítulo 1

Capítulo 2

Capítulo 3

Abstract

The use of plant-based indicators for irrigation management has been widely studied. However, the high number of measurements necessary to identify spatial variability in orchards makes this system difficult to be carried out in large commercial areas. The alternative may be the use of remote sensing. Development of high resolution airborne sensors during the last years brings about new possibilities for detecting plant water status remotely in large areas, and therefore to conduct a more efficient irrigation management for water use.

The aim of this PhD thesis is the development of a tool for vineyard spatial variability management, by using high resolution remote sensing imagery. To achieve it, two methodologies to re-design irrigation sectors were firstly compared, with the goal of reducing yield variability. Methods were based on using structural vegetative indices such as Plant Cell Density (PCD) obtained from multispectral images, and leaf water potential measurements (Ψ_L).

It is also presented the development of Crop Water Stress Index (CWSI) for the four grapevine varieties Pinot-noir, Chardonnay, Syrah and Tempranillo, as a tool for quantify vine water status with remote sensing thermal imagery. CWSI was empirically developed with infrared temperature sensors to subsequently generate CWSI maps by acquiring high resolution thermal images. CWSI was developed and validated with Ψ_L measurements at different phenological stages.

Effectiveness aspects to consider such as the optimal moment of the day to detect vine water status with aerial thermal images, the minimum spatial resolution required, or the most appropriated aerial platform, were also studied in this PhD thesis. The implementation of this technology in viticulture will permit to make a more efficient irrigation management taking into account vineyard spatial variability.

Resumen

El uso de indicadores del estado hídrico de los cultivos para la optimización del riego en cultivos leñosos ha sido ampliamente estudiado. Sin embargo, el elevado número de puntos de medidas necesarios para caracterizar la variabilidad espacial de una parcela, hace que sea un sistema de difícil aplicación en grandes extensiones comerciales. La alternativa se basa en el uso de la teledetección. Con el desarrollo en los últimos años de sensores aerotransportados de alta resolución, se abren nuevas posibilidades para detectar el estado hídrico de los cultivos en grandes extensiones y poder realizar un manejo del riego más eficiente.

Esta tesis doctoral tiene como principal objetivo desarrollar una herramienta que permita manejar la variabilidad espacial de los viñedos, mediante la utilización de la teledetección de alta resolución. Para tal fin, en primer lugar se han comparado dos metodologías para re-definir los sectores de riego, con el objetivo de disminuir la variabilidad productiva. Los métodos se basaron en el uso de índices estructurales de vegetación, tales como el Plant Cell Density (PCD) obtenidos a partir de imágenes multiespectrales, y con medidas del potencial hídrico de hoja (Ψ_L).

Se presenta también el desarrollo del Crop Water Stress Index (CWSI) en las cuatro variedades de viña Pinot-noir, Chardonnay, Syrah y Tempranillo, como herramienta para cuantificar el estado hídrico mediante la teledetección térmica. El CWSI se desarrolló empíricamente con sensores de temperatura infrarrojo para posteriormente poder generar mapas de CWSI mediante la adquisición de imágenes aéreas térmicas de alta resolución. El CWSI se desarrolló y validó con medidas de Ψ_L en las distintas fases fenológicas.

Aspectos de operatividad, tales como el momento idóneo del día para detectar el estado hídrico mediante imágenes aéreas térmicas, la resolución espacial mínima requerida, o la plataforma aérea más adecuada, también han sido estudiados en esta tesis. La implementación de esta tecnología en la viticultura permitirá realizar un manejo del riego más eficiente teniendo en cuenta la variabilidad espacial del estado hídrico en un viñedo.

Introducción

1. Antecedentes

La escasez de agua en el mundo podría limitar la producción y el abastecimiento de alimentos (UNESCO, 2010). Esta situación puede verse agravada debido al efecto del cambio climático, ya que todo parece indicar que en los próximos años habrá un aumento de la escasez de agua por la disminución de las precipitaciones y un aumento de la aridez y fenómenos extremos como olas de calor y sequías. Además, la población mundial está creciendo a un ritmo de 80 millones de personas al año, lo que implicará una mayor demanda de alimento y de agua dulce. La mayor parte del crecimiento poblacional ocurrirá en países en desarrollo, principalmente en regiones con un clima árido y semiárido, donde el recurso agua es limitado.

La agricultura es el principal motor de crecimiento en la mayoría de las economías en vías de desarrollo, y a la vez el sector mayor consumidor de agua. Se estima, según la FAO, que la superficie mundial de regadío es de 220 millones de hectáreas y que el regadío consume un 69% de los recursos hídricos dulces, llegando incluso al 90% en algunas regiones. Sin embargo, el riego en la agricultura es necesario para hacer frente a la demanda de alimentos de una demografía creciente, en particular, en las zonas urbanas. A medida que la población aumenta (aprox. 75 millones cada año), los recursos per cápita disponibles son más restringidos, por lo que se hace necesaria una mayor productividad. Bajo estas circunstancias, realizar un manejo del agua de riego eficiente y hacer pequeñas reducciones en períodos determinados pueden traducirse en ahorros de agua importantes. A la vez, la adopción de estrategias de riego adecuadas permiten mejorar la eficiencia productiva (Kg alimento/m^3 de agua). Esto es especialmente cierto en el caso de la vid, ya que es el cultivo leñoso que ocupa una mayor superficie en el mundo (FAO, 2009).

La viña ha sido tradicionalmente un cultivo de secano. Además, en España el riego en viticultura ha estado prohibido durante décadas por restricciones legales. Después del levantamiento de la prohibición del riego en el año 1996, la implantación de sistemas de riego, mayormente localizados, ha incrementado hasta que a día de hoy en zonas semiáridas, y con el objetivo de producir vinos de alta calidad es impensable no disponer de una buena instalación de riego. Bajo estas condiciones, pequeñas aportaciones de agua tienen un efecto directo sobre la producción (Ferreyra et al. 2003), y composición de la uva (Girona et al. 2009). Para regar eficientemente la viña es necesario saber cuánto y cuándo regar. Por ello, las prácticas de riego más habituales en la región mediterránea implican la adopción de estrategias de *riego deficitario controlado* (RDC). El RDC está fundamentado en reducir el aporte de agua en aquellos períodos fenológicos en el que un déficit hídrico controlado no afecte sensiblemente la producción ni la calidad de la cosecha y que cubra la demanda evaporativa del cultivo durante el resto del año. En viña, la adopción de esta técnica ha demostrado unas mejoras en la composición de las uvas (Williams & Mattews 1990), además de unos ahorros importantes de agua. Por ejemplo, se conoce que la adopción de estrategias de RDC en variedades tintas, durante la fase de post-envero mejoran sustancialmente la composición de la uva (Girona et al. 2009, Basile et al. 2011).

Sin embargo, estrategias de déficit en variedades blancas durante el período de post-envero afectan negativamente sobre la calidad de la uva (Basile et al. 2012). Por lo tanto, la elección de la estrategia de riego debe tener en cuenta la variedad, la intensidad del déficit hídrico y el momento fenológico en que se adopta.

La programación técnica del riego de los viñedos se realiza en base a las necesidades hídricas, utilizando el método del balance hídrico y calculando la evapotranspiración de referencia (ET_o) a partir del modelo de Penman-Monteith (Allen et al. 1998) y el coeficiente de cultivo (K_c) en función del cultivo y estado fenológico. No obstante, cuando se adopta un riego deficitario, imponer un riego basado en el concepto de balance hídrico implica definir el estrés hídrico de la planta sobre la base de fracciones de ET_o. Este método puede producir cierto nivel de incertidumbre, ya que el desarrollo del estrés hídrico no solamente depende del porcentaje de déficit de riego, sino también de la capacidad de retención de agua del suelo, del clima, material vegetal y condiciones de crecimiento (Reynold y Naylor, 1994). Además, la variabilidad espacial natural de los viñedos, dónde factores del medio físico (orografía del terreno o propiedades del suelo) y las prácticas culturales (poda, riego o aplicación de fertilizantes) condicionan de manera importante la respuesta del cultivo, implica unas necesidades hídricas diferentes en las distintas subzonas de un viñedo. En consecuencia, a la hora de programar el riego, es preciso hacer un manejo diferencial y aportar distintas cantidades de agua en las distintas subzonas en función de sus requerimientos hídricos. Para ello, es necesario disponer de indicadores del estado hídrico, tales como el potencial hídrico de hoja (Ψ_L) o la temperatura de la hoja (T_c), que permitan detectar el estado hídrico de grandes extensiones y puedan ser utilizados como herramienta de programación del riego (Girona et al. 2006).

En este sentido, existe un especial interés en el sector vitivinícola en mejorar el manejo del viñedo teniendo en cuenta su heterogeneidad. Para ello, el uso de las nuevas tecnologías basadas en la teledetección y sistemas de información geográfica se presentan como unas herramientas de gran utilidad para gestionar los viñedos más eficientemente. Actualmente, la heterogeneidad productiva y de calidad de la uva en un viñedo se resuelve utilizando algunas aplicaciones basadas en la teledetección. Algunas aplicaciones se basan en realizar vendimias selectivas clasificando el viñedo en subzonas en función de su vigorosidad vegetativa utilizando índices de vegetación, tales como el *Normalized Difference Vegetation Index* (NDVI), o el *Plant Cell Density* (PCD) (Bramley et al. 2003). Sin embargo, la teledetección también puede utilizarse como una herramienta de gestión del riego. Para realizar un manejo del riego eficiente es necesario, en primer lugar, disponer de un diseño de los sectores de riego acorde con la variabilidad espacial del viñedo. Así, la obtención de mapas de vigorosidad vegetativa utilizando la teledetección puede ser una herramienta útil para rediseñar el sistema de riego de un viñedo. La detección del estado hídrico de los cultivos a partir de la temperatura de la hoja (T_c), también forma parte de las actuales líneas de investigación de la teledetección. Con el desarrollo de esta tecnología, será posible detectar remotamente el estado hídrico de grandes extensiones, aportar distintas cantidades de agua en cada subzona del viñedo en

función de sus necesidades hídricas, y adoptar las estrategias de riego más convenientes para cada variedad de viña en cuestión, con el consiguiente ahorro de agua.

2.   Indicadores del estado hídrico

2.1.   *Potencial hídrico de hoja*

El potencial hídrico de hoja (Ψ_L) es el indicador comúnmente más utilizado para determinar el estado hídrico en frutales y viña (Williams y Araujo, 2002; Schultz, 2003). El método estándar para realizar la medida es utilizar la cámara de presión (Scholander) (Figura 0.1). La cámara de presión da una medida de la tensión que se produce en el xilema de una planta intacta debido a la evaporación de agua desde el tejido por transpiración y a las resistencias al movimiento del agua desde el suelo hasta el tejido (Scholander et al., 1965). El potencial hídrico estimado con la cámara de presión es el valor negativo de la presión requerida para comenzar a obtener líquido en la superficie expuesta del xilema a presión atmosférica (Boyer, 1967; Ritchie y Hinckley, 1975; Campbell, 1985; Turner, 1987; Kirkham, 2005).
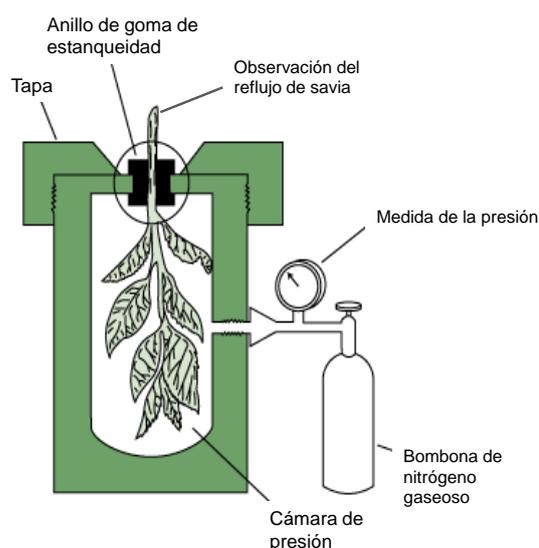
(Fuente: Plant physiology)

Figura 0.1. Método de la cámara de presión utilizado para la medida del potencial hídrico foliar.

El Ψ_L es por lo tanto, el indicador más sencillo para determinar el estado hídrico de las plantas, ya que está íntimamente relacionado con las respuestas de la planta al estrés a corto y medio plazo. En base a este indicador, es posible manejar eficientemente el riego (Girona et al. 2006), ya que integra la influencia del suelo, planta y condiciones climáticas sobre las necesidades hídricas. En viña, numerosos estudios han relacionado las respuestas productivas (Williams y Arujo, 2002; Grimes y Williams, 1990; Ojeda y otr. 2002) y de calidad de la uva (Girona y otr. 2009; Ginestar y otr. 1998; Intrigliolo, 2009) con el estado

hídrico determinado a partir del Ψ_L. Sin embargo, la medida del Ψ_L es a escala foliar, resulta compleja, y requiere de un espacio de tiempo limitado al mediodía, lo que hace que sea un sistema de difícil aplicación en grandes extensiones comerciales.

2.2. *La temperatura de la hoja*

La temperatura de la hoja o del dosel vegetativo (T_c) ha sido también ampliamente reconocida como indicador del estado hídrico de los cultivos (Jackson et al. 1977; Gates, 1964; Tanner 1963). Inicialmente, con el desarrollo de los primeros sensores de temperatura infrarrojo, se utilizó la diferencia de temperatura entre la existente a nivel de cubierta vegetal y la del aire (T_c-T_a) (Jackson et al. 1977). El concepto se basa en que las plantas sometidas a un estrés hídrico tienden a cerrar los estomas para evitar una mayor pérdida de agua, lo que hace disminuir su transpiración, así como su capacidad de realizar la fotosíntesis. En consecuencia, T_c-T_a aumenta a medida que las plantas presentan un mayor estrés hídrico.

Sin embargo, la temperatura de la cubierta vegetativa también está afectada por otros factores ambientales, tales como la humedad relativa, el viento o la radiación, y por lo tanto, no puede por sí sola ser un buen indicador del estado hídrico de los cultivos. Por ese motivo, T_c-T_a se normalizó teniendo en cuenta estos factores y desarrollando un índice denominado Crop Water Stress Index (CWSI) (Idso et al. 1981).

El uso de este indicador ha sido mayormente con medidas puntuales utilizando termómetros o sensores de temperatura infrarrojo (Jones and Leinonen, 2003; Jones, 2004). Su aplicación a través de imágenes para el uso de la teledetección ha estado limitada debido a la baja resolución espacial de los sensores térmicos desarrollados hasta el momento.

2.3. *Crop Water Stress Index*

Una importante contribución a la investigación ha sido el desarrollo del *Crop Water Stress Index* (CWSI), formulado por Idso et al. (1981) y Jackson et al. (1981). Este índice normalizado enmascara los efectos de otros parámetros ambientales que afectan de forma directa en la relación entre temperatura del dosel vegetativo y estado hídrico. El CWSI nos proporciona un valor entre 0 a 1 dependiendo del nivel de estrés hídrico del cultivo. Existen distintas metodologías para la obtención del CWSI, y se describen a continuación:

2.3.1. *Método empírico*

Idso et al. (1981) mostró que el CWSI se podía obtener empíricamente en varios cultivos a partir del desarrollo de una línea base denominada 'non-water stressed baseline (NWSB)'. La NWSB se determina a partir de la relación entre T_c-T_a y el déficit de presión de vapor (DPV) para plantas que se encuentren en condiciones hídricas adecuadas y

presenten una máxima transpiración. El CWSI se obtiene a partir de la temperatura del dosel vegetativo (T_c), según:

$$CWSI = \frac{(T_c - T_a) - (T_c - T_a)_{LL}}{(T_c - T_a)_{UL} - (T_c - T_a)_{LL}} \qquad (1)$$

donde (T_c-T_a) es la diferencia de temperatura medida de la hoja - aire, (T_c-T_a)$_{LL}$ el esperado *lower limit o non-water stressed baseline* de (T_c-T_a) en el caso de un dosel potencialmente transpirando, y (T_c-T_a)$_{UL}$ el esperado diferencial en el caso de un dosel sin transpirar. Ambas líneas base son función del déficit de presión de vapor.
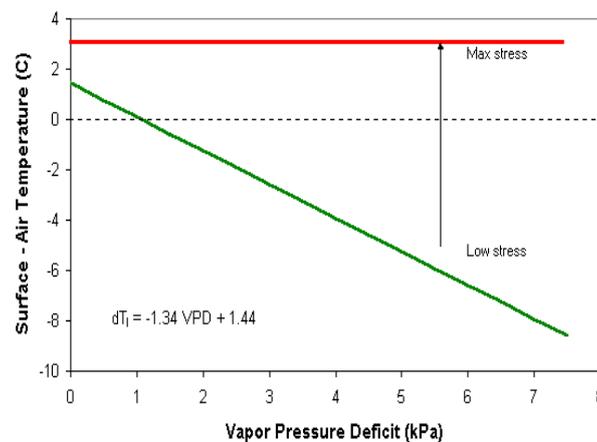
Figura 0.2. Ejemplo de Crop water stress index según el método de Idso, mostrando la distancia relativa de las medidas entre el lower y upper baselines, en función del deficit de presión de vapor. (Idso et al. 1981).

El método empírico se ha desarrollado principalmente en cultivos anuales y hortícolas, y en menor medida en frutales y viña, debido a la complejidad que supone obtenerlo para cubiertas no homogéneas. Algunos ejemplos son: Idso et al. (1982) desarrolló las NWSB para una amplia variedad de cultivos extensivos y hortícolas. Otros estudios se desarrollaron en trigo (Alderfasi y Nielsen, 2001; Yuan et al. 2004; Gontia y Tiwari, 2008), alfalfa (Abduljabbar et al. 1985; Payero et al. 2005), maíz (Nielsen and Gardner 1987; Yazar et al. 1999; Irmak et al. 2000), algodón (Wanjura et al. 1990), judías (Erdem et al. 2006) y melón (Orta et al. 2003), entre otros. En frutales, Testi et al. (2008) desarrolló el CWSI para pistachero, Glenn et al. (1989) en melocotonero, Tormann (1986) en nectarina y Sepaskhah y Kashefipour (1994) en limonero dulce.

No obstante, este método es dependiente del clima y debido a eso, un CWSI para un mismo cultivo puede ser diferente bajo distintas condiciones de radiación solar y viento (Hipps et al. 1995; Zolnier et al. 2001; Al-Faraj et al. 2000). En condiciones de bajo DPV, hay poca diferencia entre la temperatura del dosel vegetativo de plantas bien regadas y estresadas, mientras que los errores de medida tienen la misma magnitud, por lo que existe una mejor señal de CWSI a DPV altos. Algunos autores han demostrado la menor utilidad

de este método en lugares con condiciones climáticas húmedas, (DPV<2KPa), ya que existe la probabilidad de generar errores significativos en el cálculo de CWSI (Hipps et al. 1985; Jones 1999). Sin embargo, Gardner and Shock (1989) sugirieron que una línea base común, podría utilizarse en distintas localizaciones con un DPV desde 1 a 6 KPa.

2.3.2. Método balance energético

Jackson et al. (1981) y Jackson et al. (1982) desarrollaron el método teórico para calcular el CWSI. Éste método contempla además del déficit de presión de vapor y el viento, las diferencias en la radiación neta y resistencia del cultivo (ambas aerodinámica y superficial). Años más tarde, Jackson et al. (1988) presentó una actualización de la metodología. Así, el CWSI se determinó en base a la ecuación del balance energético de una superficie:

$$R_n = G + H + \lambda E \tag{2}$$

donde R_n es la radiación neta (W m^{-2}), G es el flujo de calor hacia la superficie (W m^{-2}), H es el flujo de calor sensible (W m^{-2}) hacia el aire encima de la superficie, y λE es el flujo de calor latente (W m^{-2}).

La ecuación que relaciona la diferencia de temperatura entre el dosel vegetativo y el aire con el déficit de presión de vapor ($e_s - e_a$), la radiación neta, y la resistencia aerodinámica y del cultivo, se obtuvo según:

$$T_c - T_a = \frac{r_a I_c R_n}{\rho C_p} \cdot \frac{\gamma(1 + r_c/r_a)}{\Delta + \gamma(1 + r_c/r_a)} - \frac{e_s - e_a}{\Delta + \gamma(1 + r_c/r_a)} \tag{3}$$

donde ρC_p son la densidad y calor específico del aire, T_c es la temperatura del dosel vegetativo, T_a la temperatura del aire, I_c es un coeficiente de intercepción, e_s el vapor de presión del aire saturado a T_c, e_a el vapor de presión del aire, γ es la constante psicométrica, Δ es la pendiente de la relación entre la presión de saturación y la temperatura, r_c y r_a son la resistencia del dosel vegetativo y aerodinámica, respectivamente.

El límite superior e inferior de T_c-T_a se determinan según:

$$(T_c - T_a)_{UL} = \frac{r_a Ic_u R_n}{\rho C_p} \tag{4}$$

$$(T_c - T_a)_{LL} = \frac{r_a I_{cl} R_n}{\rho C_p} \cdot \frac{\gamma}{\Delta + \gamma} - \frac{e_s - e_a}{\Delta + \gamma} \tag{5}$$

Sin embargo, la diferencia de temperatura para la mayoría de cultivos bajo un estado hídrico adecuado será mayor que el límite inferior, ya que exiben resistencia al flujo del agua, incluso cuando el agua no es un factor limitante. En esos casos, el límite inferior se modificará sustituyendo γ por $\gamma^* = \gamma\ (1 + r_{cp}/r_a)$, donde r_{cp} es la resistencia al vapor de agua del dosel vegetativo a transpiración potencial.

La resistencia aerodinámica (r_a) se calcula a partir de la siguiente ecuación:

$$r_a = \frac{4.72[Ln((z-d)/z_o)]^2}{1 + 0.54u} \tag{6}$$

donde u es la velocidad del viento (Allen et al. 1994) y z, d y z_o son respectivamente, la altura de referencia del sensor (2 metros por encima del dosel), altura de desplazamiento, y la rugosidad de la cubierta vegetal.

Éste método teórico presenta la dificultad de tener que estimar variables muy sensibles a la variación, tales como las propiedades de resistencia aerodinámica de un cultivo o la radiación neta absorbida por la hoja. Por ejemplo, el cálculo de parámetros de la resistencia aerodinámica del dosel vegetativo de un cultivo tiene el inconveniente de ser altamente sensible a la anchura de la cubierta vegetal, a prácticas de manejo del cultivo y puede variar según la especie y variedad (Jackson et al. 1981). Entonces, las líneas base obtenidas mediante esta metodología no pueden ser transportadas en distintas localidades, debido a que también son dependientes del lugar o incluso del año, ya que R_n, temperatura y r_a pueden variar. Este requerimiento, conjuntamente con la necesidad de medir con precisión la temperatura de la hoja, limita la expansión de éste método a nivel práctico.

Algunos estudios han desarrollado este método en trigo (Wang et al. 2005), algodón (Wanjura et al. 1984), melocotonero (Wang et al. 2010), o manzano (Andrews et al. 1992), entre otros, utlizando sensores de temperatura infrarrojo. Gontia y Tiwari (2008) comparó el método empírico con el teórico en trigo sin encontrar diferencias significativas entre ambos. Además, algunos estudios han validado el CWSI obtenido a partir de imágenes aéreas térmicas con medidas de conductancia estomática, en olivos (Berni et al. 2009b).

En los últimos años se han desarrollado nuevas metodologías para el cálculo del CWSI, basadas en modificaciones del método del balance energético. Alves y Pereira (2000) propusieron una nueva línea base siguiendo las estimaciones de Wanjura et al. (1995), quién demostró que un dosel vegetativo es capaz de refrigerarse solamente alrededor de un par de grados por encima de la temperatura ambiente de un bulbo húmedo (T_w). Éste método tiene a ventaja de no requerir de la variable r_c. Entonces, la 'non-water stressed' baseline puede expresarse según:

$$T_s - T_w = \frac{\gamma}{\Delta + \gamma} \frac{r_a(R_n - G)}{\rho c_p} \tag{7}$$

donde T_s es la temperatura del bulbo húmedo *(T$_w$)* y Δ se puede calcular según $(T_a + T_w)/2$.

Jones et al. (1999) también sugirió una modificación del método básico teórico, sustituyendo $(T_c - T_a)_{LL}$ a T_{wet} y $(T_c - T_a)_{UL}$ a T_{dry}. Los valores teóricos de la temperatura de referencia de la superficie de una hoja pueden calcularse utilizando una modificación del balance energético de la hoja (Jones 1992). Este método propuesto por Jones et al. (1999) fue proporcional a la conductancia estomática y se define según:

$$CWSI = \frac{(T_{dry} - T_c)}{(T_c - T_{wet})} \tag{8}$$

O también:

$$CWSI = g_{lw}(r_{aw} + s/\gamma)r_{HR}) \tag{9}$$

donde g_{lw} es la conductancia estomática, r_{aw} es la 'boundary layer resistance' al vapor de agua, s es la pendiente de la curva que relaciona presión de saturación de vapor con temperatura, γ es la constante psicronométrica, r_{HR} es la resistencia paralela al calor y transferencia radiativa.

Para una superficie seca con las mismas propiedades radiativas y aerodinámicas, las pérdidas de calor sensible serán iguales a la radiación neta absorbida. Por lo tanto, se puede estimar T_{dry} (=T_{max} de la ecuación de Idso) según:

$$T_{dry} - T_a = \frac{r_{HR}R_{ni}}{\rho C_p} \tag{10}$$

La temperatura de la correspondiente superficie húmeda (T_{wet}) puede calcularse según:

$$T_{wet} - T_a = \frac{r_{HR}r_{aw}\gamma R_{ni}}{\rho C_p[\gamma(r_{aw}) + sr_{HR}]} - \frac{r_{HR}\delta e}{\gamma r_{aw} + sr_{HR}} \tag{11}$$

En trigo se realizó un estudio comparativo entre el método empírico propuesto por Idso et al. (1981), el método teórico (Jackson et al. 1988) y el propuesto por Alves y Pereira (2000), concluyendo que el método empírico presentaba largas fluctuaciones de valores y frecuentemente valores fuera del rango entre 0-1, mientras que los otros dos métodos se relacionaron satisfactoriamente con el potencial hídrico foliar y presentaron todos los valores entre el rango de 0 y 1 (Yuan et al. 2004). Leinonen et al. (2006) también comparó

en viña tres métodos para estimar la conductancia estomática (g_s) utilizando el CWSI. Los métodos que se compararon fueron a) método del balance energético, sin el uso de superficies de referencia, b) solamente con el uso de T_{dry} (Eq.10) y c) el uso de T_{dry} y T_{wet} (Eq. 10 y 11). Las conclusiones del estudio recomendaron el uso de T_{dry} como superficie dereferencia, ya que es más fácil de obtener una superficie seca (hoja sin transpiración) que una húmeda. Por el contrario, el método del balance energético se descartó debido a sus claras limitaciones, ya que es difícil de obtener valores precisos de radiación neta absorbida por la hoja.

2.3.3. Método con superficies de referencias

Este método se presenta como el más simple para el cálculo del CWSI. Se basa en utilizar superficies naturales o artificiales a modo de referencia para calcular 'T_{wet}' y 'T_{dry}'. Las referencias comúnmente más utilizada son mojar el dosel vegetativo con agua en ambos lados o bien utilizar paneles húmedos (=T_{wet}) o por otro lado, cubrir las hojas con vaselina (=T_{dry}), con el propósito de evitar la transpiración. También se ha utilizado en algunos estudios papel de filtro húmedo o seco. Cohen et al. (2005), Meron et al. (2003; 2010) utilizaron en algodón paneles húmedos como superficies de referencia artificiales húmedas (wet artificial reference surfaces, WARS) y T_{dry} se estimó añadiendo 5.0 ºC a la temperatura del aire de un bulbo seco.

Möller et al. (2007) comparó distintas metodologías para el cálculo del CWSI en viña, basadas en el modelo teórico desarrollado por Jones et al. (1999) y en distintos métodos de obtención de T_{wet} y T_{dry} mediante el uso de superficies de referencia. Su estudio concluyó que el uso de WARS para obtener T_{wet} y T_{aire}+5ºC para obtener T_{dry} fue el que mostró una mejor relación con el Ψ_L durante toda la estación. También Ben-Gal et al. (2009) y Alchanatis et al. (2010) compararon ambos métodos en algodón. Sin embargo, a nivel práctico el uso de superficies de referencia para calcular el CWSI presenta ciertas limitaciones. Una primera limitación es la utilización de un mismo valor arbitrario de º5C para el cálculo de T_{dry}. Es conocido que cuando se produce el cierre estomático debido al estrés hídrico, la temperatura de la hoja depende de su capacidad de intercambiar calor con el aire. Esta capacidad de intercambio de calor depende en parte, de la anchura o forma de la hoja (Gates and Papian 1971; Nobel 2009). Por lo tanto, (T_c-T_a) de un dosel sin transpirar dependerá de estos parámetros y podrá ser distinto según el cultivo, variedad y fase fenológica. Otra limitación se basa en la necesidad de disponer de referencias en cada una de las imágenes a procesar. Por el momento, creemos que este método tiene pocas posibilidades de ser utilizado directamente y continuadamente como herramienta para programar el riego.

3. Teledetección

Podemos definir el término teledetección como '*la medida o adquisición de información de alguna propiedad de un objeto o fenómeno, mediante un instrumento que no está en contacto físico directo con el objeto o fenómeno bajo estudio*' (Colwell, 1983).

La principal ventaja del uso de la teledetección en viticultura se basa, a diferencia de las medidas puntuales mencionadas anteriormente, en que permite adquirir información precisa de la variabilidad espacial y temporal del viñedo.

3.1. Sistemas de obtención de imágenes

En la actualidad existen distintas plataformas capaces de proporcionar información sobre la vegetación, tales como satélites, aviones o avionetas tripuladas o no tripuladas (*unmanned aerial vehicles*, *UAV*). Sin embargo, la elección de la plataforma óptima para instalar el sensor influenciará en la resolución espacial, espectral y temporal de las imágenes.

El concepto de *resolución espacial* se refiere al objeto más pequeño que se puede distinguir en la imagen, lo que se suele conocer como píxel. La resolución espacial depende por lo tanto, de las características de la óptica del sensor y altura sobre el nivel del suelo de la plataforma. La *resolución espectral* consiste en el número de canales espectrales (y su ancho de banda) que es capaz de registrar imágenes un sensor. Los nuevos sensores, llamados espectrómetros o hiperespectrales llegan a tener hasta 256 canales con un ancho de banda muy estrecho para poder separar de forma precisa distintos objetos por su comportamiento espectral. La *resolución temporal* se refiere a la frecuencia con que una plataforma es capaz de proporcionar imágenes de un mismo punto de la superficie terrestre. En este sentido, los satélites, disponen de una menor resolución temporal respecto a las plataformas aéreas.

En la actualidad existen satélites, tales como Ikonos o Quickbird capaces de proporcionar imágenes multiespectrales (en el visible y en el infrarrojo próximo) con resoluciones espaciales hasta 60 cm. Sin embargo, existen ocasiones en que los datos que necesitamos requieren de una mayor resolución espacial o de una mayor frecuencia temporal, y estos satélites no pueden ofrecerlo. Además, los satélites que actualmente disponen de sensores térmicos (Terra-Aster), solamente son capaces de proporcionar imágenes con un tamaño de píxel alrededor de 90 metros, con lo cual los hace impracticables para aplicaciones agrícolas. La posibilidad de disponer de un avión preparado con cámaras multiespectrales o térmicas de alta resolución permite mejorar las prestaciones de los satélites actualmente en órbita, abordando nuevas aplicaciones operativas con una mayor frecuencia de adquisición de imágenes.

3.2. Reflectividad

Los sensores instalados en las distintas plataformas son capaces de medir la radiación electromagnética reflejada y/o emitida por la superficie terrestre. El espectro está dividido en varias regiones (Fig. 0.3). La región visible (VIS), llamado así porque es la única radiación electromagnética que puede detectar nuestros ojos, se comprende entre 0,4 a 0,7 μm, y aproximadamente se corresponde con la región fotosintéticamente activa (PAR). Dentro del visible distinguimos tres bandas elementales como pueden ser el azul (de 0,4 a 0,5 μm), el verde (de 0,5 a 0,6 μm) y el rojo (de 0,6 a 0,7 μm), mientras que para el infrarrojo, nos quedamos con el infrarrojo cercano o próximo (de 0,7 a 1,3 μm) y una estrecha franja de longitud de onda del infrarrojo medio (de 1,3 a 2,8 μm).
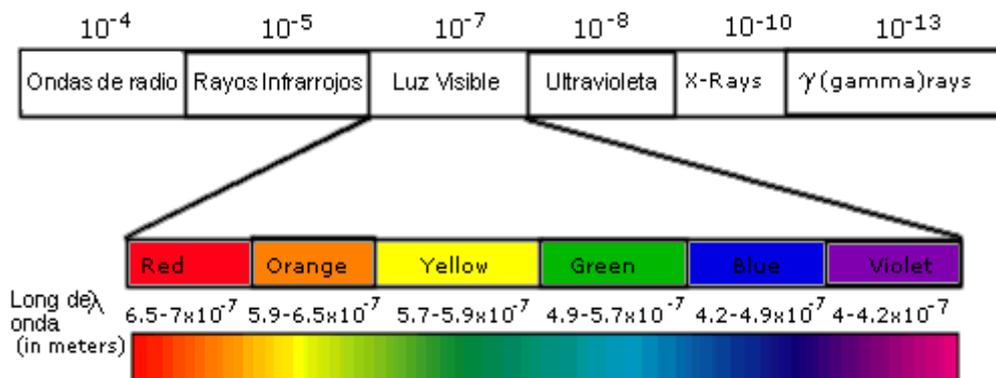
Figura 0.3. Espectro electromagnético

Mediante la combinación de las bandas espectrales es posible obtener, para cada píxel de la imagen, información cuantitativa de los parámetros biofísicos relacionados con la dinámica de la vegetación, principalmente a través de la medición de la reflectividad y temperatura de la superficie terrestre. Por lo tanto, con la combinación de distintas bandas espectrales es posible obtener una gran cantidad de índices, los cuales se relacionan con las propiedades de la vegetación.

3.2.1. Imágenes multiespectrales

Las cámaras en color tradicionales suelen proporcionan tres bandas de información por cada imagen (rojo, verde y azul), tratando de imitar el proceso de visión del sistema humano. Sin embargo, en una imagen multiespectral, el número de bandas empleadas para representar una escena contempla una mayor cantidad de bandas. Con la combinación de las bandas del rojo e infrarrojo se obtienen los denominados *Índices de vegetación,* los cuales se definen como un parámetro obtenido a partir de la combinación de dos o más valores de reflectancia a distintas longitudes de onda, para resaltar alguna propiedad de la

vegetación. Existen distintas categorías de índices que van desde la identificación de cambios estructurales en la vegetación (Johnson et al. 2003; Bramley et al. 2003), la estimación de la pérdida de constituyentes bioquímicos de la clorofila (Björkman & Powles, 1982) o agua (Peñuelas et al. 1995), detección de cambios en los pigmentos foliares (Gamon et al. 1992) o en la fluorescencia clorofílica (McFarlane et al. 1980).

Los índices de vegetación estructurales son posiblemente los más conocidos y utilizados, ya que fueron la primera herramienta eficaz para la detección de las propiedades de las cubiertas vegetales. Se basan en determinar la vegetación activa densa a partir del contraste entre la reflectividad en el rojo y en el infrarrojo cercano. Por lo tanto, cuando mayor sea el contraste entre en estas bandas, mayor será el vigor de la vegetación, entendido como una mayor cobertura del suelo y una mayor actividad fotosintética. Por otro lado, cambios en la cubierta vegetal, tales como amarilleamiento de la vegetación, vegetación seca o sequía, suelen traducirse en cambios en la reflectividad en las bandas del rojo y infrarrojo. Los índices de vegetación estructurales más utilizados en aplicaciones de la teledetección son el *Normalized Difference Vegetation Index* (NDVI), o el *Plant Cell Density index* (PCD), los cuales se definen como:

$$NDVI = \frac{\varphi_{NIR} - \varphi_R}{\varphi_{NIR} + \varphi_R} \qquad\qquad\qquad (12)$$

$$PCD = \frac{\varphi_{NIR}}{\varphi_R} \qquad\qquad\qquad (13)$$

donde φ_{NIR} es la reflectividad en el infrarrojo cercano y φ_R es la reflectividad en el rojo, en el ancho de banda correspondiente.

Estos índices se han utilizado en teledetección para identificar y mapear diferencias intraparcelarias del vigor vegetativo con el propósito de relacionarlas con la variabilidad de la cosecha (Martinez-Casasnovas et al. 2009; Lamb et al. 2001), calidad de la uva (Trought and Bramley, 2011; Johnson et al. 2001) o necesidades hídricas (Acevedo-Opazo et al. 2008).

3.2.2. Imágenes térmicas

Las imágenes térmicas se obtienen midiendo la energía de la radiación electromagnética emitida por la superficie de un cuerpo y que es función de su temperatura. Para la estimación de la temperatura se utilizan sensores térmicos capaces de medir las bandas en la región del espectro infrarrojo térmico, entre 7 y 13 µm.

Tal y como se ha mencionado con anterioridad, una de las aplicaciones de las imágenes térmicas en la teledetección consiste en medir la temperatura de la cubierta vegetativa del cultivo y en el consiguiente desarrollo del *Crop Water Stress Index* (CWSI). Este índice se

considera un buen indicador del estado hídrico de los cultivos (Tanner, 1963; Idso et al. 1978; Jackson et al. 1977). Recientemente, con la posibilidad de adquirir imágenes térmicas de alta resolución obtenidas con sensores térmicos aerotransportados (Berni et al. 2009a), ha aumentado la posibilidad de utilizar esta tecnología como herramienta para detectar la variabilidad del estado hídrico en parcelas comerciales y así poder tomar decisiones de riego en función de ello. Algunos estudios han demostrado en cultivos leñosos como olivar, la posibilidad de detectar y mapear la variabilidad del estado hídrico a partir de la diferencia de temperatura de la hoja y el aire (T_c-T_a) (Sepulcre-Cantó et al. 2006) o mediante el CWSI (Berni et al. 2009b). El uso de mapas de CWSI en viñedos puede ser un método simple, coste-efectivo para un manejo eficiente del riego en función de su estado hídrico.

Referencias

Abdul-jabbar, A.S., Lugg, D.G., Sammis, T.W., Gay, L.W (1985) Relationship between Crop water stress index and alfalfa yield and stress between irrigation and evapotranspiration. Trans. ASAE, 28, 2, 454-461.

Acevedo-Opazo, C., Tisseyre, B., Guillaume, S., Ojeda, H (2008) The potential of high spatial resolution information to define within vineyard zones related to vine water status. Precis Agric 9:285–302.

Alchanatis, V., Cohen,Y., Cohen, S., Moller, M., Sprinstin, M., Meron, M., Tsipris, J., Saranga,Y., Sela, E (2010) Evaluation of different approaches for estimating and mapping crop water status in cotton with thermal imaging. Precision Agriculture, 11, (1), 27-41.

Aldefasi, A.A., Nielsen, D.C (2001) Use of crop wáter stress index for monitoring water status and scheduling irrigation in wheat. Agricultural Water Management 47, 69-75.

Al-Faraj, A., Meyer, G.E., Schade, G.R., Horst.G.L (2000) Dynamic analysis of moisture stress in tall fescue (Festuca arundinacea) using canopy temperature, irradiation, and vapor deficit. Trans. ASAE 43(1): 101-109.

Allen, R.G., Smith, M., Pereira, L.S., Perrier, A (1994) An update for the calculation of reference evapotranspiration. ICID Bull. 43(2):35-92.

Allen, R.W., Pereira, L.S., Raes, D., Smith, M (1998) Crop evapotranspiration. Guidelines for computing crop water requirements. FAO Irrigation and Drainage Paper No. 56. 300 pp.

Alves, I., Pereira, L.S (2000) Non-water-stressed baselines for irrigation scheduling with infrared thermometers:a new approach. Irrigation Sci. 19, 101–106.

Andrews, P.K., Chalmers, D.J., Moremong, M (1992) Canopy-air temperature differences and soil water as predictors of water stress of apple trees grown in a humid, temperate climate. J.Amer.Soc.Hort.Sci. 117 (3), 453-458.

Basile, B., Marsal, J., Mata, M., Vallverdú, X., Bellvert, J., Girona, J (2011) Phenological sensitivity of Cabernet Sauvignon to water stress: vine physiology and berry composition. Am J Enol Vitic 62:452–461.

Basile, B., Girona, J., Behboudian, M.H., Mata, M., Rosello, J., Ferré, M., Marsal, J (2012) Responses of ''Chardonnay'' to deficit irrigation applied at different phenological stages: vine growth, must composition, and wine quality. Irrigation Science. 30:397–406.

Ben-Gal, A., Agam, N., Alchanatis, V., Cohen, Y., Yermiyahu, U., Zipori, I., Presnov, E., Sprintsin, M., Dag, A (2009) Evaluating water stress in irrigated olives: correlation of soil water status, tree water status, and thermal imagery. Irrigation Science. 27:367–376

Berni, J.A., Zarco-Tejada, P.J., Suarez, L., Fereres, E (2009a) Thermal and narrow-band multispectral remote sensing for vegetation monitoring from an unmanned aerial vehicle. IEEE Transactions on Geoscience and Remote Sensing. 47, 722-738.

Berni, J.J., Zarco-Tejada, P.J., Sepulcre - Cantó, G., Fereres, E., Villalobos, F (2009b) Mapping canopy conductance and CWSI in olive orchards using high resolution thermal remote sensing imagery. Remote sensing of Environment. 113, 2380-2388.

Björkman, O., Powles, S (1982) Inhibition of photosynthetic reactions under wáter stress: Integration with light level. Planta, 161, 490-504.

Boyer, J.S (1967) Leaf water potentials measured with a pressure chamber. *Plant Physiology*. 42(1): 133-137.

Bramley, R.G.V., Lamb, D.W (2003) Making sense of vineyard variability in Australia. In: Precision viticulture. Proceedings of the IX Congreso Latinoamericano de Viticultura y Enología, Santiago, Chile, pp 35–44.

Campbell, G.S (1985) Soil Physics with Basic. Elsevier, Amsterdam.

Cohen, Y., Alchanatis, V., Meron, M., Saranga, Y., Tsipris, J (2005) Estimation of leaf water potential by thermal imagery and spatial analysis. J Exp Bot. 56 (417), 1843–1852

Colwell, R.N. (ed.) (1983) Manual of Remote Sensing. Falls Church, Virginia.

Erdem, Y., Sehirali, S., Erdem, T., Kenar, D (2006) "Determination of Crop water stress index for irrigation scheduling of Beans (Phaseolus vulgaris. L)". Turk . J . Agric. 30:195-202.

FAO (2009) Agriculture indices (FAOSTAT). http://faostat.fao.org. Accessed 14 July 2011.

Ferreyra, E.R., Sellés, G., Ruiz, S.R., Sellés, M.I (2003) Efecto del estrés hídrico aplicado en distintos períodos de desarrollo de la vid Chardonnay en la producción y calidad del vino. Agricultura Técnica (Chile) 63(3): 227-286.

Gamon, J.A., Penuelas, J., Field, C.B (1992) *A Narrow-Waveband Spectral Index That Tracks Diurnal Changes in Photosynthetic Efficiency*. Remote Sensing of Environment 41:35-44.

Gardner, B.R., Shock, C.C (1989) Interpreting the crop water stress index. ASAE, 89, 2642.

Gates, D.M (1964) Leaf temperature and transpiration. Agron. J. 56, 273-277.

Gates, D.M., Papian, L.E (1971) Atlas of energy budgets of plant leaves. Academic Press, London, 279 p.

Glenn D.M., Worthington, J.W., Welker, M.J., Farland, M (1989) Estimation of peach tree water use using infrared thermometry. J. Am. Soc. Hort. Sci. 114: 737-741.

Ginestar, G., Eastham, J., Gray, S., Iland, P (1998) Use of sap-flow sensors to schedule vineyard irrigation. I. Effects of post-veraison water deficits on water relations, vine growth, and yield of Shiraz grapevines. Am J Enol Vitic. 49:413–420.

Girona, J., Mata, M., del Campo, J., Arbonés, A., Bartra, E. Marsal, J (2006) The use of midday leaf water potential for scheduling deficit irrigation in vineyards. Irrigation Science. 24,115–127.

Girona, J., Marsal, J., Mata, M., del Campo, J., Basile, B (2009) Phenological sensitivity of berry growth and quality of 'Tempranillo' grapevines (Vitis vinifera L.) to water stress. Aust J Grape Wine Res. 15:268–277.

Glenn D.M., Worthington, J.W., Welker, M.J., Farland, M (1989) Estimation of peach tree water use using infrared thermometry. J. Am. Soc. Hort. Sci. 114: 737-741.

Gontia, N.K., Tiwari, K.N (2008) Development of crop water stress index of wheat crop for scheduling irrigation using infrared thermometry. Agricultural Water Management 10, 1144-1152.

Grimes, D.W., Williams, L.E (1990) Irrigation effects on plant water relations and productivity of 'Thompson Seedless' grapevines. Crop Sci. 30:255-260.

Hipps, L.E., Ashrar, G., Kanemasu, E.T. (1985) A theoretically-based normalization of the environmental effects on foliage temperature. Agricultural and Forest Meteorology 35, 113–122.

Idso, S.B., Jackson, R.D., Reginato, R.J (1978) Extending the "degree day" concept of plant phenological development to incude water stress effects. Ecology, 59:431-433.

Idso, S.B., Jackson, R.D., Pinter, P.J., Reginato, R.J., Hatfield, J.L (1981) Normalizing the stress-degree-day paameter for environmental variability. Agr For Meteorol. 24, 45-55.

Intrigliolo, D.S., Castel, J.R (2009) Response of *Vitis vinifera* cv. 'Tempranillo' to partial rootzone drying in the field: Water relations, growth, yield and fruit and wine quality. Agricultural Water Management. 96 (2): 282-292.

Irmak, S., Dorota, Z.H., Bastug, R (2000) Determination of crop water stress index for irrigation timing and yield estimation of corn. Agron. J. 92, 1221-1227.

Jackson, R.D., Reginato, R.J., Idso, S.B (1977) Wheat canopy temperature: a practical tool for evaluating water requirements. Water Resour. Res., 13: 651-656.

Jackson, R.D., Idso, S.B., Reginato, R.J., Pinter, P.J (1981) Canopy temperature as a crop water stress indicator. Water Resources Res., 7: 1133-1138.

Jackson, R.D (1982) Canopy temperature and crop water stress. Advances in irrigation, Vol 1, Academic Press, New York, 43-85.

Jackson, R.D., Kustas, W.P., Choudhury, B.J (1988) A reexamination of the crop water stress index. Irrigation Sci. 9, 309–317.

Johnson, L.F., Bosch, D.F., Williams, D.C., Lobitz, B.M. (2001) Remote sensing of vineyard management zones implications for wine quality. Appl Eng Agric. 17(4):557–560.

Johnson, L.F., Roczen, D. E., Youkhana, S. K., Nemani, R. R., Bosch, D. F (2003). Mapping vineyard leaf area with multi-spectral satellite imagery. Computers and Electronics in Agriculture. 38, 33–44. doi:10.1016/S0168-1699(02)00106-0.

Jones, H.G (1992) Plants and microclimate, 2nd edn. Cambridge: Cambridge University Press.

Jones, H.G (1999) Use of infrared thermometry for estimation of stomatal conductance as a possible aid to irrigation scheduling. Agric For Meteorol. 95(3):139–149.

Jones, H.G (2004) Application of thermal imaging and infrared sensing in plant physiology and ecophysiology. Advances in Botanical Research. 41,107–163.

Jones, H.G., Leinonen, I (2003) Thermal imaging for the study of plant water relations. Journal of Agricultural Meteorology. 59, 205–214.

Kirkham, M.B (2005) Principles of Soil and Plant Water Relations. Elsevier Academic Press, Amsterdam, xiv + 500 pp.

Lamb, D., Hall, A., Louis, J (2001) Airborne remote sensing of vines for canopy variability and productivity. Aust Grapegrow Winemak. 449, 89–92.

Leinonen, I., Grant, O. M., Tagliavia, C. P. P., Chaves, M. M., & Jones, H. G. (2006). Estimating stomatal conductance with thermal imagery. Plant, Cell and Environment, 29, 1508−1518.

Martinez-Casasnovas, J.A., Vallés, D., Ramos, M.C (2009) Irrigation management zones for precision viticulture according to intrafield variability. In: EFITA conferences, pp 523–529.

Mc Farlane, J., Watson, R., Theisen, A., Jackson, R., Ehrler, W (1980). Plant stress detection by remote measurement of fluorescence. Applied Optics, 19, 3287-3289.

Meron, M., Tsipris, J., Charitt, D (2003) Remote mapping of crop water status to assess spatial variability of crop stress. In: Strafford J, Werner A (eds) Precision agriculture. Proceedings of the fourth European conference on precision agriculture. Academic Publishers, Berlin, pp 405–410.

Meron, M., Tsipris, J., Alchanatis, V., Cohen, Y., Orlov, V (2010) Crop water stress mapping for site specific irrigation by thermal imagery and artificial reference surfaces. Precision Agriculture, 11, 148-162.

Möller M., Alchanatis, V., Cohen, Y., Meron, M., Tsipris, J., Naor, A., Ostrovsky, V., Sprintsin, M. Cohen, S (2007) Use of thermal and visible imagery for estimating crop water status of irrigated grapevine. J Exp Bot 58(4):827–838.

Nielsen, D.C., Gardner, B.R. (1987) Scheduling irrigations for corn with the crop water stress index (CWSI). Appl. Agric. Res. 2, 5, 295-300.

Nobel, P.S (2009) Physicochemical and environmental plant physiology. 4th ed. Academic press, Amsterdam, Boston. 582 p.

Ojeda, H., Andary, C., Kraeva, E., Carbonneau, A., Deloire, A (2002) Influence of pre- and postveraison water deficit on synthesis and concentration of skin phenolic compounds during berry growth of vitis vinifera cv. Shiraz. Am. J. Enol. Vitic. 53(4): 261-267.

Orta, A.H., Erdem, Y., Erdem, T (2003) Crop water stress index for watermelon. Scientia Hort. 98, 121-130.

Payero, J.O., Neale, C.M.U., Wright, J.L (2005). Non-water stressed baselines for calculating crop water stress index (CSWI) for alfalfa and tall fescue grass. Trans. ASAE, 48(2): 653-661.

Peñuelas, J., Filella,I., Biel, C., Serrano, L., Save, R (1995) *The Reflectance at the 950-970 Region as an Indicator of Plant Water Status*. International Journal of Remote Sensing 14:1887-1905.

Reynolds, A.G., Naylor, A.P (1994) 'Pinot-noir' and 'Riesling' grapevines respond to water stress duration and soil water-holding capacity. Hort Sci 29(12): 1505-1510.

Ritchie, G.A., Hinckley, T.M (1975) The Pressure Chamber as an Instrument for Ecological Research. Advance in Ecological Research. 9, 165-254.

Roby, G., Harbertson, J.F., Adams, D.A., Matthews, M.A (2004) Berry size and vine water deficits as factors in winegrape composition: anthocyanins and tannins. Australian Journal of Grape and Wine Research 10, 100–107.

Scholander, P.F., Hammel, H.T., Bradstreet, E.D., Hammingsen, E.A (1965) Sap pressure in vascular plants. Science 148, 339-346.

Schultz, H.R (2003) Differences in hydraulic architecture account for near-isohydric and anisohydric behaviour of two field-grown *Vitis vinifera* L. cultivars during drought. Plant, Cell & Environment. 26, 8, 1393-1405.

Sepaskhah, A.R., Kashefipour, S.M (1994) Relationships between leaf water potential, CWSI, yield and fruit quality of sweet lime under drip irrigation. Agricultural Water Management. 25, 1, 1994, 13–21.

Sepulcre-Canto, G., Zarco-Tejada, P., Jimenez-Muñoz, J., Sobrino, J., de Miguel, E. et al. (2006) Detection of water stress in a olive orchard with thermal remote sensing imagery. Agricultural and Forest Meteorology, 136, 44.

Tanner, C.B (1963) Plant temperatures. Agron. J. 55, 210-211.

Testi, L., Goldhamer, D., Iniesta, F., & Salinas, M. (2008). Crop water stress index is a sensitive water stress indicator in pistachio trees. Irrigation Science, 26, 395–405.

Tormann, H (1986) Canopy temperature as a plant water stress indicator for nectarines. South African Journal of Plant and Soil. 3, 3.

Trought, M.C.T., Bramley, R.G.V (2011) Vineyard variability in Marlborough, New Zealand: characterising spatial and temporal changes in fruit composition and juice quality in the vineyard. Australian Journal of Grape and Wine Research. 17, 79-89.

Turner, N.C., Stern, W.R., Evans, P (1987) Water relations and osmotic adjustment of leaves and roots of lupins in response to water deficits. Crop Sci. 27, 977-983.

UNEP (2008). The Blue Plan's sustainable development outlook for the Mediterranean.

UNESCO (2010). 3er Informe de las Naciones Unidas sobre el Desarrollo de los Recursos Hídricos en el mundo.

Yazar A., Howell A.T., Dusek D.A., Copeland K.S (1999) Evaluation of crop water stress index for LEPA irrigated corn. Irrig. Sci. 18, 171-180.

Yuan, G., Luo, Y., Sun, X., Tang, D (2004) Evaluation of a crop water stress index for detecting water stress in winter wheat in the North China Plain. Agricultural Water Management 64, 29-40.

Wang, L., Yu Qiu, G., Zhang, X (2005) Application of a new method to evaluate crop water stress index. Irrigation Science, 24, 49-54.

Wang, X.Z., Yang, W.P., Wheaton A.D., Cooley, N., Moran, B (2010) Automated canopy temperature estimation via infrared thermography: A first step towards automated plant water stress monitoring. Journal of Computers and Electronics in Agriculture, Vol. 73, 1, 74-83, ISSN 0168-1699.

Wanjura, D.F., Hatfield, J.L., Upchurch, D.R., 1990. Crop water stress index relationships with crop productivity. Irrig. Sci. 11, 93–99.

Wanjura, D.F., Upchurch, D.R., Mahan, J.R (1995) Control of irrigation scheduling using temperature-time thresholds. Trans. ASAE, 38, 2, 403-409.

Wanjura, D.F., Kelly, C.A., Wendt, C.W., Hatfield, J.L (1984) Canopy temperature and water stress of cotton crops with complete and partial ground cover. Irrigation Science. 5, 37-46.

Williams, L.E., Araujo, F.J (2002) Correlations among predawn leaf, middday leaf and midday stem wáter potential and their correlations with other measures of soil and plant water status in vitis vinifera. J. Am. Soc. Hort. Sci 127(3):448-454.

Williams, L.E. and Matthews, M.A (1990) Grapevine. In: Irrigation of agricultural crops (Agronomy Monograph No. 30). Eds. B.A. Steward and D.R. Nielsen (ASA-CSSA-SSSA: Madison, WI) pp. 1019–1055.

Zolnier, S., Gates, R.S., Anderson, R.G., Nokes, S.E., Duncan, G.A (2001) Non-water-stressed baseline as a tool for dynamic control of misting system for propagation of poinsettias. Trans. ASAE 44(1): 137-147.

Presentación del trabajo

Esta tesis doctoral se basa en utilizar herramientas de teledetección de alta resolución para el manejo de la variabilidad espacial intraparcelaria de los viñedos. Para ello, la tesis se ha estructurado en dos partes: i) caracterización de la variabilidad intraparcelaria de un viñedo y estudio de posibles alternativas para re-diseñar los sectores de riego en función de la variabilidad, con el propósito de obtener una uniformidad productiva, ii) desarrollo del *Crop Water Stress Index* (CWSI) como indicador del estado hídrico de la viña, y generación de mapas estacionales de CWSI para ser utilizados como herramienta de manejo del riego en viñedos. Esta tesis doctoral se ha centrado en las variedades de viña de Pinot noir, Chardonnay, Tempranillo y Syrah.

La tesis se distribuye en tres capítulos que se resumen a continuación:

En el **Capítulo 1**, se presenta un estudio de caracterización de la variabilidad de un viñedo y se determinan las propiedades físicas del suelo que mayor efecto tienen sobre la variabilidad espacial del estado hídrico en un viñedo. Además, se exponen y comparan dos metodologías para delimitar zonas o sectores de riego, con el propósito de homogeneizar la producción. Las metodologías estudiadas fueron en base a la variabilidad del estado hídrico, obtenida con medidas de potencial hídrico foliar (Ψ_h) y en base al índice de vegetación estructural *Plant Cell Density* (PCD), obtenido a partir de imágenes aéreas multiespectrales.

En el **Capítulo 2** se demostró la viabilidad de utilizar el *Crop Water Stress Index* (CWSI) como indicador del estado hídrico en un viñedo de Pinot noir. El desarrollo del CWSI se realizó a partir del método empírico, obteniendo la 'non-water-stressed baseline' a partir de datos de temperatura del dosel vegetativo de una viña sin estrés hídrico. Posteriormente, se validó el CWSI en el viñedo entero con medidas de potencial hídrico foliar (Ψ_h), al mismo tiempo que se adquirieron las imágenes térmicas aéreas del viñedo con una avioneta no tripulada (UAV). Otros aspectos metodológicos como la resolución espacial óptima de la imagen térmica y el momento idóneo del día para detectar el estrés hídrico a partir de imágenes térmicas aéreas han sido estudiados en este capítulo.

En el **Capítulo 3** se han desarrollado las ecuaciones de CWSI para las variedades de viña Pinot noir, Chardonnay, Tempranillo, y Syrah. Sin embargo, se conoce que la respuesta de la viña al déficit de presión de vapor (DPV) puede ser diferente en función del momento fenológico. Así, en este capítulo también se desarrollaron las ecuaciones de CWSI en las distintas fases fenológicas y la validación estacional con medidas de potencial hídrico foliar (Ψ_h). Se valoró el efecto de utilizar las ecuaciones de cada momento fenológico y variedad sobre la relación entre CWSI y Ψ_h. Con esta información es posible obtener mapas de CWSI durante toda una campaña de riego y así programar el riego en función del estado hídrico.

Derivada de esta tesis doctoral se han publicado los siguientes trabajos:

Revistas incluidas en el SCI:

Bellvert, J., Marsal, J., Mata, M., Girona, J. (2012) Identifying irrigation zones across a 7.5-ha 'Pinot noir' vineyard based on the variability of vine water status and multispectral images. Irrigation Science, 30, 499-509.

J. Bellvert, P.J. Zarco-Tejada, J. Girona, E. Fereres. (2013) Mapping crop water stress index in a `Pinot-noir´ vineyard: comparing ground measurements with thermal remote sensing imagery from an unmanned aerial vehicle. Precision Agriculture.
DOI 10.1007/s11119-013-9334-5.

Revistas y libros no incluidos en el SCI:

J. Bellvert and J. Girona (2012) The use of multispectral and thermal images as a tool for irrigation scheduling in vineyards. Book chapter. The use of remote sensing and geographic information systems for irrigation management in Southwest Europe. Options Méditerranéennes. 67 p.131-137. ISSN: 1016-1228-ISBN: 2-85352-482-5.

J. Bellvert, J.P. Zarco-Tejada, J. Girona, E. Fereres (2013) La teledetección como herramienta para el manejo del riego en viñedos. TIERRAS. 206, 56-61.

Aportaciones a congresos:

Bellvert J, Zarco-Tejada PJ, Gonzalez-Dugo V, Girona J, Fereres E (2013) Scheduling vineyard irrigation based on mapping leaf water potential from airborne thermal images. Precision Agriculture'13. ed. John Stafford. p.699-704.

Póster a congreso: INNPACTO project: A tool for scheduling irrigation using airborne high resolution thermal imagery. Bellvert J, Zarco-Tejada PJ, Girona J, Mata M, Bonastre N, Paris C, González-Dugo V, Romero R, Fereres E. Congreso: European Precision agriculure conferences. Lleida, junio 2013.

Póster a congreso: Determinación del estado hídrico de viñedos mediante imágenes térmicas de alta resolución obtenidas con un vehículo aéreo no tripulado. J. Bellvert, P.J. Zarco-Tejada, J. Girona, E. Fereres. XV Congreso de la Asociación Española de Teledetección (AET). Madrid, Octubre 2013.

J. Bellvert, J. Girona, J.P. Zarco-Tejada y E. Fereres (2011) Utilización del Crop Water Stress Index (CWSI) para la programación del riego en viñedos. Agricultura, Agua y Energía. Madrid, Marzo 2011.

Objetivos

Los objetivos de esta Tesis Doctoral son los siguientes:

1. Estudiar la influencia de las características físicas del suelo sobre la variabilidad del estado hídrico de un viñedo.

2. Determinar la efectividad de dos metodologías de re-diseño de los sectores de riego -potencial hídrico foliar (Ψ_h) e índice de vegetación estructural (Plant Cell Density)- para reducir la variabilidad productiva en un viñedo.

3. Evaluar el Crop Water Stress Index (CWSI) como indicador del estado hídrico en viña: validación del CWSI con el potencial hídrico foliar (Ψ_h) y obtención de mapas de CWSI utilizando imágenes térmicas de alta resolución desde un vehículo aéreo no tripulado (UAV).

4. Evaluar el efecto de la variedad y fenología en el desarrollo del CWSI y en sus validaciones con el potencial hídrico foliar (Ψ_h), para las variedades de viña Pinot noir, Chardonnay, Tempranillo y Syrah.

5. Responder a aspectos metodológicos para la detección del estado hídrico en viñedos mediante imágenes térmicas aéreas, tales como: i) la resolución espacial óptima de la imagen, y ii) momento óptimo del día para adquirir las imágenes.

Capítulo 1

Identifying irrigation zones across a 7.5-ha 'Pinot noir' vineyard based on the variability of vine water status and multispectral images

J. Bellvert, J. Marsal, M. Mata & J. Girona

Programa Uso eficiente del agua, Institut de Recerca i Tecnologia Agroalimentàries (IRTA), Centre UdL-IRTA, 191 Av. Rovira Roure, 25198 Lleida, Spain

Abstract Vine water status, yield, and berry composition are variables within a vineyard. There is current interest in defining zones of similar yield and berry composition. The aim of this study was to compare two methods for identifying homogeneous zones in terms of yield within a 7.5-ha `Pinot noir´ vineyard. The two methods were based on: spatial distribution of average midday leaf water potential ($\Psi_L$) and plant cell density (PCD = near infrared / red) which is a vegetation index. A proposal for splitting the vineyard into eight new irrigation zones was assessed. A `blind´ zonation based on regular polygons of equal sizes was also established as a standard for comparison. Coefficients of variation (C_v) in yield for both methods were compared with that of the blind zonation. In 2006 and 2007, a *k*-means cluster analysis indicated that variability in Ψ_L was mainly effected by soil properties. In both years, the vineyard was fully irrigated (100 % ETc). The two methods did not improve yield C_v for full irrigation in 2006 and 2007 compared to blind zonation. In 2009, regulated deficit irrigation (RDI) was applied resulting in higher variability in Ψ_L and yield. The Ψ_L method of zonation significantly reduced coefficient of variation under RDI but PCD method did not despite the reduction in C_v by 16.7 %. We recommend irrigation zonation based on Ψ_L when RDI is applied.

Resumen

El estado hídrico de la viña, la producción y la composición de la uva presentan una variabilidad espacial dentro de un viñedo. Recientemente, hay un interés en definir zonas con similitudes en cuanto a términos productivos y de composición de la uva. El objetivo de este estudio fue comparar dos métodos para identificar zonas homogéneas en términos productivos en un viñedo de 7-ha de `Pinot-noir´. Los dos métodos se basaron en: distribución espacial del potencial hídrico foliar promedio (Ψ_L) y el índice vegetativo plant cell density (PCD = infrarrojo cercano/rojo). Se evaluó una propuesta basada en dividir el viñedo en ocho nuevas zonas de riego. Como estándar de comparación, se estableció una zonificación 'ciega' basada en polígonos regulares de la misma medida. Se compararon los coeficientes de variación (C_v) de la producción de los dos métodos con el del método de zonificación 'ciega'. En los años 2006 y 2007, un análisis de agrupación k-means indicó que la variabilidad del Ψ_L estaba básicamente afectada por las propiedades del suelo. En ambos años, el viñedo se regó en la totalidad de sus necesidades hídricas (100% ETc). En estos dos años 2006 y 2007, ninguno de los dos métodos fue capaz de mejorar el C_v de la producción comparándolos con la zonificación ciega. En el 2009, se adoptó una estrategia de riego deficitario controlado (RDC), obteniendo una mayor variabilidad en Ψ_L y también en la producción. El método de zonificación basado en el Ψ_L redujo significativamente el coeficiente de variación cuando se adoptó una estrategia de RDC, pero en cambio el método del PCD no, a pesar de obtener una disminución del C_v del 16.7%. Cuando se adopte una estrategia de RDC, recomendamos zonificar los sectores de riego en utilizando el método del Ψ_L.

Introduction

In semi-arid regions of the Mediterranean basin efficient irrigation management is necessary to obtain high quality grapes. There is current interest in obtaining homogeneity in terms of yield and berry composition within vineyards. Grapevine water status has a direct effect on yield (e.g. Intrigliolo and Castel 2010) and on berry composition (e.g. Basile et al. 2011) but soil physical properties are deemed as being foremost important in causing spatial variability. Soil properties may influence grapevine water status if irrigation requirements are not met. Differences in yield (Bramley and Hamilton 2004) and berry composition (Bramley 2005) have been reported across irrigated vineyards. Variability in canopy vigour, yield, and fruit composition within a vineyard can be the result of grapevines responding differently to the same irrigation protocol across different vineyard zones. Designing an irrigation system without taking into account spatial variability of the soil and plant water status can potentially increase variability in yield and berry composition across a vineyard. A widespread problem in many vineyards is that awareness of the faulty irrigation design happens after the system is set up.

The problem of variability within a vineyard has sometimes been addressed by splitting the block into several individual plots and treating each plot as a single management unit for cultivation and harvest (Bramley and Lamb 2003; Bramley and Hamilton 2004; Johnson et al. 2001). Another approach is applying different irrigation amounts in various zones of a vineyard. For instance, Proffitt and Malcolm (2005) managed irrigation in vigorous areas differently from less vigorous areas in order to reduce vegetative growth in the former. Information about the causes of spatial vineyard variability was provided by Ortega et al. (2003) and Taylor et al. (2005). But information is scant about the use of a tool capable of re-designing irrigation zones of a vineyard for achieving uniformity in yield and berry composition. Only Martinez-Casasnovas et al. (2009) proposed a method for re-defining irrigation management zones according to within-field variability using yield, soil properties, and vegetative indices obtained from multispectral images.

Irrigation design based on soil properties is costly and requires a large number of sampling. This study presents the alternative of using vine water status and spectral vegetative indices for re-defining irrigation zones. The measurement of leaf water potential (Ψ_L) with a pressure chamber has been used successfully for scheduling irrigation in vineyards (Girona et al. 2006). Remote sensing technology and geographic i*nformation systems* (GIS) are valuable tools for zonal irrigation designing within a vineyard. Spectral vegetative indices, such as normalized difference vegetation index (NDVI) and plant cell density (PCD), are obtained from multispectral images combining different wavelengths specifically in the blue, green, red and near infrared bands. Some authors have related these indices to yield (Arnó et al. 2005; Lamb et al. 2001; Martínez-Casasnovas et al. 2009), trunk diameter (Proffitt and Malcolm 2005), and vine water status (Acevedo-Opazo et al. 2008; Kriston-Vizi et al. 2008). However, studies are scant where these indices are used as tools to re-design irrigation zones within a vineyard. We know of no study that

demonstrated the usefulness of using these indices to diminish yield variability within a vineyard.

Our first aim was to study the influence of physical soil characteristics on the variability of vine water status within a 7.5-ha `Pinot noir´ vineyard. Then, the effectiveness of two methods proposed for re-designing irrigation zones (Ψ_L and PCD index) were compared for reducing yield variability within this vineyard. During the first two years the Ψ_L method was evaluated for fully irrigated conditions and in the third year both Ψ_L and PCD methods were evaluated when RDI was applied.

Materials and Methods

Study site

The study was conducted in a 16-year-old `Pinot noir´ (*Vitis vinifera* L.) vineyard during 2006, 2007 and 2009. The 7.5-ha commercial vineyard was located at 41º 39'N, 00º 30'E (WGS84, UTM zone 31N) in Raïmat, Lleida, Catalonia, Spain. Vines were planted 1.7 m apart in rows 3.1 m apart (1900 vine / ha). They were cordon-trained to an espalier type canopy system at a height of 0.9 m. Canopy dimensions were maintained by vertical shoot positioning in July and hedging shoots above the top wire twice during growing season. Irrigation system was divided into four regular sectors. Drip emitters were pressure compensating with a nominal flow of 3.7 l. h^{-1} and spaced 0.85 m apart. Uniformity coefficients of the emitter flows were calculated according to Burt (2004) and had an average of 82%.

Climatic conditions and irrigation strategies were different from year to year. Table 1.1 presents a summary of the main climatic variables and irrigation and crop coefficients used during the irrigation season. Much of the rainfall in 2007 and 2009 occurred during vegetative growth. Irrigation of the entire vineyard was managed by Raïmat winery, applying the same amount of water in each of the four sectors during three years. Irrigation season was from April to October. Frequency of irrigation was the same for the three years and varied from 3 days per week to 4 days per week. Crop evapotranspiration (ET_c) was calculated by multiplying ET_o (potential evapotranspiration) by irrigation coefficient (K_i).Values of K_i had been obtained by Raïmat winery in cooperation with the Irrigation Technology Department of IRTA (Xavier Bordes, Raïmat winery, personal communication) and were very similar to crop coefficients (K_c) proposed by Allen et al. (1998). In 2006 and 2007 full irrigation was applied while in 2009 regulated deficit irrigation (RDI) was implemented from mid June to the end of September. Details of the RDI application are given in Girona et al. (2006). In general, 66% of crop evapotranspiration was replaced by irrigation.

A total of 161 measurement locations were defined on a regular grid within the vineyard. Each location was geo-referenced with global positioning system (GPS) equipment according to the European Datum 1950.

Tabla 1.1. Summary of the main climatic variables during irrigation period (April – September) and crop coefficients (Kc) used for irrigation scheduling during the three years of experiment

			April	May	June	July	August	September
2006	Temp (Avg.)	℃	14.1	18.8	22.0	26.4	21.7	20.6
	T max	℃	26.8	34.7	35.1	37.9	33.2	27.5
	ET_o	mm	108.1	145.2	157.1	177.7	152.2	99.9
	Rainfall	mm	2.8	1.0	2.7	3.0	1.5	75.8
	Crop coefficient	(K_c)	0.15	0.40	0.65	0.60	0.60	0.54
2007	Temp (Avg.)	℃	13.9	17.6	21.3	23.5	22.7	19.1
	T max	℃	28.3	31.8	33.3	35.5	39.2	26.9
	ET_o	mm	88.3	139.7	153.7	176.5	142.7	103.8
	Rainfall	mm	76.5	21.5	24.4	1.6	1.4	11.0
	Crop coefficient	(K_c)	0.20	0.40	0.63	0.75	0.75	0.45
2009	Temp (Avg.)	℃	12.0	18.8	22.7	24.4	24.7	19.6
	T max	℃	25.6	31.6	36.3	36.0	36.6	27.0
	ET_o	mm	91.8	142.6	157.9	173.7	147.3	106.5
	Rainfall	mm	112.7	7.1	16.2	31.2	40.6	53.0
	Crop coefficient	(K_c)	0.20	0.33	0.55	0.45	0.35	0.25

Soil physical properties

A total of 81 soil profiles were dug within the regular grid of the vineyard in 2006. The following soil properties were studied: texture (percentages of sand, loam and clay), depth, concentration of organic matter (OM), electrical conductivity (EC_e) from the saturated paste extracts (1:2.5 ratio), pH, calcium carbonate equivalent (CC_{eq}), and soil water holding capacity (SWHC). The last parameter was determined following the recommendations of Richards (1965). In 2009 a topographic analysis in the vineyard was made, measuring the altitude in each spot using a real-time kinematic global positioning system (RTK-GPS) with a precision on the millimetric scale.

Vine water status

Leaf water potential (Ψ_L) was measured with a pressure chamber (Soil Moisture 3005, Soil Moisture Corp., Sta. Barbara, CA, USA) following the recommendations of Turner and Long (1980). All measurements were done at noon (1/2 hour on either side of solar noon) selecting a fully expanded leaf exposed to direct sunlight. Two teams of four technicians each were used so that all measurements were taken in less than one hour. A total of 161 Ψ_L measurements were taken, one measurement on each vine. In 2006, Ψ_L was measured on: 19 June, 14 and 31 July and 8 August. The measurements were taken on 26 June and 31 July in 2007. They were taken on 6 and 31 July in 2009. The seasonal value of Ψ_L for each location was estimated as the average of all daily measurements made over the season in that location.

Plant Cell Density (PCD) index measurements

PCD as cited by Bramley et al. (2003), was obtained from multispectral images (spectral reflectances at different wavelengths) as an indicator of plant canopy vigour. The PCD index was computed according to Equation 13:

$$\text{PCD} = \frac{\varphi_{NIR}}{\varphi_{RED}} \qquad\qquad (13)$$

where φ_{NIR} is the spectral reflectance at near-infrared (760-900 nm) and φ_{RED} is spectral reflectance at red (630-690 nm).

PCD was only measured in 2009 when the vineyard was deficit irrigated. On 15 July 2009 (maximum vegetative growth) a digital multi-spectral image (DMSI) of the vineyard was obtained with a light aircraft (CESSNA C172S EC-JYN) at an altitude of 1 km. The DMSI sensor collects data in four wavebands: infra-red, red, green and blue. The image resolution was 2048 x 2048 pixels with 14-bit digitization and optical focal length of 24-28 mm. All imagery was collected under a clear sky. The flight was made by RS Teledetección (Lleida, Spain) and imagery was processed by SpecTerra Services (Perth, WA, Australia). PCD maps ranging from 0 to 255 values and yielding a ground-based spatial resolution of 0.5 m were obtained enabling to distinguish pixels from vine vegetation to pixels dominated by non-vine features such as soil and inter-row vegetation.

Other measurements

Berry growth was measured by sampling 18 berries every two weeks at each measurement location from mid June to August each year. Berries were weighed in the laboratory to determine the average fresh weight (FW). Trunk diameter (TD) was measured at a height of 50 cm on each vine using a digital caliper (Mitutoyo Absolute 500-181-20; Mitutoyo Corporation, kawasaki, Japan) with a 0.01 mm resolution. Yield data

were acquired from a Canlink 3000 Farmscan monitor (Bentley, WA, Australia) installed above a mechanical grape harvester in 2006 and 2007. They were manually harvested in 2009.

Statistics and data presentation

Mapping variables and statistical analysis

Yield, Ψ_L and PCD maps were obtained interpolating all data by ordinary kriging method using the spherical semivariogram model and interpolating a total of nine neighboring points and obtaining a regular grid of 0.5 m by pixel. To determine both physical and biological parameters which could affect vine water status variability in the vineyard, a methodology which took into account the typology and number of available data was adopted for 2006 and 2007 data. Ψ_L data were classified using the multivariate k-means clustering analysis and obtaining three different areas: Low Ψ_L (L), Medium Ψ_L (M) and High Ψ_L (H). Using this methodology made it possible to convert Ψ_L maps (obtained by ordinary kriging) to reclassified conglomerate maps (three clusters). These analyses were carried out in ArcMap (version 9.3; ESRI Inc. Redlands, CA, USA) using the spatial analyst extension.

K-means clustering is a non-hierarchical method of data aggregation that minimizes the distances within the clusters whilst the Euclidean distance between clusters (i.e. distance between cluster centres) is maximized. K-means clustering has been successfully used in precision agriculture for the management of zones based on yield, elevation and soil electrical conductivity (Arnó 2009; Bramley and Hamilton 2004; Cuppit and Whelan 2001).

ANOVA was used for testing the significant differences in Ψ_L among the three clusters. It was also used to test whether the soil properties and vine attributes of each cluster differed from those of the other clusters. Furthermore, using the 2006 and 2007 data, regressions were done between Ψ_L and each of SWHC, soil depth, yield, and trunk diameter; using in all cases a quadratic model. Version 4.2 of SAS (SAS 2002) was used for statistical analyses.

Yield thresholds and analysis for proposed re-designing of irrigation zones

Yield thresholds in response to Ψ_L and PCD index were established in 2009 following three sequential steps: i) calculating boundary lines between yield and Ψ_L and PCD index according to the method of Schmidt et al. (2000) that was based on splitting data into groups, calculating boundary points for each group and finally fitting the boundary lines; ii) visually splitting the boundary lines into two different parts of different tendency that can be separated by a likely intersection point; and iii) using the non-linear regression

procedure (NLIN) from SAS following the Marquardt method to estimate the actual intersection point (threshold) and deriving the corresponding statistics (SAS 2002). PCD data were acquired from the averaged pixel values of each sampled location where Ψ_L was measured.

Three different methods of re-designing irrigation zones were used. A "blind" design was first made by splitting the block into eight regular zones of identical areas each being less than 1.6 ha. The other two proposed designs were based on measurements of Ψ_L and PCD index. Borders for zones in the last two designs were decided by grouping measured locations with similar characteristics. Proposed irrigation zones were initially formed by first including at least three adjacent measured locations under the same specific threshold. The establishment of these thresholds values was explained in the previous paragraph. New measured locations were included in the same irrigation zone if they were within the range specified by the threshold found for Ψ_L and PCD index. New defined zones were adjacent to other zones and not included in them.

The yield's coefficient of variation (C_v) for the years 2006, 2007, and 2009 were compared for the three methods of zonation (blind, Ψ_L and PCD). In 2006 and 2007, C_v of yield was obtained using the proposed irrigation re-designing of 2009. All map analysis and data acquisition was carried out with ArcMap (version 9.3; ESRI Inc. Redlands, CA, USA) using the spatial analyst extension. Statistical analysis was carried out using SAS version 4.2 (SAS 2002).

Results

Soil characteristics

The soil was silty-loam (USDA-SCS, 1975). There was a similar distribution of sand, silt, and clay with soil depth. Sand content showed the highest spatial C_v. The pH of the saturated paste from 81 soil samples averaged at 8.43 ± 0.03 (SE). Soil pH was slightly more basic in depth than in the top of the soil. Electrical conductivity (EC_e) of the saturated soil paste averaged at 0.49 ± 0.08 dS/m. There was no difference in EC_e between top soil and subsoil. The value (%) of calcium carbonate equivalent ($CC_{eq.}$) averaged at 28.05 ± 0.77 and was slightly lower in the top layer of the soil than in subsoil. The average concentration (%) of organic matter (OM) was 1.09 ± 0.05. OM in the top layers of soil was significantly higher than in the subsoil, reaching a maximum of 3.3 % in the former. Soil depth and soil water holding capacity (SWHC) co-varied significantly ($P < 0.0001$) with a coefficient of determination (r^2) of 0.61. No correlation was found between soil texture components (sand, silt and clay) and electrical conductivity (dS/m). However, the linear relationship between EC_e and pH was highly significant ($r^2 = 0.77$, $P < 0.0001$).

Analysis of Ψ_L variation

For 2006 and 2007 three clusters were identified based on Ψ_L. Table 1.2 shows averages of Ψ_L for these clusters that were significantly different in each of the two years (P < 0.0001). For 2006 the maximum value (MPa) of Ψ_L was -0.65 and the minimum value was -1.23. The corresponding values were -0.52 and -1.25 in 2007. Fig. 1.1 indicates that the pattern of within-vineyard Ψ_L variations was fairly stable from one year to the next. Zones with higher Ψ_L values were localized during both years at the north and south-eastern part of the block (yellow colour). Lower Ψ_L values were in the south and north-western part of the block (red colour). Fig. 1.1 (c & f), shows the Ψ_L map and clustering for both years indicating clearly the pattern of the three different clusters of vine water status. Soil and grapevine parameters were also stable between both years and most of them showed significant differences between clusters of Ψ_L (Table 1.2). Table 1.2 shows that soil texture parameters of silt and sand had no significant influence on Ψ_L variability for both years, but clay fraction did. Organic matter concentration had a significant influence on Ψ_L only in 2006 (P = 0.003) with higher values in well watered clusters. EC_e had a significant effect on Ψ_L block variability (P = 0.001) in both years. Areas with high EC_e were coincidental with areas of Low Ψ_L values. In 2006, pH was higher in high Ψ_L clusters. A significant effect on Ψ_L was found in both years with SWHC and soil depth (P < 0.0001). Differences in vine water status were related to differences in yield. In both years, yield was significantly different (P < 0.0001) among zones of Ψ_L, being lower where Ψ_L was low. Likewise, berry fresh weights at harvest and trunk diameter were significantly different (P < 0.0001) among Ψ_L clusters. Smaller berry size and lower trunk diameter were found in the most stressed zones. Elevation did not vary significantly in the vineyard.

Correlated parameters with yield

Fig. 1.2 shows quadratic relationships between yield and parameters that could be used for re-designing irrigation zones: Ψ_L, SWHC, TD and soil depth. Only Ψ_L and soil depth had highly significant relationship with yield (P < 0.0001). SWHC also had a significant relationship with yield (P = 0.0186) despite a very low r^2 of 0.052. TD and yield were not related. The polynomial regression indicated that high values of Ψ_L and soil depth corresponded with higher yields.
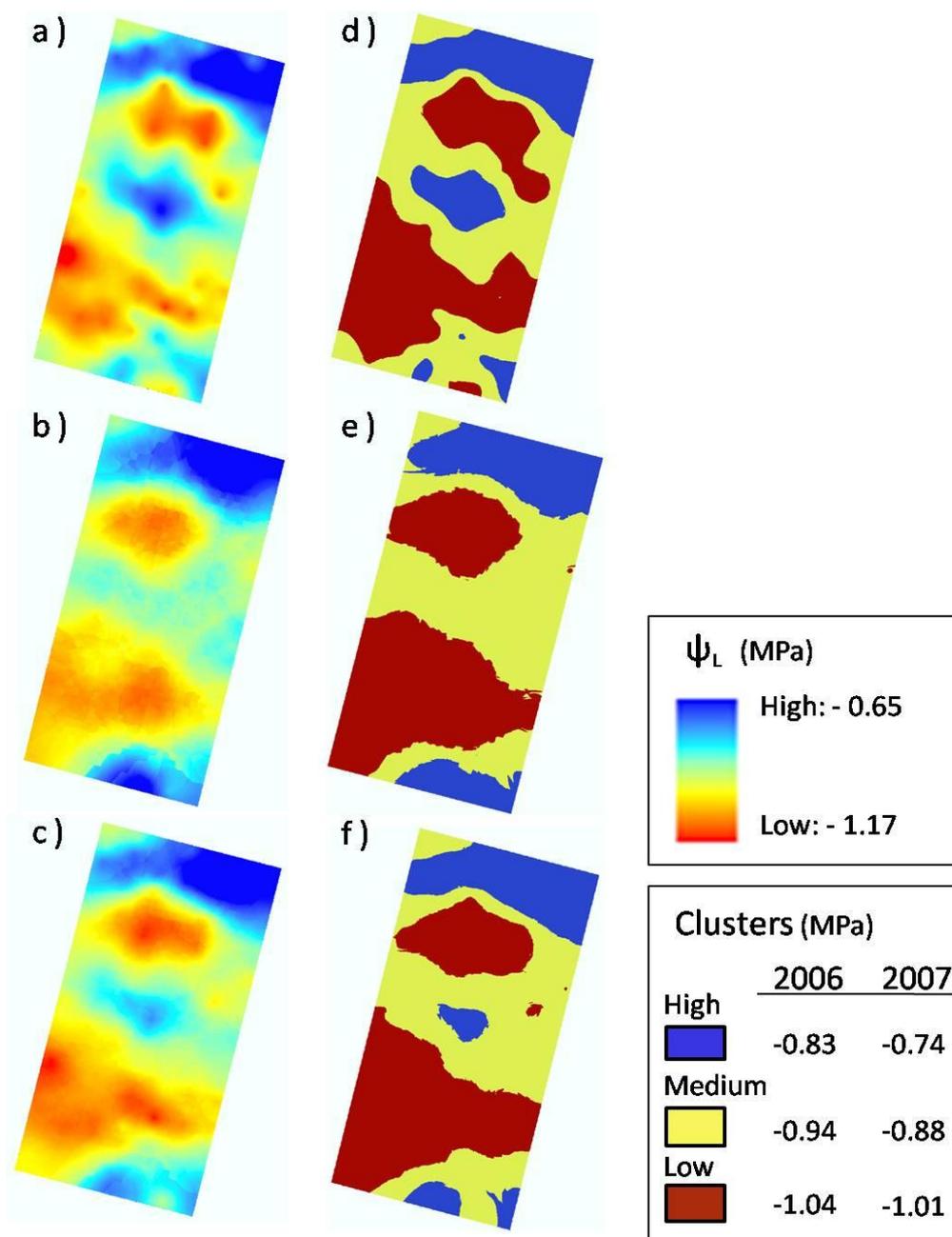
Figure 1.1. Maps of leaf water potential (Ψ_L) for High, Medium and Low clusters in 2006 (a, b), 2007 (c, d) and average of the 2 years (e, f)

Table 1.2. Multivariate k-means clustering analysis classifying soil and grapevine properties for high (H), medium (M) and low (L) weighted average of leaf water potential (WaΨ$_L$) zones in a 7.5-ha `Pinot noir´ vineyard for years 2006 and 2007. Means within column in each year followed by different letters were significantly different at *P* < 0.05 using Duncan test. The abbreviations are for: OM = organic matter, EC$_e$ = electrical conductivity, SWHC = soil water holding capacity, FW = fresh weight of berries at harvest, and TD = trunk diameter.

Zone	WaΨ$_L$ (MPa)	Clay (%)	Silt (%)	Sand (%)	OM (%)	EC$_e$ (dS/m)	pH (unitless)	SWHC (mm)	Depth (cm)	Elevation (m)	Yield (ton ha^{-1})	FW (g)	TD (mm)
Year 2006													
H	-0.83 a	25.46 a	54.01	25.53	1.16 a	0.39 b	8.47 a	143.03 a	160.03 a	282.62	13.72 a	1.34 a	53.86 a
M	-0.95 b	22.67 b	54.42	22.91	1.12 ab	0.44 b	8.39 b	124.81 ab	138.14 b	282.26	12.53 b	1.24 b	49.97 b
L	-1.04 c	24.84 a	55.22	20.19	1.06 b	0.63 a	8.37 b	113.59 b	121.86 c	281.68	12.59 b	1.14 c	50.40 b
P ≤	< .0001	0.009	n.s	n.s	0.003	0.001	0.0013	0.043	< .0001	n.s	< .0001	< .0001	0.001
Year 2007													
H	-0.74 a	25.82 a	54.23	19.69 b	1.14	0.37 b	8.44	152.37 a	172.35 a	282.08	16.74 a	1.28 a	56.01 a
M	-0.88 b	21.48 b	54.27	24.25 a	1.10	0.45 b	8.39	118.73 b	133.69 b	283.23	14.89 b	1.18 b	51.74 b
L	-1.01 c	25.46 a	55.06	19.69 b	1.09	0.56 a	8.40	112.47 b	112.47 b	281.41	13.41 c	1.09 c	51.79 b
P ≤	< .0001	< .0001	n.s	0.001	n.s	0.003	n.s	< .0001	< .0001	n.s	< .0001	< .0001	< .0001
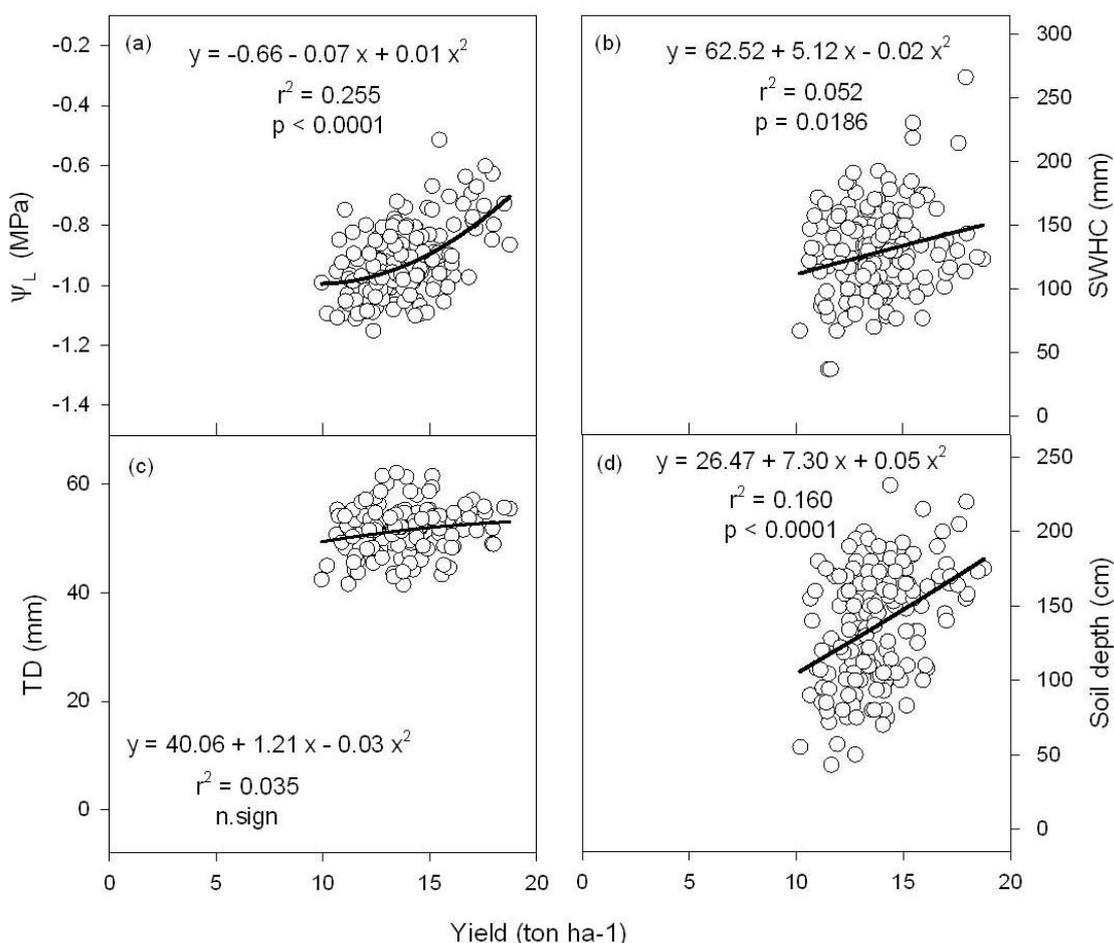
Figure 1.2. Relationships between yield and: a) leaf water potential (Ψ_L), b) soil water holding capacity (SWHC), c) trunk diameter (TD), and d) soil depth. The values are averages of 2006 and 2007 data.

Searching for yield thresholds

Yield response to Ψ_L was more marked in 2009 than in 2006 and 2007. Fig. 1.3a shows that Ψ_L values in 2009 had a large range, from -0.63 to -1.49 MPa. Therefore 2009 data were adopted for defining yield thresholds. Yield variability was also slightly higher that year reaching a maximum value of 23 and a minimum value of 4.7 ton ha^{-1}. The effect of water stress on yield followed a quadratic pattern with a maximum at highest Ψ_L value of -0.60 MPa (Fig. 1.3a). Vegetative growth, in terms of PCD index, also had a significant relationship with yield (Fig. 1.3b). Yield tended to decrease at PCD values lower than 196 (Fig. 1.3b). Thresholds found following the described methodology on boundary line and non-linear regression were slightly different, being -0.96 MPa for Ψ_L and 105 for PCD (Table 1.3). The relationship between Ψ_L and PCD index was quadratic (y= $75.31x^2+283.14x+326.26$; $r^2 = 0.39$, P < 0.0001).
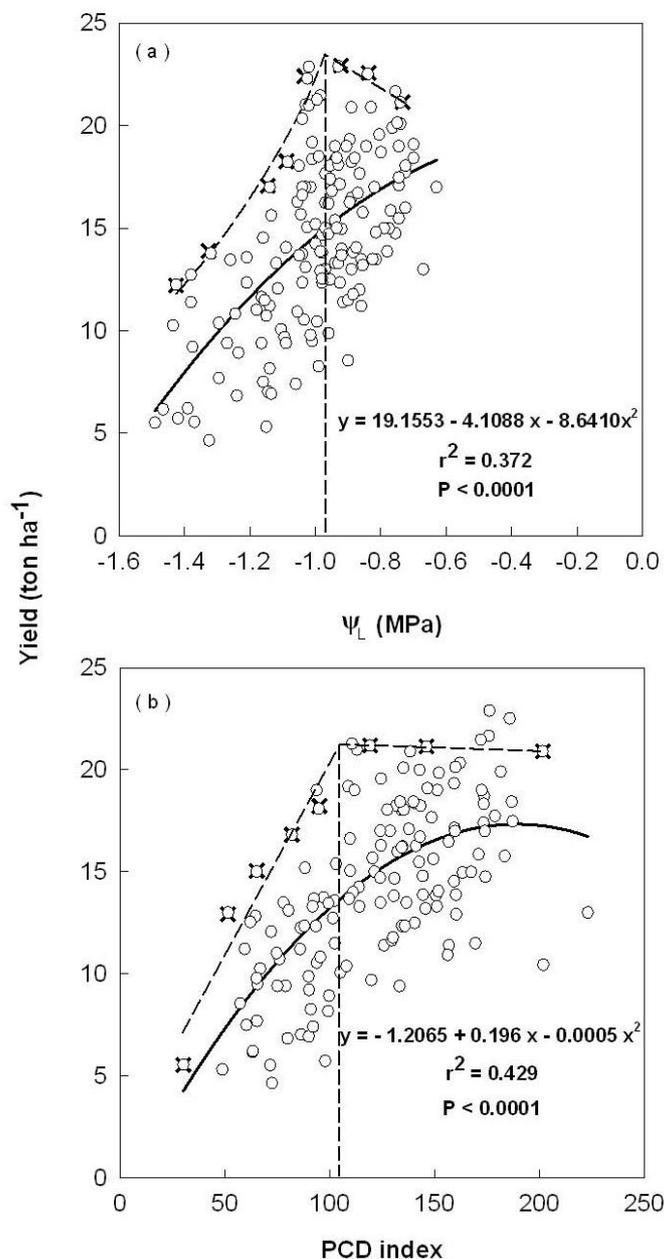
Figure 1.3. Relationships between yield and: a) leaf water potential (Ψ_L) and b) plant cell density (PCD) index in 2009. Broken lines are upper bound fitting. Two different responses are considered according to a two visually defined boundary line sections. The intersection between these sections is obtained from non-linear regression statistics protocol and show the threshold in which yield starts to decline in response to the considered factor.

Table 1.3. Boundary lines statistics for irrigation zonation based on PCD and Ψ_L according to yield responses in 2009. Thresholds of yield responses were estimated by using non-linear regression (NLIN) following Marquardt method (SAS, 2002)

Method	Interval	Boundary equations	Threshold	Std Error	95% Confidence Limits		Pr > F
PCD	x<105.2	$y = 0.187x + 1.567$	105.2	9.85	77.85	132.6	0.0035
	x>105.2	$y = -0.004x + 21.632$					
Ψ_L	x<-0.96	$y = 88.338 \times e^{1.398x}$	-0.96	0.03	-1.05	-0.87	<.0001
	x>-0.96	$y = -9.674x + 14.178$					

Thresholds of yield responses were estimated by using nonlinear regression (NLIN) following Marquardt method (SAS 2002)

Proposed re-designing of irrigation zones

A proposal of eight re-formulated irrigation zones is presented in Fig. 1.4. Areas (ha) of irrigation zones 1 to 8, proposed on the basis of Ψ_L values and marked in Fig. 4c, were respectively: 0.65, 0.94, 0.74, 1.57, 1.56, 0.73, 0.52 and 0.76. Areas of irrigation zones based on PCD index were 0.70, 0.79, 1.16, 1.06, 0.68, 0.86, 1.28 and 0.94 ha for zones 1-8, respectively (Fig. 1.4e). A statistical analysis comparing C_v of yield for both methods compared to the blind irrigation zone design (Fig. 1.4a) indicated no significant differences in 2006 and 2007. There were significant differences among the three methods (P = 0.046) in 2009. For 2009 the blind irrigation zones had the greatest yield variability. Re-designing of irrigation zones based on PCD index maps slightly reduced C_v of yield to around 16.7%. But the yield in PCD-based zones did not significantly differ from those of blind zones. The method based on Ψ_L had significant differences with the blind method by reducing yield variability to around 26.5 %. Within-vineyard yield variability increased over the three years reaching maximum C_v values in the last year because of RDI application (Table 1.4).

Discussion

Implications of vineyard spatial variability

Spatial variability in vineyards is mostly effected by vine water status and soil physical properties. However, the influence of soil properties on grapevine can be different between irrigated and non-irrigated plots. In non-irrigated plots, soil characteristics have an important impact on grapevine water status and as a consequence on yield and fruit composition (Morlat and Bodin 2006; Van Leeuwen et al. 2004). In irrigated vineyards effects of soil properties on vine water status should not be as marked because water supply to the plant is guaranteed by the irrigation and less from water reservoir in the soil.

The first step in our zonation attempt was to search for a criterion based on which spatial variability of yield could be explained. Candidate parameters were Ψ_L, soil depth, SWHC, and TD (Fig.1.2). Because only Ψ_L and soil depth were statistically related to the yield, the other parameters were not considered. Soil depth had the inconvenience of requiring a large number of sampling. Moreover, the effect of soil depth on yield will be subdued under irrigation. Ψ_L seemed to be the best candidate in terms of correlation to yield, though its determination has the problem of having to perform a large number of manual measurements within a short time either at midday or at predawn. Despite this practical limitation, Ψ_L was adopted as a parameter to study yield heterogeneity by cluster analysis.

The k-means clustering analysis of Table 1.2 indicated that variability in Ψ_L affected the yield and in turn was influenced by different soil properties. Differences in soil depth and SWHC could have led to differences in the volume of soil that roots could have explored, increasing the volume of plant available water that could have positive impact on yield. In fact, a significant relationship was found between soil depth and Ψ_L and between soil depth and yield in 2006 and 2007. Soil EC_e can be influenced by both static and changing factors including water quality, soil texture, mineralogy, soil water content, bulk density and temperature (Friedman 2005; Fulton et al. 2010; Johnson et al. 2003). The EC_e content here was related to the soil and not to water which was of a good quality according to the standards defined by Ayers et al. (1985) (data not shown). Some studies have explored soil EC_e as an indicator of soil texture for mapping vineyard spatial variability based on soil texture (Corwin and Lesch 2005; Fulton et al. 2010). However, in our study EC_e was significantly related only to silt content. C_v for EC_e was high which means that areas with maximum EC_e values of 2.0 dS/m could have had limited root water uptake and in some zones within the vineyard vines could be exposed to incipient saline conditions. But this was only observed for a limited number of locations and in the top layers. Higher EC_e and lower yields corresponded with more stressed zones (Table 1.2). So the effect of EC_e, if any, is confounded by the reduction in soil water content.

Cluster analysis of 2006 and 2007 data, based on three vine water status levels, allowed to distinguish the most water stressed parts (47 % of the area) of the block from the less

stressed parts (24 % of the area). These areas showed a temporal stability of grapevine Ψ_L (Fig. 1.1). This temporal stability means that low and high grapevine water status zones remained located in the same part of the block over the three years of study. Probably because of the influence that vine water status had on yield, these results were similar to those of Bramley and Hamilton (2004) who found temporal stability in the pattern of within-vineyard yield. However, due to different climatic conditions and irrigation strategies adopted between the three years (e.g. RDI applied only in 2009), Ψ_L values presented significant differences among years.

The use of remote sensing imagery in 2009 made it possible to explore the PCD as an alternative for the basis of re-designing irrigation zones. The 2009 data indicated the existence of significant relationships (P < 0.0001), despite low r^2 values, between PCD index and other measured parameters such as Ψ_L ($r^2 = 0.39$), soil depth ($r^2 = 0.26$), SWHC ($r^2 = 0.24$), and TD ($r^2 = 0.39$). Proffitt and Malcolm (2005) reported a significant relationship between PCD index and trunk circumference ($r^2 = 0.72$, P < 0.01). Acevedo-Opazo et al. (2008) demonstrated that significant differences existed in pre-dawn Ψ_L between the highest and lowest canopy vegetative zones of a vineyard based on multispectral images. Basically, and in agreement with Dobrowski et al. (2003), the PCD index gives information about the plant vegetative vigour although vegetative vigour is highly dependent on plant water status (Koundouras et al. 2008). Thus, this significant relationship between PCD index and Ψ_L demonstrated that vine vegetative growth was at least partially affected by vine water status. It was therefore justified to compare both related methods as a possible tool for re-designing irrigation zones with the aim of trying to reduce yield variability.

Proposal for re-designing irrigation zones

The use of RDI in 2009 increased yield variability compared to previous years. We think this higher variability was due to water stress in vines growing in zones with shallower soils. This is similar to what Lampinen et al. (1995) found when comparing different soil types under RDI. Maximum yield in 2009 was higher than those in 2006 and 2007. Besides the natural year-to-year variation of yield, the higher rainfall in 2009 for April could have made a contribution (Table 1.1). Fig. 3a shows that yield losses started from a threshold Ψ_L value of -0.96 MPa. Yield was reduced to 79% when a value of -1.49 MPa was reached. Adoption of RDI therefore increased within-vineyard yield variability. Vegetative growth differences measured with PCD index were also significantly related with yield variability. Yield losses were observed at PCD values below 105 (Fig. 1.3b).

Proposed designing of irrigation zones based on three methods (blind, Ψ_L and PCD) caused significant differences in yield between the two irrigation strategies of full irrigation (in 2006 and 2007) and RDI (2009). Results shown in Table 1.4 for years 2006 and 2007 demonstrate that yield uniformity was higher in all proposed irrigation zones when vineyard was fully irrigated and no significant improvement on reducing yield variability was found by applying either Ψ_L or PCD methods for zoning. The analysis in

Table 1.4 assumes that the spatial variation of PCD was the same in the three years of study although it was measured only in 2009. The best tool for re-designing irrigation zones in 2009 was on the basis of Ψ_L which significantly reduced yield variability with respect to a blind zonation. In all cases, except in the proposed irrigation zones 3 and 5, the Ψ_L method presented a significant decrease in C_v of yield. PCD method did not reduce C_v significantly compared to the blind method. In certain conditions PCD may not be correlated to Ψ_L. Examples could be found in the proposed irrigation zones 3, 5, 6, 7 and 8 (Fig. 1.4). In locations where vegetative vigour is high (high PCD) transpiration also increases and it may happen that water supply is not enough for that location as compared to vines with lower vigour in other locations (Williams et al. 2003). This will lead to lower Ψ_L in the grapevine due to increased water loss through transpiration (Rossouw, 2010). This would be true for proposed irrigation zones 6 and 8 (Fig. 1.4). Secondly, it was demonstrated that these vegetative indices could be affected by crop management practices such as pruning or differences in vine training systems (vertical shoot positioning). In those cases quantity of near infrared leaf reflectance and PCD values would be reduced, but plant water status would have been improved by the accompanied reduction in transpiration (e.g. proposed irrigation zones 3, 5 and 7).

The results of this study indicated that although differences in soil characteristics within the vineyard existed and affected vine water status, a new design of irrigation zones based on soil characteristics may not always be justified if full irrigation is applied. However, the adoption of RDI may exacerbate the influence of low water available in the soil on plant water status and the zonation will be worthwhile. The usefulness and efficiency of this approach will require further evaluation. Girona et al. (2006) demonstrated a reduction of yield and berry fresh weight variability by irrigating each elemental plot independently by using Ψ_L as a plant-based indicator. According to their results, it is expected that yield variability within the block would be lower than what we have found if each proposed zone had been irrigated independently. Moreover, some studies have demonstrated the effect of Ψ_L on berry composition (e.g. Basile et al. 2011). Our perception from this study is that re-designing irrigation zones on the basis of vine water status and using Ψ_L measurements as a tool for irrigation in each proposed irrigation zone could be the most appropriate alternative for obtaining uniformity of yield and possibly for improving berry composition within the vineyard under deficit irrigation.
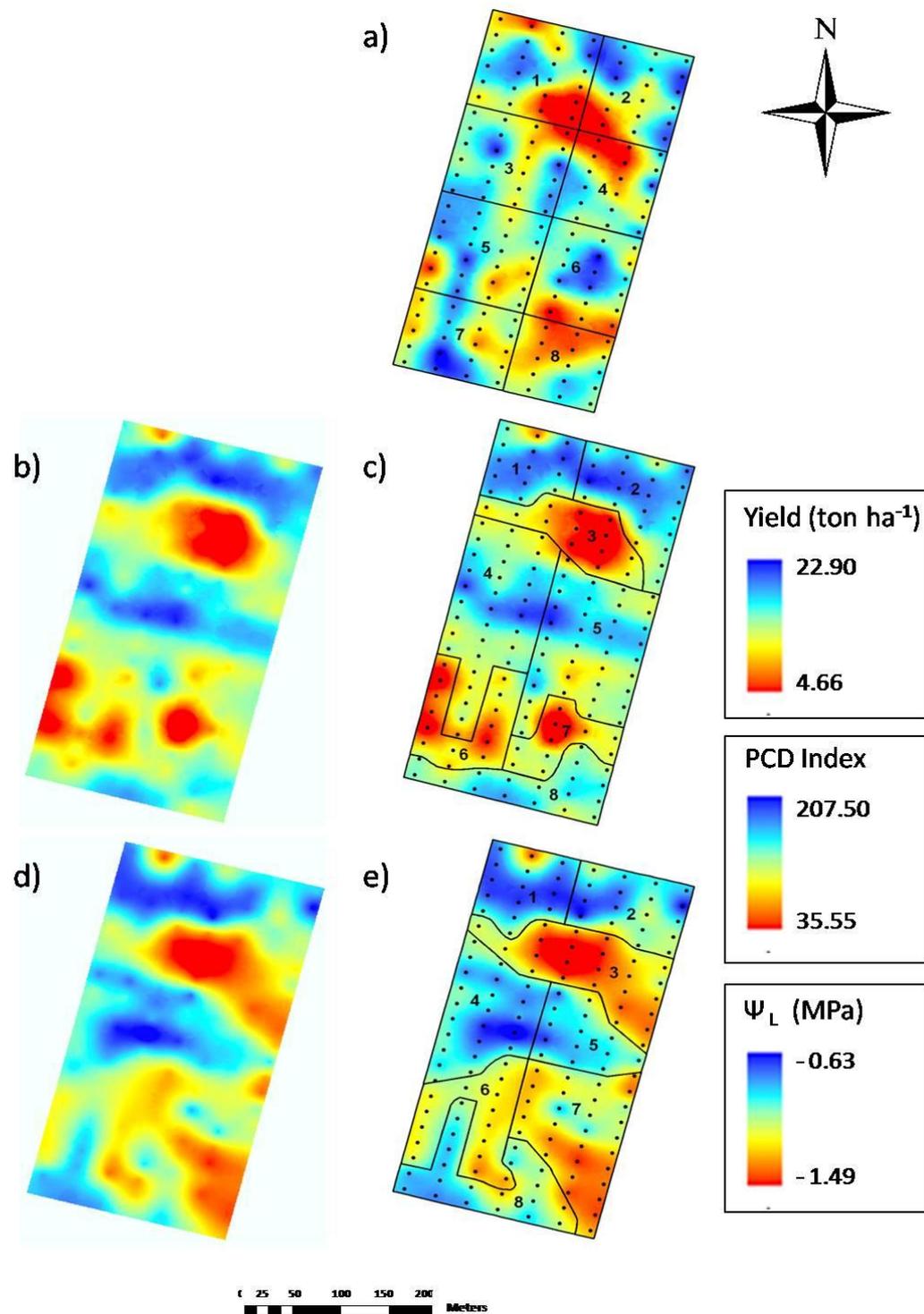
Figure 1.4. Maps of: a) yield, b) leaf water potential (Ψ_L), and d) plant cell density index (PCD); and proposed re-designing of irrigation zones based on a) blind c) Ψ_L and e) PCD in 2009. Points in bold show the 161 measurement locations in the vineyard.

Table 1.4. Comparison of yield variability in terms of coefficient of variation (C_v) in the proposed re-designs of irrigation zones, comparing a blind design with plant cell density index (PCD) and leaf water potential (Ψ_L) during the three years of study. For 2009 different letters following average values indicate significant differences at P < 0.05 using Duncan's test. There were no significant differences in average values in 2006 and in 2007. C_v of yield in 2006 and 2007 was obtained using the proposed re-designing of irrigation zones in 2009.

Irrigation zones	C_v of yield (2006)			C_v of yield (2007)			C_v of yield (2009)		
	Blind	Ψ_L	PCD	Blind	Ψ_L	PCD	Blind	Ψ_L	PCD
1	12.29	5.80	7.36	20.34	19.71	19.75	35.71	13.17	14.84
2	8.59	7.78	7.53	15.88	15.62	11.94	27.94	21.68	22.49
3	8.69	6.69	8.49	15.41	26.24	22.81	26.72	27.89	37.47
4	5.81	9.92	8.84	18.03	16.34	13.82	32.53	18.36	18.44
5	5.87	8.17	6.27	17.73	13.33	11.49	24.30	22.12	16.35
6	5.29	9.65	6.89	14.33	17.86	19.26	31.93	25.25	31.03
7	8.44	14.70	7.82	15.24	15.81	16.51	25.22	19.31	30.72
8	9.12	8.45	8.70	18.21	19.52	16.49	27.96	23.18	22.06
Avg ± SE	8.01 ± 0.82	8.90 ± 0.96	7.74 ± 0.32	16.90 ± 0.71	18.05 ± 1.39	16.51 ± 1.41	29.04 ± 1.40 a	21.37 ± 1.59 b	24.18 ± 2.85 ab
Significance	n.s.			n.s.			0.0460		

For 2009, different letters following average values indicate significant differences at P < 0.05 using Duncan's test. There were no significant differences in average values in 2006 and in 2007. Cv of yield for the 2006 and 2007 data was obtained using the proposed re-designing of irrigation zones in 200

Conclusions

Spatial variability of vine water status within vineyard was consistent over the three years of study and was mainly affected by soil properties such as depth, SWHC and EC_e. Yield was considered the most affected by vine water status variability. However, a simulation on re-designing irrigation zones based on Ψ_L when full irrigation was applied did not significantly reduce C_v of yield. But C_v of yield was reduced when RDI was applied.

Re-designing irrigation zones based on the PCD index did not significantly decrease yield variability. But we propose the feasibility of this technology be explored in further work.

References

Acevedo-Opazo, C., Tisseyre, B., Guillaume, S., Ojeda, H (2008) The potential of high spatial resolution information to define within-vineyard zones related to vine water status. Precision Agriculture 9:285-302

Allen, R.G., Pereira, L.S., Raes, D., Smith, M (1998) Crop evepotranspiration. Guidelines for computing crop water requirements. FAO Irrigation and Drainage paper nº56, pp 300

Arnó, J., Martínez-Casasnovas, J.A., Blanco, R., Bordes, X., Esteve, J (2005) Viticultura de precisión en Raïmat (Lleida): experiencias durante el periodo 2002-2004. ACE, Revista de enología, 64

Arnó, J (2009) Una investigación sobre la variabilidad intraparcelaria en viña y el uso de sensores láser en viticultura de precisión. phD, University of Lleida (Spain)

Ayers, R.S., Wescot, D.W (1985) Water quality for agriculture. FAO Irrigation and Drainage paper nº 29, rev.1

Basile, B., Marsal, J., Mata, M., Vallverdú, X., Bellvert, J., Girona, J (2011) Phenological sensitivity of Cabernet Sauvignon to water stress: vine physiology and berry composition. American Journal of Enology and Viticulture, AJEV-D-11-00003R1 (in-press)

Bramley, R.G.V., Lamb, D.W (2003) Making sense of vineyard variability in Australia. In: Precision Viticulture. Proceedings of the IX Congreso Latinoamericano de Viticultura y Enología, Santiago, Chile, pp 35-44

Bramley, R.G.V, Pearse, B., Chamberlain, P (2003) Being Profitable Precisely – a case study of Precision Viticulture from Margaret River. Australian and New Zealand Grapegrower and Winemaker – Annual Technical Issue, 473a, pp 84-87

Bramley, R.G.V., Hamilton, R.P (2004) Understanding variability in winegrape production systems: 1. within vineyard variation in yield over several vintages. Australian Journal of Grape and Wine Research 10:32-45

Bramley, R.G.V (2005) Understanding variability in winegrape production systems: 2. Within vineyard variation in quality over several vintages. Australian Journal of Grape and Wine Research 11:33-42

Burt, C.M (2004) Rapid field evaluation of drip and microspray distribution uniformity. Irrigation and drainage systems 18: 275-297

Corwin, D.L., Lesch, S.M (2005) Apparent soil electrical conductivity measurement in agriculture. Comput Electron Agric 46:11–43

Cuppitt, J., Whelan, B.M (2001) Determinig potential within-field crop management zones. In: ECPA 2011 – 3rd European Conference on Precision Agriculture. Vol 1. Eds. S. Blackmore and G. Grenier (agro Montpellier, Ecole Nationale Superieure Agronomique de Montpellier: France), pp 7-12

Dobrowski, S.Z., Ustin, S.L., Wolpert, J.A (2003) Grapevine dormant pruning weight prediction using remotely sensed data. Australian Journal of Grape and Wine Research 9:177-182

Friedman, S.P (2005) Soil properties influencing apparent electrical conductivity: a review. Comput Electron Agric 46:45–70

Fulton, A., Schwankl, L., Lynn, K., Lampinen, B., Edstrom, J., Prichard, T (2010) Using EM and VERIS technology to assess land suitability for orchard and vineyard development. Irrig Sci. DOI 10.1007/s00271-010-0253-1

Girona, J., Mata, M., del Campo, J., Arbonés, A., Bartra, E., Marsal, J (2006) The use of midday leaf water potential for scheduling deficit irrigation in vineyards. Irrigation Science 24:115-127

Girona, J., Marsal, J., Mata, M., del Campo, J., Basile, B (2009) Phenological sensitivity of berry growth and quality of "Tempranillo" grapevines (Vitis vinífera L.) to water stress. Australian Journal of Grape and Wine Research 15:268-277

Grimes, D.W., Williams, L.E (1990) Irrigation effects on plant water relations and productivity of 'Thompson Seedless' grapevines. Crop Sci. 30:255–60.

Intrigliolo, D., Castel, J.R (2009) Response of grapevine cv. 'Tempranillo' to timing and amount of irrigation: water relations, vine growth, yield and berry and wine composition. Irrig Sci. DOI 10.1007/s00271-009-0164-1

Johnson, L.F., Bosch, D.F., Williams, D.C., Lobitz, B.M (2001) Remote sensing of vineyard management zones implications for wine quality. Applied Engineering in Agriculture. Vol. 17:4:557-560

Johnson, C.K., Mortensen, D.A., Wienhold, B.J., Shanahan, J.F., Doran, J.W (2003) Site-specific management zones based upon soil electrical conductivity in a semiarid cropping system. Agron J 95:303–315

Koundouras, S.*,* Tisialtas, I.T.*,* Zioziou, E., Nikolaou, N *(*2008*)* Rootstock effects on the adaptive strategies of grapevine (*Vitis vinifera* L. cv. Cabernet Sauvignon) under contrasting water status: leaf physiological and structural responses. Agriculture, Ecosystems and Environment 128:86–96

Kriston-Vizi, J., Umeda, M., Miyamoto, K (2008) Assessment of the water stress status of mandarin and peach canopies using visible multispectral imagery. Bio-systems Engineering 100:338-345

Lamb, D., Hall, A., Louis, J (2001) Airborne remote sensing of vines for canopy variability and productivity. Australian Grapegrower and Winemaker 449:89-92

Lampinen, B.D., Shackel, K.A., Southwick, S.M., Olson, B., Yeager, J,T., Goldhamer, D (1995) Sensitivity of yield and fruit-quality of French prune to water-deprivation at different fruit-growth stages. Journal of the American Society for Horticultural Science 120:2:139-147

Martinez – Casasnovas, J.A., Vallés, D., Ramos, M.C (2009) Irrigation management zones for precision viticulture according to intra-field variability. EFITA conferences, pp 523-529

Morlat, R., Bodin, F (2006) Characterization of viticultural terroirs using a simple field model based on soil depth – II. Validation of the grape yield and berry quality in the Anjou vineyard (France) Plant and Soil 281:55-69

Myers, B.J (1988) Water-stress integral – a link between short-term stress and long-term growth. Tree physiology 4:4:315-323

Ortega, R., Esser, A., Santibañes, O (2003) Spatial variability of wine grape yield and quality in Chilean vineyards: economic and environmental impacts. Proceedings of the 4th European conference on precision agriculture, Berlin, Germany, pp 499-506

Proffitt, T., Malcolm, A (2005) Zonal vineyard management through airborne remote sensing. Australian & New Zeland Grapegrower & Winemarker 502:22-27

Richards, L.A (1965) Physical conditions of water in soil. Methods of soil analysis. Agronomy nº 9, American Society of Agronomy, Madison, WI, USA, pp 128-152

Rossouw, G.C (2010) The effect of within-vineyard variability in vigour and water status on carbon discrimination in Vitis vinifera L. cv Merlot. Thesis at Stellenbosch University, department of viticulture and oenology, Faculty of AgriSciences

SAS (2002) Enterprise Guide version 4.2 (SAS Institute Inc. Cary, NC, USA)

Schmidt, U., Hanspeter, T., kaupenjohann, M (2000) Using boundary line approach to analyze N_2O flux data from agricultural soils. Nutrient Cycling in Agroecosystems 57: 119-129

Taylor, J., Tisseyre, B., Bramley, R., Reid, A (2005) A comparison of the spatial variability of vineyard yield in European and Australian production systems. Proceedings of the 5th European conference on precision agriculture, pp 907-915

Turner, N.C., Long, M.J (1980) Errors arising from rapid water loss in the measurement of leaf water potential by pressure chamber technique. Austr J Plant Physiol. 7:527-537

USDA-SCS (1975) Soil Taxonomy: A Basic System of Soil Classification for Making and Interpreting Soil Surveys. U.S. Dept. of Agric. Handb. 436. U.S. Govt. Print. Off. Washington, DC. pp 754

Van Leeuwen, C., Fraint, P., Choné, X., Tregoat, O., Koundouras, S., Dubourdieu, D (2004) Influence of climate, soil, and cultivar on terroir. Am. J. Enol. Viticulture 55:207–217

Williams, L.E., Phene, C.J., Grimes, D.W., Trout, T.J (2003) Water use of mature Thompson Seedless grapevines in California. Irrigation Science 22:11-18

Capítulo 2

Mapping crop water stress index in a `Pinot-noir´ vineyard: comparing ground measurements with thermal remote sensing imagery from an unmanned aerial vehicle

J. Bellvert[a], P.J. Zarco-Tejada[b], J. Girona[a], E. Fereres[b,c]

[a]*Programa Uso eficiente del agua, Institut de Recerca i Tecnologia Agroalimentàries (IRTA), Centre UdL-IRTA, 191 Av. Rovira Roure, 25198 Lleida*

[b]*Instituto de Agricultura Sostenible (IAS), Consejo Superior de Investigaciones Científicas (CSIC), Córdoba*

[c]*Departamento de Agronomía, Universidad de Córdoba (UCO), Córdoba*

Abstract Characterizing the spatial variability in water status across vineyards is a prerequisite for precision irrigation. The crop water stress index (CWSI) indicator was used to map the spatial variability in water deficits across an 11-ha `Pinot noir´ vineyard. CWSI was determined based on canopy temperatures measured with infrared temperature sensors placed on top of well-watered and water-stressed grapevines in 2009 and 2010. CWSI was correlated with leaf water potential (Ψ_L) ($R^2 = 0.83$). This correlation was also tested with results from high resolution airborne thermal imagery. An unmanned aerial vehicle equipped with a thermal camera was flown over the vineyard at 07:30, 09:30, and 12:30 h (solar time) on 31 July 2009. At about the same time, Ψ_L was measured in 184 grapevines. The image obtained at 07:30 was not useful because it was not possible to separate soil from canopy temperatures. Using the airborne data, the correlation between CWSI and Ψ_L had an R^2 value of 0.46 at 09:30 h and of 0.71 at 12:30 h, suggesting that the latter was the more favorable time for obtaining thermal images that were linked with Ψ_L values. A sensitivity analysis of varying pixel size showed that a 0.3 m pixel was needed for precise CWSI mapping. The CWSI maps thus obtained by airborne thermal imagery were effective in assessing the spatial variability of water stress across the vineyard.

Resumen   La caracterización de la variabilidad espacial del estado hídrico de un viñedo es un prerrequisito para el riego de precisión. El indicador crop water stress index (CWSI) se utilizó para mapear la variabilidad espacial del estrés hídrico en un viñedo de 11-ha de `Pinot-noir´. En los años 2009 y 2010, se determinó el CWSI en base a la medida de la temperatura de la cubierta vegetativa de viñas regadas en la totalidad de sus necesidades hídricas y viñas estresadas, utilizando sensores de temperatura infrarrojo . El CWSI se relacionó con el potencial hídrico foliar (Ψ_L) ($R^2 = 0.83$). Ésta correlación también se evaluó con imágenes térmicas aéreas de alta resolución. El día 31 de Julio del 2009, un vehículo aéreo no tripulado, equipado con una cámara térmica voló por encima de un viñedo a las 07:30, 09:30, y 12:30 h (hora solar). En el mismo momento, se midió el Ψ_L en 184 viñas. La imágen obtenida a las 07:30 se descartó porque no fue posible discriminar entre la temperatura del suelo y la de la vegetación. Con los datos aéreos, la correlación entre CWSI y Ψ_L presentó un R^2 de 0.46 a las 09:30 h y de 0.71 a las 12:30 h, sugeriendo que el momento más favorable para obtener imágenes térmicas que se relacionen con el estado hídrico de la viña es alrededor del mediodía. Un análisis de sensibilidad que consistió en variar el tamaño del píxel mostró que para obtener mapas de CWSI con suficiente precisión es necesario adquirir píxeles de 0.3 m. Así, la evalución de la variabilidad espacial del estrés hídrico de viñedos con mapas de CWSI obtenidos con imágenes térmicas aéreas resultó efectiva.

Introduction

Spatial variability in water requirements across a field limits the efficient use of irrigation water. Uniform irrigation across a variable field will result in unintended water stress in some parts with overwatering in others. Water may therefore be wasted in both cases and for winegrapes this has important implications regarding berry composition (Basile et al., 2011). It is thus imperative that spatial variability be characterized before irrigation can be judiciously applied. Efficient use of irrigation water is especially important for grapevines as they occupy the highest area of any fruit crop in the world (FAO, 2010). Four criteria have so far been used for identifying spatial variability across vineyards: soil properties (Wetterlind et al., 2008; Fulton et al., 2011), yield (Bramley and Hamilton, 2004; Martinez-Casasnovas et al., 2009), spectral vegetation indexes (Bramley et al., 2005; Acevedo-Opazo et al., 2008a), and vine water status (Bellvert et al., 2012; Acevedo-Opazo et al., 2008b).

Mapping spatial variability on the basis of the above criteria has some constraints. Using soil properties requires collection of large number of samples which is costly. Yield is not only affected by soil spatial variability, but also by cultural practices. Spectral vegetation indices are sensitive to vine vigour, so they are highly affected by cultural practices including fertilization and pruning methods. Measurement of leaf water potential (Ψ_L) using a pressure chamber is time consuming and costly. An alternative was therefore explored by measuring crop water stress index (CWSI) (Idso et al., 1981) which has shown a strong relationship with Ψ_L in grapevine (Möller et al., 2007). Determination of CWSI requires the measurement of three environmental variables: canopy temperature (T_c), air temperature (T_a) and vapour pressure deficit (VPD).Temperature has so far been mostly measured with infrared temperature sensors or with thermal images taken from near ground level (Jones et al., 2002; Zia et al. 2009). However, the advent of modern remote sensing technology offers the possibility of inexpensive and precise airborne measurements. An example is using thermal imaging sensors onboard unmanned aerial vehicles (UAV; Berni et al., 2009a). As far as the authors know, the use of this technology for determining CWSI has not been explored for grapevines.

The aim of the study was to map CWSI across a vineyard using airborne imaging from a UAV as well as comparing these results to ground measurements of CWSI and Ψ_L. The objectives were to determine: i) the most favorable spatial resolution for imaging, in terms of pixel size, for the highest accuracy; and, ii) the best time of day for data collection and mapping. Most grape growing areas which require irrigation have immediate access to the information arising from airborne remote sensing. Examples include sites in Europe, South Africa, USA and Australasia. Ground measurements, as described here, are possible in other areas. Results of this research could therefore be useful to most grapevine growing areas where judicious irrigation across a variable field is needed to optimise grape yield and quality.

Materials and Methods

The study was carried out during the 2009 and 2010 growing seasons in an 11-ha `Pinot noir´ (*Vitis vinifera L.*) commercial vineyard located in Raimat (41º 39'N, 00º 30'E), Lleida, Spain. The vines were 16 years old and planted 1.7 m apart along 3.1 m rows (1900 vines ha^{-1}) with north-south row orientation. They were cordon-trained to an espalier type canopy system at a height of 0.9 m. Width of the canopy ranged from 0.25 to 0.80 m. Canopy management practices aimed to produce high-quality grapes by limiting canopy growth and by vertical shoot positioning in July. The soil was of silty-loam texture and variable in depth, ranging from 0.60 to 1.90 m. Climate of the area is Mediterranean, and the annual rainfall was 411 mm in 2009 and 300 mm in 2010. Reference evapotranspiration (ET$_o$) was 1003 mm in 2009 and 1049 mm in 2010. The whole irrigated area was divided into four regular sectors and irrigation management of the entire vineyard was carried out following the schedule developed at Raimat winery. The irrigation season was from April until October. Frequency of water applications varied from 3 to 4 days per week. The same amount of water was applied to each of the four sectors. Irrigation water was applied through a drip irrigation system with emitter discharge of 3.7 l·h^{-1}. Emitters were spaced 0.85 m apart on a single drip line per vine row.

In a small area within the vineyard, two irrigation treatments were set up to measure canopy temperature under different levels of water status. The treatments were: i) well-watered control, where irrigation replaced 100% of ET$_o$, and ii) stressed, where water was applied only after midday leaf water potential (Ψ_L) dropped below -1.2 MPa in 2009 and below -1.6 MPa in 2010.

Measurement of canopy temperature and CWSI

Four IRTS; infrared temperature sensors (model PC151LT-0; Pyrocouple series, Calex electronics Limited, Bedfordshire, UK) were installed at the start of the experiment about one meter above two grapevines in each irrigation treatment. Canopy temperature was measured from 23 June − 5 August in 2009 and from 8 July − 12 August in 2010. The calibrated IRTS were installed aiming vertically downward (nadir view) in such a way that by visual inspection and with several leaf temperature measurements with a hand-held infrared thermometer (Fluke 62 mini, Fluke Europe, Eindhoven, Netherlands) ensured that 100% of the temperature signal came from leaves. A similar instrumental set-up was used by Sepulcre-Canto et al. (2006). The sensor angular field of view was 15:1 with an accuracy of ±1%. All IRTS were connected to a datalogger (model CR200X; Campbell Scientific Inc, Logan, USA) that recorded temperatures every minute and stored the 15-min averages.

CWSI was calculated as:

$$CWSI = \frac{(T_c - T_a) - (T_c - T_a)_{LL}}{(T_c - T_a)_{UL} - (T_c - T_a)_{LL}} \qquad (1)$$

where T_c-T_a is canopy- air temperature difference; LL is the T_c-T_a values for lower limit, UL is the upper limit of the same. T_c-T_a is a linear function of vapour pressure deficit (VPD) (non-water-stressed baseline, NWSB). The NWSB was calculated for the two years following the procedure described in Testi et al. (2008). Only data from clear days (95% of days) with wind speed below 6 m s^{-1} (at a height of 10 m) were used in the assessment of CWSI. This is because differences in solar radiation could affect the NWSB and wind speed could also effect changes in the aerodynamic conductance (Hipps et al. 1985). Hourly values of T_c-T_a were regressed against vapour pressure deficits (VPD) separately for the different hours of the day, from 07:00 to 18:00 h. Each point was obtained from half hourly averages of T_c, T_a and VPD, using the T_c of the well-watered grapevines. To obtain $(T_c$-$T_a)_{LL}$, the average NWSB of the two years was corrected taking the minimum values of T_c-T_a for each VPD. The upper limit $(T_c - T_a)_{UL}$ was obtained by simulating the NWSB for a hypothetical slightly negative VPD, that represents the vapour pressure difference generated by the temperature differential T_c-T_a when VPD=0 (Idso et al., 1981). T_a and VPD were obtained from a portable weather station (Watchdog 2000; model 2475 Plant growth, Spectrum Technologies, Inc. Plainfield, Illinois, USA) located on one side of the vineyard.

Airborne imagery

A thermal camera (Miricle 307K; Thermoteknix Systems Ltd, Cambridge, UK) was installed on an unmanned aerial vehicle (UAV) developed at the Laboratory for Research Methods in Quantitative Remote Sensing (Quantalab; IAS-CSIC, Córdoba, Spain), as described by Zarco-Tejada et al. (2012). The camera has a resolution of 640x480 pixels, is equipped with a 14.25-mm f1.3 lens and is connected to a computer via a USB 2.0 protocol. The spectral response was in the range of 8-12 µm. The camera was calibrated in the laboratory to obtain radiance values, and then upwelling and downwelling sky temperature were measured during the flight. In addition, indirect calibrations were conducted using surface temperature measurements to improve the calibration. The accuracy of this method was evaluated by Berni et al. (2009a,b), who have demonstrated an accuracy less than 1 K. The UAV flew over the vineyard at 07:30, 09:30 and 12:30 solar time (09:30, 11:30 and 14:30 local time) on 31 July 2009 at 200 m altitude. Unless otherwise specified, all times referred to here are solar times. Each flight took around 11 minutes, with a flying pattern consisting of five longitudinal lines of 700 m separated by 70 m. The swath of the image was 165 x 221 m and longitudinal and transversal overlapping was 90% and 57%, respectively. Air temperature was 23.2 ºC at 07:30 h, 26.6 ºC at 09:30 h and 32.3 ºC at 12:30 h. Images obtained had 0.3 m spatial resolution enabling the capture of only grapevine canopy and excluding soil, background targets and shadows. Further image processing conducted in the laboratory enabled a pixel re-sampling of the same images acquired on 31 July 2009. Newly obtained re-sampled images of pixel sizes of 0.6, 0.8, 1.0, 1.2, 1.5 and 2.0 m were used to study the influence of pixel size on canopy

temperature detection for determining the minimum and best possible spatial resolution that may be required in assessing T_c of vineyards.

Field data collection

Leaf water potential (Ψ_L) was measured weekly at 12:00 h on the four vines above which IRTS were installed in the two irrigation treatments. Two fully expanded leaves exposed to direct sunlight were measured on each vine. A Scholander pressure chamber (Soil Moisture Equipment Corp., Santa Barbara, CA, USA) was used following the recommendations of Turner and Long (1980). On 28 July 2009, Ψ_L and stomatal conductance (g_s) were measured every hour from 07:30 to 16:30 h on six vines of each irrigation treatment. A steady-state diffusion porometer (model 1600; Li-Cor Inc., Lincoln, Nebraska, USA) was used to measure g_s.

Concomitant to the flights at 09:30 and 12:30 h on 31 July, Ψ_L was measured in the monitored areas to relate the canopy temperature obtained from aerial thermal imagery to a ground-based water stress indicator. Leaf water potential was measured in 184 vines on one leaf per vine, selected on a regular grid within the experimental vineyard. Each location was geo-referenced with global positioning system (GPS) equipment according to the European Datum 1950. To carry out these measurements, two teams, each equipped with a pressure chamber on a truck carried out all the measurements so that they could be performed within one hour around the time of flying.

Data analysis

Image processing methods were used to extract T_c from pixels located in the vines where Ψ_L was measured. Pixels were manually selected in each vine to ensure that only pure canopy vegetative pixels were taken (Fig.2.1a). The thermal imagery acquired at each flight time was re-sampled using a pixel aggregate technique through cubic convolution. Exactly the same region of interest created for the very high resolution thermal imaging was used to extract the aggregated pixels from the lower resolution mosaics. The same pixel neighborhoods were used for the assessment of the CWSI- leaf water potential relationships (Fig.2.1b). CWSI was calculated using Eq.1 and a vineyard CWSI map was developed based on interpolating T_c for all vines within the vineyard. Version 4.2 of SAS (SAS, 2002) was used for statistical analyses.
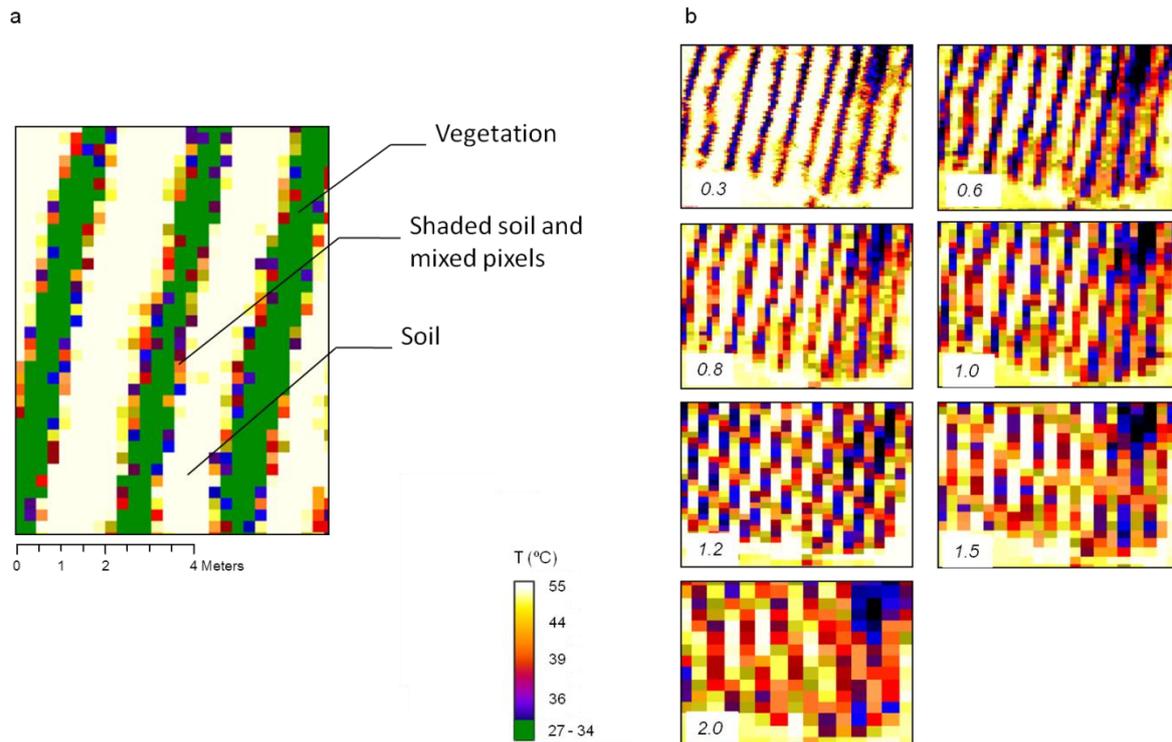
Figure 2.1. Image detail showing: a) the differences in pixel temperatures that enabled the identification of pure crown vegetation pixels, soil and both shaded soil and mixed pixels; and b) the image differences at spatial pixel resolutions of 0.3, 0.6, 0.8, 1.0, 1.2, 1.5 and 2.0 cm. Vegetation (in green) was identified in the interval of temperatures between 27 to 34 ºC.

Results

Airborne thermal imagery and vineyard water status variability

Figure 2.2 presents the thermal image of the vineyard collected at 12:30 h on 31 July 2009 from the UAV, and where the Ψ_L were measured. There was marked variability in canopy temperatures throughout the vineyard. Maximum canopy temperatures corresponded with stressed grapevines, reaching values of 40 ºC. The temperature of the stressed canopies was greater than air temperature by a maximum difference of 7.5 ºC. On the other hand, well-watered grapevines had lower T_c than T_a due to the cooling effect of transpiration. Maximum T_c-T_a for well-watered grapevines ranged from -1 to -3 ºC.
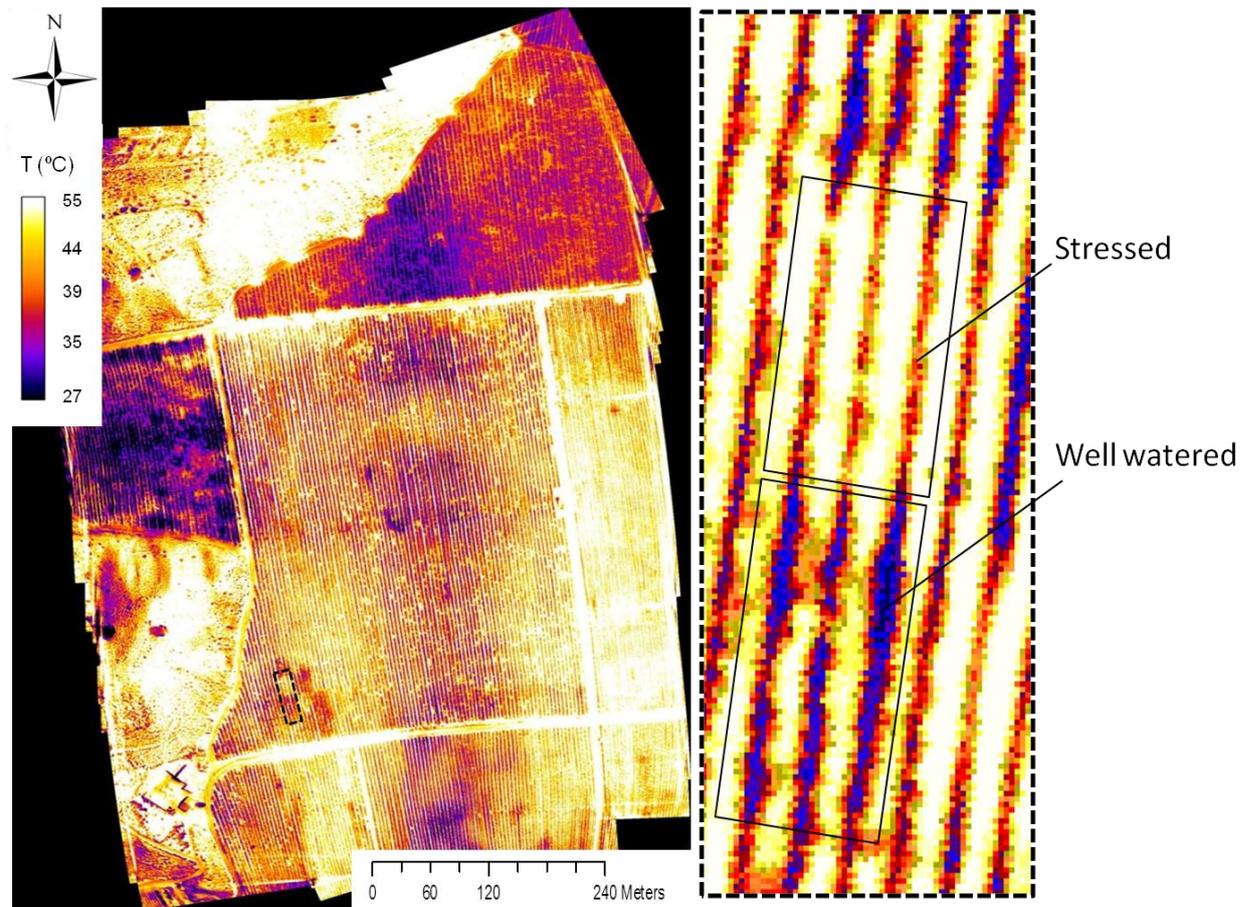
Figure 2.2. Airborne thermal image obtained over the study vineyard at 12:30 h on 31 July 2009 with the rectangle in bold indicating the area within which leaf water potential (ΨL) was measured.

Relationships between T_c-T_a and Ψ_L at different times

Surface temperatures measured from the UAV at 07:30 h did not allow the extraction of pure canopy temperatures because of the difficulty in finding sufficient differences between T_c and soil temperature at that time, even though T_c at 07:30 was 15 ℃ for well-watered grapevines and 23 ℃ for stressed grapevines. The corresponding soil temperature values ranged from 16 ℃ to 34 ℃. These differences in soil temperature values were because of the effect of vegetation cover in the well watered parts of the vineyard. Leaf water potential was correlated better with T_c-T_a at 12:30 h as compared to 09:30, having a much higher correlation coefficient (R^2) (Fig. 2.3). A maximum T_c-T_a value of 7.8 ℃ was found at 12:30 h, which corresponded with a Ψ_L of -1.7 MPa. At 12:30 h, only well-watered vines with Ψ_L values above -0.8 MPa had negative T_c-T_a values. On the other hand, almost all vines at 09:30 h presented negative values of T_c-T_a. The lowest T_c-T_a was -8.0 ℃, corresponding to Ψ_L values higher than -0.8 MPa. Only the more stressed vines had T_c-T_a values of 0.0 ℃ at 09:30 hr.
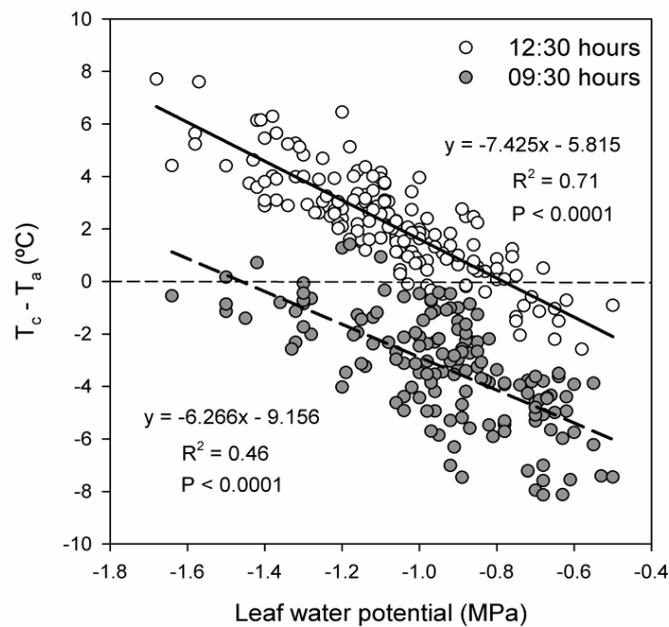
Figure 2.3. Relationship between leaf water potential (Ψ_L) measured in 184 vines and difference of canopy and air temperatures (Tc-Ta) for the measured vines. Temperature was measured using thermal camera imagery from an unmanned aerial vehicle (UAV) at 09:30 h (full circles) and at 12:30 h (empty circles).

Spatial pixel resolution imagery for the vineyard

High spatial resolution imagery enabled the retrieval of pure-vine canopy temperature (Fig.2.1b), while the lower spatial resolution imagery contained pixels with mixed information of canopy, shadows and soil background, making it difficult to detect differences in T_c. An increase of pixel size from 0.3 to 0.6 m at 12:30 h greatly affected the relationship between T_c-T_a and Ψ_L, reducing the correlation coefficient (R^2) from 0.71 to 0.38. In general, the correlation between the two variables decreased as pixel size increased from 0.6 to 2 m. There was no significant relationship between the two for the 1.20-m resolution at 12:30 h. At 09:30 h, R^2 only decreased from 0.46 to 0.42 when pixel size increased from 0.3 to 0.6 m. At the same time, R^2 decreased from 0.42 to 0.30 as pixel size increased from 0.6 to 2 m (Table 2.1). The higher effects of pixel mixture on these relationships at 12:30 h as compared to 09:30 h were due to the higher soil temperatures at midday than earlier in the morning.

Table 2.1. Relationships between leaf water potential (x) measured in 184 vines and differences of canopy and air temperatures (y) obtained with thermal camera imagery from an unmanned aerial vehicle (UAV) at spatial pixel resolutions of 0.3, 0.6, 0.8, 1.0, 120, 1.5 and 2.0 cm at 09:30 and at 12:30 h

Pixel Resolution (m)	09:30 h		12:30 h	
	Equation	R^2	Equation	R^2
0.3	y = -6.266x-9.156	0.46	y = -7.425x-5.815	0.71
0.6	y = -5.833x-9.156	0.42	y = -5.115x - 2.799	0.38
0.8	y = -6.207x-9.448	0.41	y = -4.855x - 0.845	0.27
1.0	y = -5.879x-8.996	0.39	y = -5.054x-0.253	0.22
1.2	y = -5.670x-8.625	0.36	y = -3.189x+0.786	0.05
1.5	y = -5.460x-7.737	0.34	y = -6.721x-0.207	0.28
2.0	y = -6.631x-8.224	0.30	y = -7.080x-0.557	0.29

Crop water stress index (CWSI)

Validation of CWSI at individual grapevine level

The first attempt to relate CWSI to Ψ_L measurements was performed by using data obtained from the IRTS installed above the grapevines. There was a diurnal variation of the NWSB (relationship between T_c-T_a vs. VPD for a well-watered grapevine) for both years, as found by Testi et al. (2008) in pistachio trees. The slope of the baselines at different hours of the day was rather stable, with the exception of the 12:00 h plot which was flatter. Also the intercept increased in the morning and decreased in the afternoon, except at 12:00 (data not shown). Figure 2.4a presents a scatter plot of T_c-T_a versus VPD for all data collected from 10:00 to 16:00 h in 2009 and 2010. The intercept for 2010 baseline was 4.97 (95% confidence interval: 5.45- 4.49; P<0.0001), slightly higher than for 2009 that was 3.47 (95% confidence interval: 3.78-3.15; P<0.0001). These differences could be explained because the intercept is a function of net radiation (R_n) and it is expected to increase with solar radiation (Jackson et al. 1981). The averaged R_n ($W \cdot m^{-2}$) was 122 in 2009 and 144 in 2010. However, although there existed significant differences between years (F = 28.73; P < 0.0001), the ANCOVA analysis revealed no significant differences with slopes (VPD*year), which indicated that T_c-T_a responded similarly to VPD in both years. The average NWSB for the two years (bold line) is also shown in Fig.2.4a. Minimum values of T_c-T_a versus VPD relationship were similar during both years and were used to determine a corrected NWSB, which was used as a lower limit (LL) in the calculation of the CWSI (Eq.1). Fig.2.4a shows the minimum T_c-T_a values used to determine the lower limit. The LL converged at T_c-T_a values of approximately 2.5 ℃ when VPD was zero, down to minus 6℃ for a VPD of 5 kPa. The upper limit (UL in Eq. 1) had a value of 6℃ when VPD was 0 and reached 8℃ for a VPD of 5 kPa (Fig.2.4b).

The midday Ψ_L measurements in the two irrigation treatments correlated linearly with CWSI for the two years (Fig.2.5). The relationship was significant (R^2=0.43; P<0.0001) for 2009, in spite of the relatively narrow range of Ψ_L values (it varied only between -0.8 and -1.2 MPa). Whereas in 2010, with the wider fluctuations in Ψ_L between -0.7 and -1.7 MPa, a stronger relationship was found (R^2=0.85; P<0.0001). Pooling the data for two years (solid bold line in Fig.2.5) provided a strong relationship between the two parameters (R^2=0.83; P<0.0001).
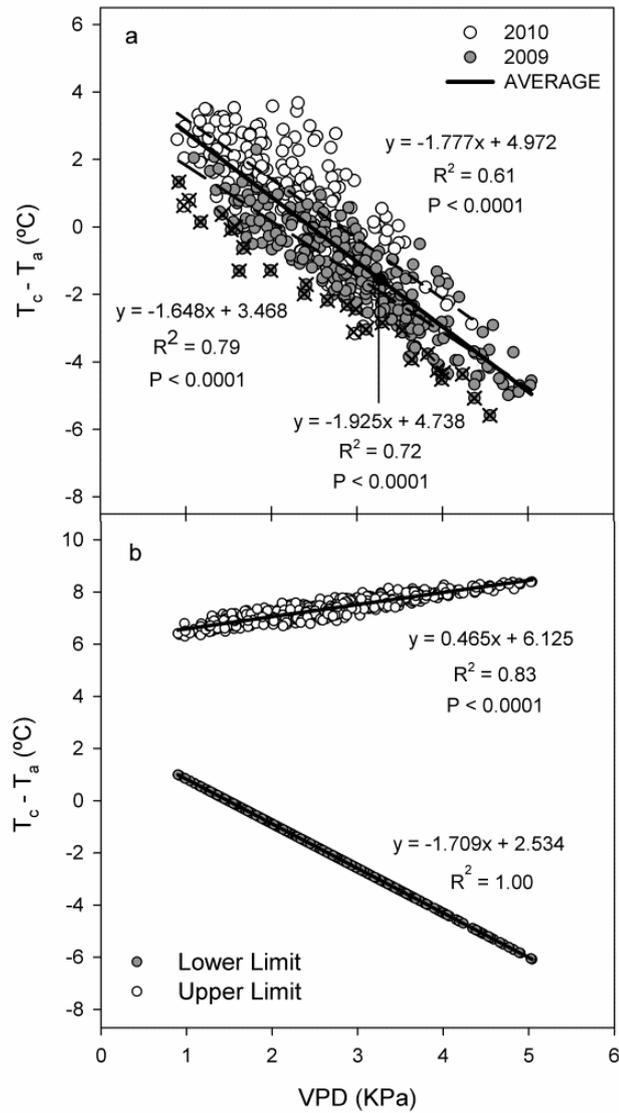
Figure 2.4. Relationship between (Tc-Ta) and VPD for determination of crop water stress index (CWSI) in `Pinot-noir´ grapevine showing: a) the non-water-stressed baseline (NWSB) between 10:00 and 16:00 h for 2009 and 2010, and b) lower and upper limits of this relationship. The bold line in Panel a is the averaged NWSB for both years. The marked points indicate the minimum (Tc-Ta) values used for estimating (Tc-Ta)$_{LL}$.
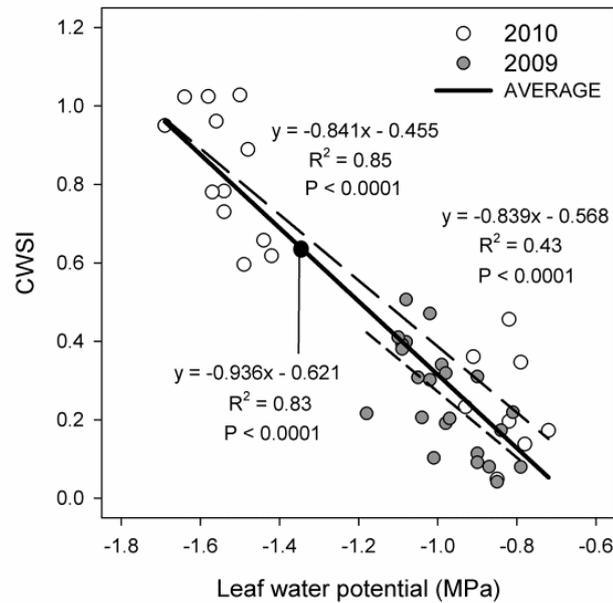
Figure 2.5. Relationship between CWSI and midday leaf water potential (Ψ_L) in well-watered and water-stressed `Pinot-noir´ grapevine for 2009 (full circles) and 2010 (empty circles). The bold line is the averaged relationship of both years. The CWSI data are based on the measurements using infra-red thermal sensors (IRTS in the text) on the ground.

Validation of CWSI at vineyard level

Thermal imagery at 12:30 had the strongest relationship with Ψ_L. Thus, from meteorological data at the time of the flight and taking into account the NWSB and UL of Fig.2.4, CWSI was calculated as follows:

$$\text{CWSI} = \frac{(T_c - T_a) - (-1.709 \cdot \text{VPD} + 2.534)}{(0.465 \cdot \text{VPD} + 6.125) - (-1.709 \cdot \text{VPD} + 2.534)} \qquad (14)$$

where T_c is the actual canopy temperature obtained from the thermal image, T_a was 32.27 ºC and VPD was 2.37 kPa (CWSI $=T_c$ - 30.75 / 8.75).
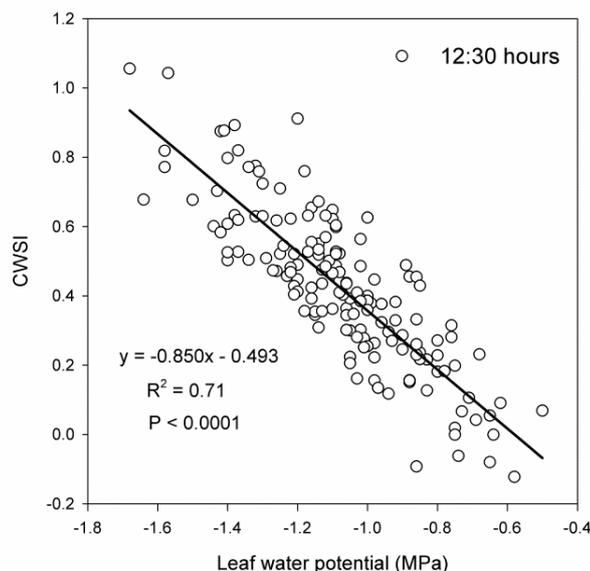
Figure 2.6. Relationship between CWSI and midday leaf water potential (Ψ_L) measured in 184 vines of `Pinot-noir´ vineyard at 12:30 h. CWSI was obtained from thermal camera imagery from an unmanned aerial vehicle (UAV).

There is general consensus in the literature that well-watered vines have midday Ψ_L values ranging from -0.6 to -0.8 MPa; Ψ_L in moderately stressed vines ranges between -1.0 and -1.2 MPa, and severely-stressed vines have Ψ_L lower than -1.5 MPa (Williams and Araujo, 2002). From Figure 2.6, it appears that the CWSI values of well-watered vines should be less than 0.2 (Ψ_L~ -0.6 to -0.8 MPa). The CWSI of moderately stressed vines ranges between 0.3 and 0.5 (Ψ_L~ -1.0 to -1.2 MPa), and severely stressed vines have a CWSI equal or above 0.7 (Ψ_L< -1.5 MPa).

Discussion

Time of the day for obtaining thermal images

A suitable time interval for obtaining thermal images needs to be identified where it reflects the vine water status, as well as being a deciding factor for the surface area that could be imaged each day.

Early morning (07:30 h) was found not to be a suitable time for detecting water stress with thermal imaging because of the small differences found between soil and canopy temperatures. Differences in the relationship of T_c-T_a and Ψ_L between the two measuring times of 09:30 and 12:30 h could be influenced by the two following factors: the time taken to measure Ψ_L because of changes that could occur in Ψ_L during this time interval, and shading.

Fig. 2.7a shows the diurnal changes of Ψ_L for well-watered and water-stressed vines confirming the results of Van Zyl (1987). It is known that Ψ_L values in grapevine remain rather stable for a few hours at noon. The interval between the first pair of vertical dotted lines in Fig. 2.7 shows the time period of 09:00 – 10:00 h and that between the second pair shows the time period of 12:00 – 13:00 h. In the first interval, Ψ_L decreased from -0.50 to -0.65 MPa for well-watered vines and from -1.30 to -1.50 MPa for stressed vines. However, during the second interval (12:00– 13:00 h) Ψ_L did not change much at all. For well-watered vines, it remained constant at around -0.85 MPa and for stressed vines at around -1.65 MPa. Thus, the relationship between T_c-T_a and Ψ_L at 09:30 h had a lower R^2 in part due to this dynamic nature of Ψ_L in the morning hours when plant water status is changing substantially over short time periods. The diurnal changes in g_s are also shown in Fig.2.7b, where it can be seen that there was a gradual decrease in g_s associated with a decrease in water potential. During early morning, stressed and well-watered vines presented slight differences in g_s. However, while stressed vines completely closed stomata from 10:00 h and arrived at maximum stress (lowest Ψ_L), well-watered vines still maintained stomata partly open, and g_s decreased from 320 to 90 mmol·m^{-2}·s^{-1}. During the 09:00-10:00 time interval, g_s in non-stressed vines was quite variable due to shading of leaves.

Shading of leaves could influence canopy temperature heterogeneity due to different degrees of stomatal conductance within the vine canopy (Jones et al., 2002). Gonzalez-Dugo et al. (2012) detected in mildly-stressed almonds that few areas within the crown had substantial stomatal closure while, in the rest of the crown, the stomata were still open and this increased heterogeneity of the canopy temperature. Similar results were reported by Testi et al. (2008) who found, in pistachio trees, a wide range of CWSI for similar midday Ψ_L values in a mild stress range. Therefore, probably at 09:30 h, mild stressed vines within the vineyard had different degrees of stomatal conductance and transpiration rates for similar Ψ_L values. As a consequence, for mildly stressed vines, there may exist a wide variability of T_c-T_a.
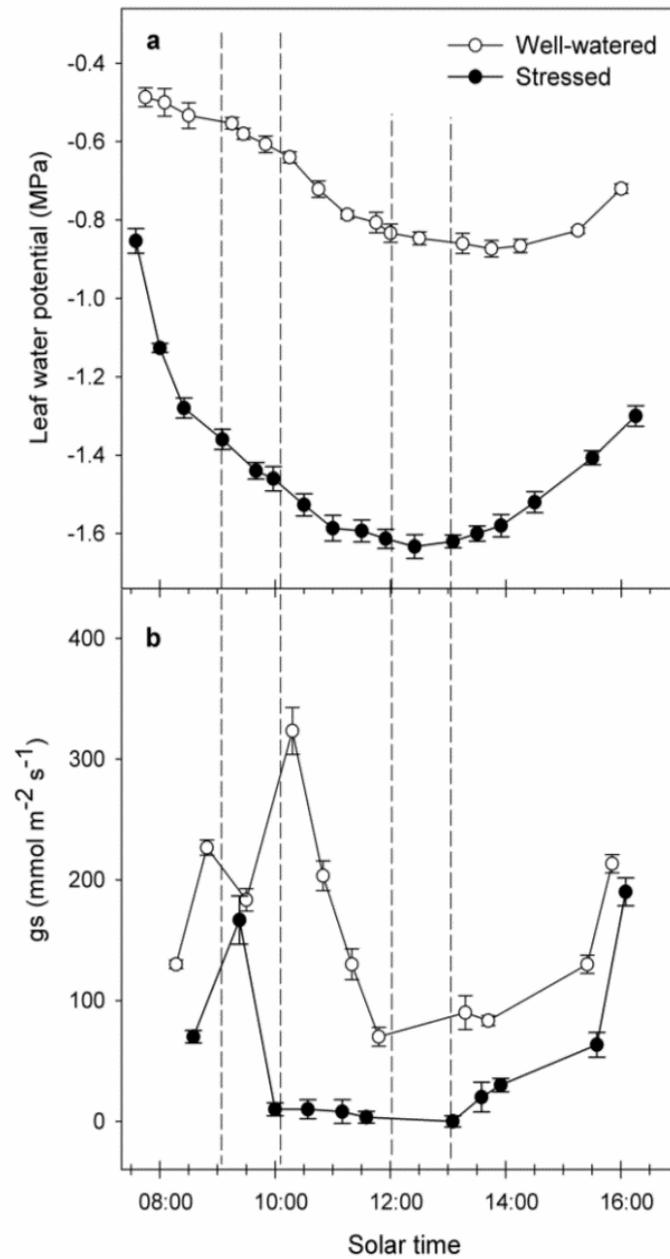
Figure 2.7. Diurnal changes in: a) leaf water potential (Ψ_L) and b) stomatal conductance (g_s) for well-watered and stressed `Pinot-noir´ vines on 28 July 2009.Vertical dotted lines indicate the time intervals starting at 09:00 and at 12:00 h. At each of this time intervals, 184 Ψ_L were measured across the vineyard.
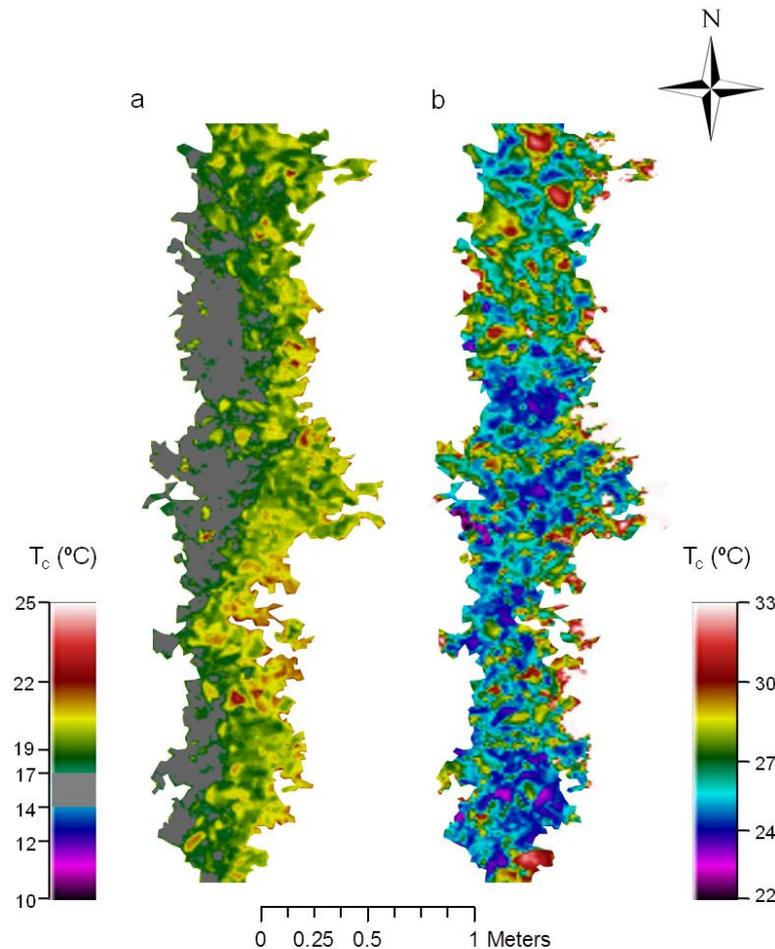
Figure 2.8. Example of the shading effect on the canopy temperature (Tc) at two different times of the day: a) 08:00 h and b) 12:00 h. Air temperatures (Ta) at 08:00 and 12:00 hours were 18.5 and 25 ºC, respectively. Rows are orientated north-south.

Thermal images capture the temperature of leaves at the top of the canopy. At 09:30 h, the zenith solar angle is lower than at midday and almost half of leaves are not exposed to direct sunlight (Fig. 2.8a). Pixels that comprised shaded leaves had lower temperature than those containing only sunlit leaves. When mixing pixels of different radiation loads, the variability in vine temperatures would be much more for the same vine water status. As a consequence, measured T_c from the viewing angle of the airborne is significantly reduced. Row orientation also makes a difference to the time of day when intercepted radiation is maximum and could influence canopy exposure to sunlight. Fig. 2.8 shows an example of the difference in T_c measured at 08:00 h and at 12:00 h on a mildly water-stressed grapevine row. T_c (ºC ± SE) at 08:00 h was 17.8±0.1 while it averaged 27.0±0.1 at 12:00 h. The corresponding T_a values were, respectively, 18.5 and 25 ºC. In part, lower value of T_c-T_a at 08:00 h, which was – 0.7 ºC, was due to the shaded leaves of one side of the vines that had leaf temperatures between 14 and 17 ºC.

The diurnal changes of Ψ_L and T_c within the canopy due to shaded leaves and/or variability in stomatal closure demonstrated that the most favorable time of day to obtain thermal images that better characterizes vine water status is around midday, e.g. during 12:00 to 13:30 h.

Spatial pixel resolution to detect water stress

Spatial pixel resolution will depend on the canopy volume of each crop. Vegetative canopy volume for grapevine is relatively low compared to woody trees or field crops. Moreover, in vines with trellis systems such as vertical shoot positioning, the canopy width seen from the top is quite narrow (around 0.25- 0.4 m) and pixel temperatures could have mixed information coming from soil, shadows and leaves.

For the two studied times of measurement, there was a similar pattern of reducing R^2 with increasing pixel size (Table 2.1). At 09:30 h, an increase of pixel size had a slightly lower effect in comparison with 12:30 h probably due to minimal temperature differences between soil and vegetation during early morning. Values of T_c-T_a increase with pixel size. The higher the pixel size, the more will be the influence of soil temperature. This will influence the CWSI values by exceeding the maximum limit of one. The results indicate that, in grapevine, it is necessary to obtain high resolution thermal imagery having at least 0.30 m pixel size.

Mapping CWSI at high resolution

CWSI calculations at individual grapevine level were used to create CWSI maps with values ranging from 0 to 1. However, T_c-T_a only responded to VPD from 10:00 to 16:00 h. During early morning and late afternoon, the correlation between T_c-T_a and VPD was poor because solar radiation has low values (R_s< 100 W· m^{-2}). At those times, solar energy hits the surface at very low altitude angles. The increase of the intercept of the NWSB during the morning is mainly explained in terms of solar radiation effect (Jackson et al., 1981) which varies throughout the day.

The CWSI map was obtained from Eq.14, using the T_c of all vines. Figure 2.9a shows in detail CWSI values of individual vines without soil interference. This is only possible with high resolution thermal imagery. By interpolating CWSI values of individual vines, it is possible to generate CWSI maps (Fig.2.9b) enabling the identification of zones of different water status levels within the vineyard. The main advantage of using CWSI maps is that it is possible to manage irrigation at large scale taking into account spatial variability of vine water status. Until now, vineyards for high quality wine production were managed and harvested by sub-block zones (Johnson et al., 2001; Bramley and Hamilton, 2004) based on the differences in berry composition within the vineyard. CWSI maps could replace the

use of Ψ_L as a grapevine water stress indicator. The measurement of Ψ_L needs a high labour input, particularly where pre-dawn Ψ_L is being used as an indicator.

Girona et al. (2006) demonstrated the feasibility of scheduling regulated deficit irrigation in individual plots of 'Pinot-noir' on the basis of Ψ_L thresholds. From relationships obtained here, it would be possible to schedule irrigation in each sector within the block by using CWSI thresholds. To do this, frequent flights would be necessary and the average CWSI for each sector will determine its irrigation needs, once a predetermined threshold is reached.

The work presented here was carried out on the cultivar 'Pinot-noir'. However, as stomatal response to VPD ranges widely among species and cultivars (Rogiers et al., 2012), relationships for other grapevine cultivars should also be determined in further studies.

Conclusions

This study demonstrated the feasibility of using high resolution thermal imagery to generate CWSI maps that can be used for precision irrigation management by incorporating the variability within a vineyard. The optimum time to obtain thermal images was around noon, when Ψ_L was more stable at its minimum diurnal values and the CWSI-Ψ_L relationship was strongest. During the morning, leaf temperature was not a good indicator of leaf water status because of shading effects.

It was found that a 0.3 m pixel size setting is the best possible in differentiating canopy temperature from the soil temperature in this vineyard canopy. This high resolution is needed in wine grapes because of the narrow canopy width. Higher pixel sizes reduced the correlation between CWSI and Ψ_L because bigger pixels must have had mixed information coming from both soil and leaves.Time interval and image resolution will be the deciding factors in determining the surface area that could be imaged each day.
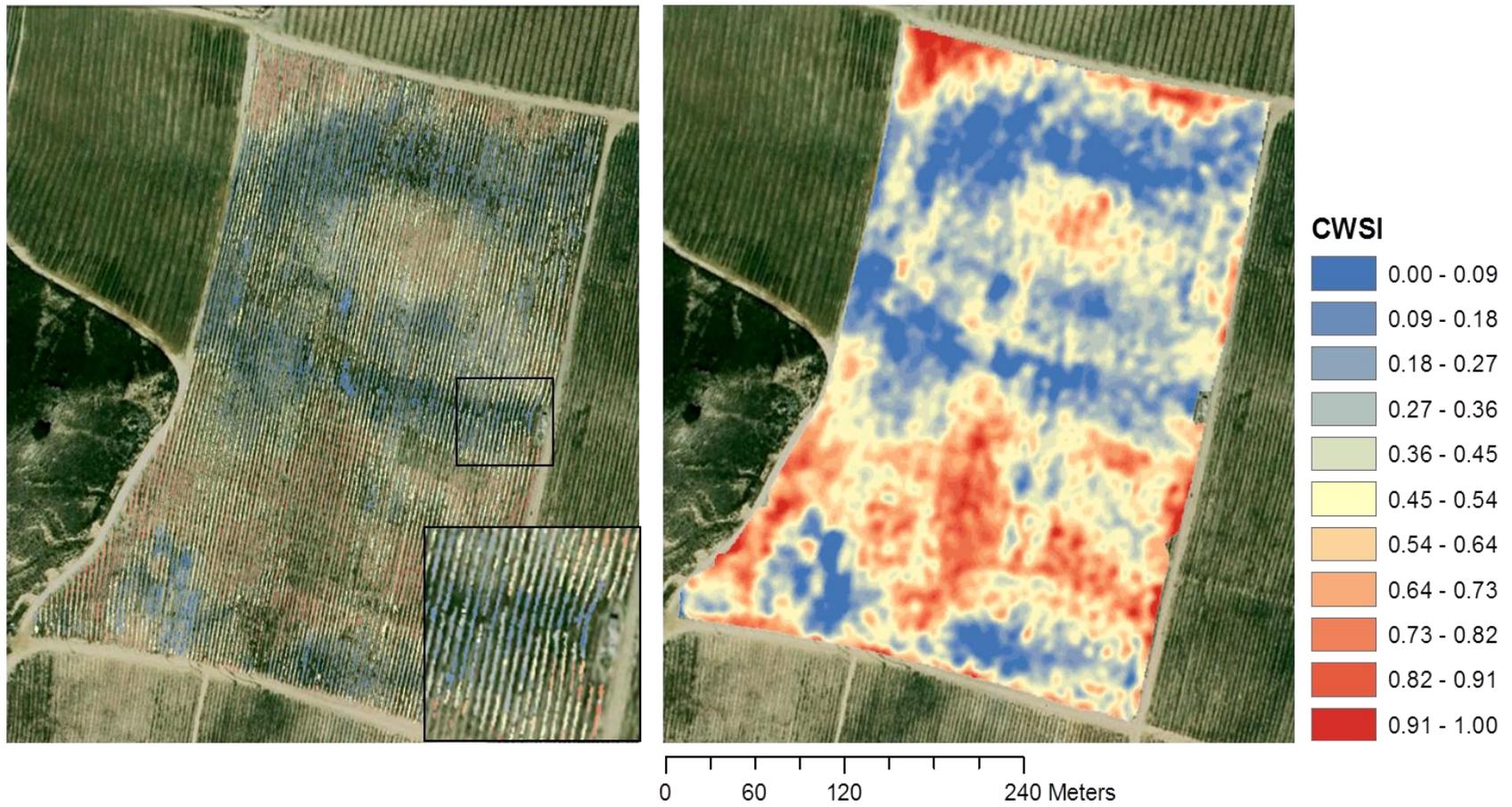
Figure 2.9. CWSI map obtained from thermal imagery at 12:30 h on 31 July 2009. An unmanned aerial vehicle (UAV) was used for the imagery

References

Acevedo-Opazo, C., Tisseyre, B., Guillaume, S., & Ojeda, H (2008a). The potential of high spatial resolution information to define within-vineyard zones related to vine water status. Precision Agriculture. 9, 285-302.

Acevedo-Opazo, C., Tisseyre, B., Ojeda, H., Ortega-Farias, S., & Guillaume, S (2008b). Is it possible to assess the spatial variability of vine water status?.J. Int. Sci. Vigne Vin. 42, 203-219.

Basile, B., Marsal, J., Mata, M., Vallverdú, X., Bellvert, J., & Girona, J (2011). Phenological sensitivity of Cabernet Sauvignon to water stress: vine physiology and berry composition. Am.J.Enol.Vitic. 62, 452-461.

Bellvert, J., Marsal, J., Mata, M., & Girona, J (2012). Identifying irrigation zones across a 7.5-ha 'Pinot-noir' vineyard based on the variability of vine water status and multispectral images. Irrigation Science. 30, 499-509.

Berni, J.J., Zarco-Tejada, J.P., Sepulcre-Cantó, G., Fereres, E., & Villalobos, F (2009a). Mapping canopy conductance and CWSI in olive orchards using high resolution thermal remote sensing imagery. Remote Sensing of Environment. 113, 2380-2388.

Berni, J.A., Zarco-Tejada, P.J., Suarez, L., & Fereres, E (2009b). Thermal and narrow-band multispectral remote sensing for vegetation monitoring from an unmanned aerial vehicle. IEEE Transactions on Geoscience and Remote Sensing. 47, 722-738.

Bramley, R.G.V., & Hamilton, R.P (2004). Understanding variability in winegrape production systems. 1. Within vineyard variation in yield over several vintages. Australian Journal of Grape and Wine Research.10, 32-45.

Bramley, R.G.V., Proffitt, A.P.B., Hinze, C.J., Pearse, B., & Hamilton, R.P (2005). Generating benefits from precision viticulture through selective harvesting. In: J.V.Stafford (ed) Precision Agriculture '05, Proceedings of the 5th European Conference on Precision Agriculture, Wageningen Academic Publishers, The Netherlands. pp. 891-898.

FAO (2010) FAO Statistical Database (online). http://faostat.fao.org/. Accessed September 2013

Fulton, A., Schwankl, L., Lynn, K., Lampinen, B., Edstrom, J., & Prichard, T (2011). Using EM and VERIS technology to assess land suitability for orchard and vineyard development. Irrigation Science. 29, 497-512.

Girona, J., Mata, M.,del Campo, J.,Arbonés, A.,Bartra, E.,& Marsal, J (2006).The use of midday leaf water potential for scheduling deficit irrigation in vineyards. Irrigation Science. 24, 115-127.

Gonzalez-Dugo, V., Zarco-Tejada, P., Berni, J.A.J., Suárez, L., Goldhamer, D., & Fereres, E (2012). Almond tree canopy temperature reveals intra-crown variability that is water stress-dependent. Agric.Forest Meteorol. 154-155, 156-165.

Hipps, L.E., Asrar, G., & Kanemasu, E.T (1985). A theoretically-based normalization of environmental-effects on foliage temperature. Agric. Forest Meteorol. 27, 59-70.

Idso, S.B., Jackson, R.D., Pinter, P.J., Reginato, R.J., & Hatfield, J.L (1981). Normalizing the stress-degree day parameter for environmental variability. Agric.Meteorol. 24, 45-55.

Jackson, R.D., Idso, S., Reginato, R., & Pinter, P. Jr (1981). Canopy temperature as a crop water stress index indicator. Water Resources Research. 17, 1133-1138.

Johnson, L.F., Bosch, D.F., Williams, D.C., & Lobitz, B.M (2001). Remote sensing of vineyard management zones: implications for wine quality. American Society of Agricultural Engineers. 17, 557-560.

Jones, H.G., Stoll, M., Santos, T., de Sousa, C., Chaves, M.M., & Grant, O.M (2002). Use of infrared thermography for monitoring stomatal closure in the field: application to grapevine. J. Exp. Bot. 53 (378) 2249-2260.

Martinez − Casasnovas, J.A., Vallés Bigorda, D., & Ramos, M.C (2009). Irrigation management zones for precision viticulture according to intra-field variability. In: Breft, A., Wolfert, S., Wien, J.E., Lokhorst, C. (Eds.), EFITA conference '09. Proceedings of the 7th EFITA Conference, Wageningen Academic Publishers, Wageningen, pp. 523-529.

Möller, M., Alchanatis, V., Cohen, Y., Meron, M., Tsipris, J., Naor, A., Ostrovsky, V., Sprintsin, M., & Cohen, S (2007). Use of thermal and visible imagery for estimating crop water status of irrigated grapevine. J. Exp. Bot. 58 (4) 827-838.

Rogiers, S.Y., Greer, D.H., Hatfield, J.M., Hutton, R.J., Clarke, S.J., Hutchinson, P.A., & Somers, A (2012). Stomatal response of an anisohydric grapevine cultivar to evaporative demand, available soil moisture and abscisic acid. Tree physiology. 32, 249-261.

SAS (2002). Enterprise Guide version 4.2 (SAS Institute Inc. Cary, NC, USA).

Sepulcre-Canto, G., Zarco-Tejada, P.J., Jimenez-Muñoz, J.C., Sobrino, J.A., de Miguel, E., & Villalobos, F.J (2006). Detection of water stress in an olive orchard with thermal remote sensing imagery. Agric. Forest Meteorol. 136, 31-44.

Testi, L., Goldhamer, D.A., Iniesta, F., & Salinas, M. (2008). Crop water stress index is a sensitive water stress indicator in pistachio trees. Irrigation Science. 26, 395-405.

Turner, N.C., & Long, M.J (1980). Errors arising from rapid water loss in the measurement of leaf water potential by pressure chamber technique. Austr. J. Plant. Physiol. 7, 527-537.

Van Zyl, J.L (1987). Diurnal variation in Grapevine Water Stress as a function of changing soil status and meteorological conditions. S. Afr. J. Enol. Vitic. 8, (2), 45-52.

Wetterlind, J., Stenberg, Bo., & Söderström, M (2008). The use of near infrared (NIR) spectroscopy to improve soil mapping at the farm scale. Precision agriculture. 9, 57-69.

Williams, L.E., & Arujo, F.J (2002). Correlations among predawn leaf, midday leaf, and midday stem water potential and their correlations with other measures of soil and plant water status in *Vitis vinifera*. J. Am. Soc. Hortic. Sci. 127, 448-454.

Zarco-Tejada, P.J., González-Dugo, V., & Berni, J.A.J (2012). Fluorescence, temperature and narrow-band indices acquired from a UAV platform for water stress detection using a micro-hyperspectral imager and a thermal camera. Remote Sensing of Environment. 117, 322-337.

Zia, S., Klaus, S., Nikolaus, M., Wenyong, D., Xiongkui, H., & Müller, J (2009). Non-invasive water status detection in grapevine (*Vitis vinifera L.*) by thermography. Int. J. Agric. &Biol. Eng. 2, 4, 46-54.

Capítulo 3

Seasonal evolution of crop water stress index in grapevine varieties determined with high resolution remote sensing thermal imagery

J. Bellvert[a], P.J. Zarco-Tejada[b], J. Girona[a], J.Marsal[a], E. Fereres[b,c]

[a]*Programa Uso eficiente del agua, Institut de Recerca i Tecnologia Agroalimentàries (IRTA), Centre UdL-IRTA, 191 Av. Rovira Roure, 25198 Lleida*

[b]*Instituto de Agricultura Sostenible (IAS), Consejo Superior de Investigaciones Científicas (CSIC), Córdoba*

[c]*Departamento de Agronomía, Universidad de Córdoba (UCO), Córdoba*

Abstract The seasonal characterization of the spatial variability in water requirements across and within vineyards could assist the viticulturist to fine tune irrigation management for quality optimization. Remotely sensed crop water stress index (CWSI) relates to crop water status, but it is not known how applicable it is to different grape varieties at different times of the season. This study focused on the determination of the lower and upper baselines for calculating CWSI for the Chardonnay, Pinot-noir, Syrah and Tempranillo varieties at different phenological stages. Baselines were determined based on canopy temperatures measured with infrared temperature sensors placed on top of well-watered grapevines in 2011. Results indicated that non-water-stressed baselines (NWSB) differed depending on variety and phenological stage. During 2011, an aircraft equipped with a thermal camera flew over the vineyards on six peculiar days throughout the season at 150 m altitude above the ground level. At the same time, leaf water potential (Ψ_L) was measured for each variety. Variety and phenological stage affected the relation between remotely sensed CWSI and Ψ_L, with phenology having greater influence on the observed than variety. For instance, one-to-one relationship between estimated and measured Ψ_L had r^2 of 0.634 and 0.729 for variety and phenology, respectively. The baselines and estimations of Ψ_L were validated in different vineyards of the same region and seasons (2013) using the same methodology as in 2011. Data obtained in 2013 was in agreement with observations during 2011. It is concluded that the use of CWSI for assessing vineyard water status requires calibration to account for the effects, primarily of phenological stage, but also, of variety. Once calibrated, this can be successfully applied to other vineyards and seasons.

Resumen   La caracterización estacional de la variabilidad espacial de los requerimientos hídricos en los viñedos puede ayudar a los viticultores a mejorar el manejo del riego, con el objetivo de optimizer la calidad. El crop water stress index, obtenido mediante la teledetección está relacionado con el estado hídrico del cultivo, pero no se conoce su aplicabilidad para distintas variedades de viña y en distintos momentos fenológicos. Este estudio se centra en la determinación de las líneas base para el cálculo del CWSI en las variedades de viña Chardonnay, Pinot-noir, Syrah y Tempranillo, en distintas fases fenológicas. En el año 2011 se determinaron las líneas base midiendo la temperatura de la cubierta vegetativa de viñas regadas en la totalidad de sus necesidades hídricas, con sensores de temperatura infrarrojo. Los resultados indicaron que las líneas base 'non-water-stressed' (NWSB) fueron diferentes en función de la variedad y fenología. En el año 2011, una avioneta tripulada equipada con una cámara térmica sobrevoló los viñedos en seis días distintos una altitud de 150 m por encima del suelo. En el mismo momento, se midió el potencial hídrico foliar (Ψ_L) para cada vaiadad. La variedad y el momento fenológico afectaron la relación entre el CWSI y el Ψ_L, teniendo la fenología una mayor influencia que la variedad. Por ejemplo, las relaciones 1:1 entre el Ψ_L estimado y el medido tuvieron un r^2 de 0.634 y 0.729 para la variedad y fenología, respectivamente. Las líneas base y estimaciones del Ψ_L también se validaron en el año 2013 en distintos viñedos de la misma región, utilizando la misma metodología que en el año 2011. Los datos obtenidos en el 2013 coincidieron con las observaciones realizadas en 2011. Se concluyó que para evaluar el estado hídrico de un viñedo, es necesario calibrar el CWSI teniendo en cuenta en primer lugar, los efectos de la fenología, pero también de la variedad. Una vez esté calibrado, puede ser aplicable con éxito en otros viñedos y temporadas.

Introduction

The crop water stress index (CWSI) was developed as a normalized index to quantify stress and overcome the effects of other environmental parameters affecting the relation between stress and plant temperature (Idso et al. 1981, Jackson et al. 1981). CWSI could be determined by at least three different methodologies. The empirical approach is based on relating canopy-air temperature difference T_c-T_a to air vapour pressure deficit (VPD) of a `non-water-stressed baseline´ (NWSB) referring for a well-watered crop transpiring at the potential rate (maximum stomatal conductance, g_s) (Idso et al. 1981). A second method is based on the energy balance equation and requires an estimate of net radiation and an aerodynamic resistance factor (Jackson et al. 1988). The other alternatives are based on using natural (Clawson et al. 1989; Leinonen and Jones 2004) and artificial (Meron et al. 2003) wet and dry reference surfaces.

The CWSI has been successfully related with leaf water potential (Ψ_L) for different grapevine varieties by using some of the latter methodologies. Examples have been reported for Pinot-noir by using the empirical approach (Bellvert et al. 2013), or for Merlot (Möller et al. 2007) and Cabernet Sauvignon (Wheaton et al. 2011) on using artificial reference surfaces. However, different criteria used for calculating CWSI prevent comparison between varieties. In addition, all the studies have shown relationships on specific days, but is not known whether the relationship between CWSI and Ψ_L would change during different phenological stages. Remotely sensed CWSI is advantageous for detection of plant water status variability within orchards (Berni et al. 2009a, Bellvert et al. 2013). If CWSI has to be a successful tool for detecting plant water status along the season in vineyards, information on the interaction between varieties and phenology in the relationship between CWSI and Ψ_L is needed.

For practical purposes, it is desirable to have a robust relationship between remotely measured CWSI to 'true' ground-based measures of crop water status throughout the season. However, stomatal control over water vapour conductance is highly sensitive to VPD (i.e. Soar et al. 2006 a,b, Poni et al. 2009, Rogiers et al. 2012) and there are clear differences in this response between varieties (Schultz and Stoll 2010, Soar et al. 2006b). These differences may affect canopy temperature and its relation with plant water status. Therefore, the response of stomata to variations in Ψ_L can be different among varieties. Some studies have also reported that stomatal responses to Ψ_L have different sensitivity between different phenological stages (Marsal and Girona, 1997 in peach; McCutchan and Shackel, 1992 in plum; Olivo et al. 2009 in grapevine). Olivo et al. (2009) reported baselines between variations of Ψ_L and vapour pressure deficit at different phenological stages in `Tempranillo´ grapevines.

Considering that VPD influences stomatal behavior and therefore canopy temperature, and that VPD varies seasonally, we hypothesize that phenology and variety would influence the determination of the crop water stress baselines in grapevines. The goal of this study was first to determine the non-water-stressed baselines (NWSB) and the CWSI

for the four grapevine varieties Pinot-noir, Chardonnay, Syrah and Tempranillo at different phenological stages. Additionally, work to establish the seasonal relationships between CWSI and Ψ_L was carried out by simultaneously measuring Ψ_L and estimating CWSI using remote sensing thermal images.

Materials and Methods

Study site

The study was carried out during the 2011 growing season in commercial vineyards of Pinot-noir, Chardonnay, Syrah and Tempranillo located in Raïmat (41º 39'N, 00º 30'E), Lleida, Spain. The areas of the plots were 11.0, 22.0, 18.4, and 14.5 ha, respectively. The vines aged twenty, eleven, nine and thirteen years old, respectively. Vines were planted in a grid of 1.7 m x 3.1 m for Pinot-noir and 2.0 m x 3.0 m for the other varieties, all of them with north-south row orientation. Canopies were cordon-trained to an espalier system at a height of 0.9 m, and their width ranged from 25 to 80 cm. Canopy management practices aimed at producing high-quality grapes by limiting canopy growth and included vertical shoot positioning in July. Climate of the area is Mediterranean, with an average annual rainfall of 291.3 mm. Reference evapotranspiration (ET_o) is around 1080 mm. Irrigation season starts in April and lasts until October. Frequency of irrigation applications varied from 3 to 4 days per week. Irrigation water was applied through a drip irrigation system with emitters spaced 0.85 m apart on single drip line per vine row, discharging 3.7 $l \cdot h^{-1}$. In a small area within each vineyard, twelve grapevines were full irrigated (100% of ET_o) to measure canopy temperature under non-stress conditions.

Canopy temperature measurements and CWSI

Two infrared temperature sensors (IRTS) (model PC151LT-0; Pyrocouple series, Calex electronics Limited, Bedfordshire, UK) were installed at the start of the experiment about one and a half meterabove two of the well-watered grapevines of each variety. Leaf water potential (Ψ_L) was weekly measured at 12:00 hours in these well-watered vines ensuring that values were above the threshold of -0.8 MPa along the season. According with Girona et al. (2006), a reference value of Ψ_L for a well-watered vine would be increase linearly from around -0.6 MPa, at the beginning of the irrigation season, up–to 0.8 MPa by early June. Two fully expanded leaves exposed to direct sunlight were measured from each vine. A Scholander pressure chamber (Soil Moisture Equipment Corp., Santa Barbara, CA, USA) was used following the recommendations of Turner and Long (1980).

Canopy temperature was measured from 10 May until 15 September, except for Syrah and Tempranillo, which finished on 30 August because of the high defoliation caused by mechanical harvest. Therefore, postharvest period was only studied in Pinot-noir and Chardonnay. The calibrated IRTS were installed aiming vertically downward (nadir view)

in such way that visual inspection and with leaf measurements using a hand-held infrared thermometer (fluke 62 mini, Fluke Europe, Eindhoven, Netherlands) ensured 100% of the temperature signal came from leaves. Moreover, canopy temperature values were validated Details of this instrumental set-up were described in Sepulcre-Canto et al. (2006). The sensors angular field of view was 15:1 with an accuracy of ±1%. This narrow angular field of view of the sensor was used in grapevines to be sure that the targeted area was pure vegetation. All IRTS were connected to a datalogger (model CR200X; Campbell Scientific, Logan, UK) that recorded temperatures every minute and stored the 15-min averages. Recorded data of well-watered grapevines was used to calculate the baselines of the crop water stress index (CWSI). The empirical CWSI is calculated as (Idso et al. 1981):

$$CWSI = \frac{(T_c - T_a) - (T_c - T_a)_{LL}}{(T_c - T_a)_{UL} - (T_c - T_a)_{LL}}$$

where T_c-T_a is measured canopy- air temperature difference; $(T_c$-$T_a)_{LL}$ lower limit of $(T_c$-$T_a)$ of a canopy which is transpiring at the potential rate, and $(T_c$-$T_a)_{UL}$ expected differential in the case of a non-transpiring canopy.

The methodology described in Bellvert et al. (2013) was used in this analysis. Each point was obtained from half hourly averages of T_c, T_a and VPD from 11:00 to 16:00 hours. Only data from clear days (95% of days) with windspeed below 6 m s^{-1} (at a height of 10 m) were used in the assessment of CWSI. A problem of the empirical method is that in some instances, the values of CWSI could exceed the range of 0.0 – 1.0 (Yuan et al. 2004). To help solve this problem, in this study we propose to use a curvilinear model to adjust the 'non-water-stressed baselines' (NWSB), from the relationship between T_c-T_a for well-watered conditions and vapour pressure deficit. The upper limit (UL) was obtained by solving the NWSB curvilinear equation for VPD=0, and then correcting for vapour pressure differences caused by the difference in T_c-T_a (Idso et al. 1981). The obtained UL followed a linear regression and represents the maximum T_c-T_a values of severely stressed grapes presumably under complete stomatal closure. The high variability of the NWSBs suggested to calculate the $(T_c$-$T_a)_{LL}$ taking the minimum values of T_c-T_a for each VPD (Bellvert et al. 2013). The lower limits (LL) were developed for a relatively wide range of VPD (1-5 KPa). Given the observed differences, the NWSBs were separated according to different phenological stages: i) from anthesis to fruit-set (berries at pea size) (Stage I), ii) from fruit-set to veraison (Stage II), iii) from veraison until harvest (stage III), and iv) from harvest until fourty days after harvest (postharvest). Air temperature (T_a) and vapour pressure deficit (VPD) were obtained from two portable weather stations (Watchdog 2000; model 2475 Plant growth, Spectrum Technologies, Inc. Plainfield, Illinois, USA) located on one side of the vineyards.

Airborne campaign

The airborne campaigns were conducted with a thermal camera (FLIR SC655, FLIR Systems, USA) installed on an aircraft (CESSNA C172S EC-JYN). The camera has a resolution of 640x480 pixels, equipped with a 24.5 mm f1.0 lens, connected to a computer via USB 2.0 protocol. The spectral response was in the range of 7.5-13 μm. The camera radiometric calibration was assessed in the laboratory using a blackbody (model P80P, Land Instruments, Dronfield United Kingdom). In addition, various calibrations were conducted at the time of each flight using surface temperature measurements to improve the calibration conducted. The accuracy of this method is discussed in Berni et al. (2009a,b), who demonstrated an accuracy below 1 K using a similar camera on board an Unmanned Aerial Vehicle (UAV). The flying pattern was carried out for 250 ha which contained the four studied plots (Fig.3.1a). It consisted in twenty longitudinal lines of 1500 meters separated by 70 meters. The flights were conducted at 12:00 solar time (14:00 local time) on 9 and 24 June, 7 July, 4 and 28 August and 12 September of 2011 at 150 m altitude above the ground level. Unless otherwise specified, all times referred here are solar times. Air vapour pressure deficit (VPD) on these days ranged from 1.89 to 4.73 KPa. Images obtained had 30-cm spatial resolution enabling the use of pure grapevine-crown pixel and excluding soil, background targets, and shadows (Fig.3.1b).

Concomitant to each flight, Ψ_L was measured to compare the temperature obtained from aerial thermal imagery with a ground-based stress indicator. Leaf water potential was measured in eighteen grapevines of each variety, with different water status, one measurement on each vine. Grapevines with different water status were selected in different locations within each plot taking into account spatial variability across vineyards. In each measured vine, aluminum paper was used between rows as a reference surface to extract canopy temperature (T_c) pixels from the same grapevines where Ψ_L was measured (Fig.3.1c). To carry out these measurements, two teams, each equipped with a pressure chamber on a truck carried out all the measurements so that they could be performed within one hour around the time of flying.
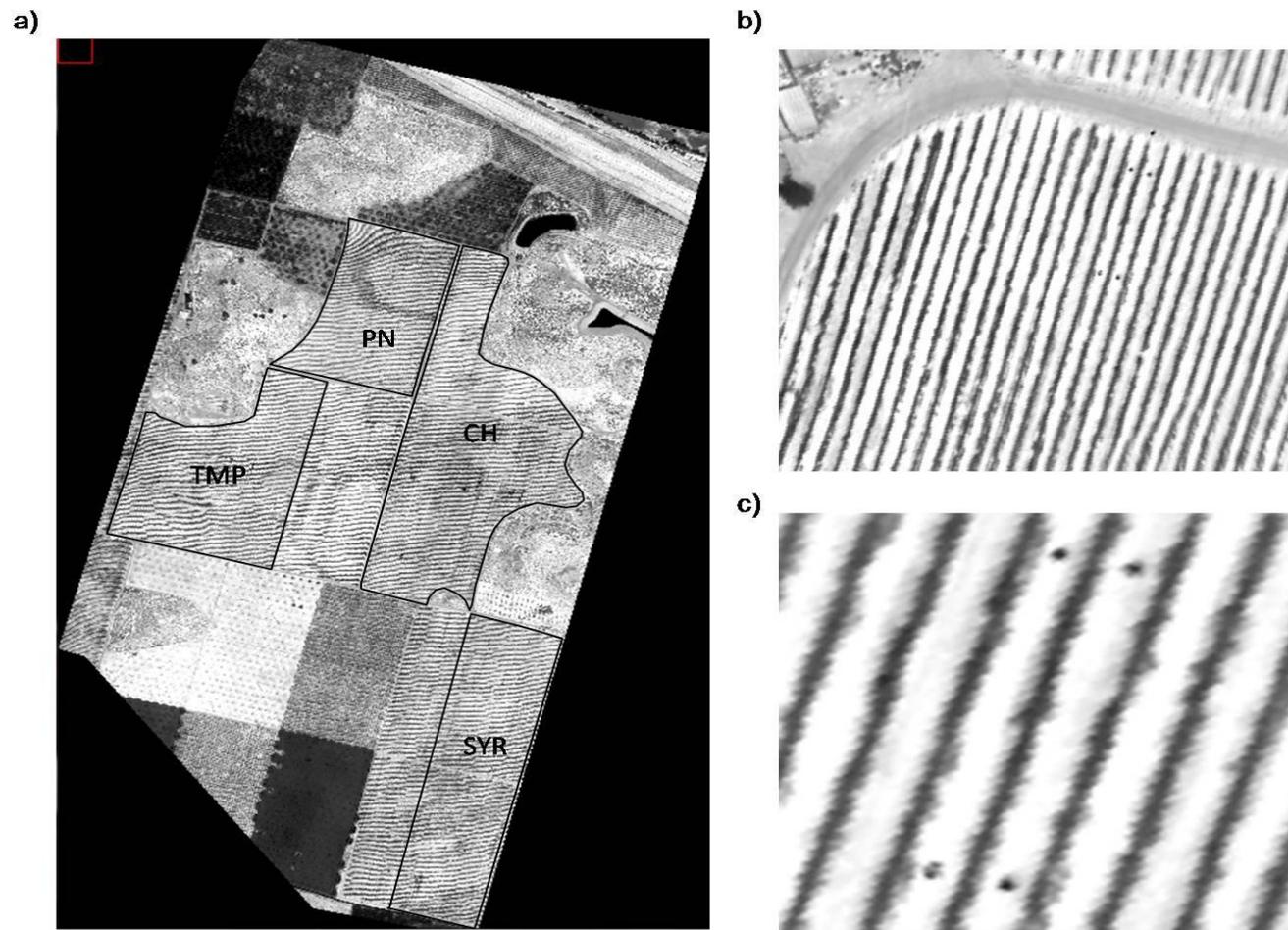
**Figure 3.1. Thermal mosaic acquired with a thermal camera FLIR SC-655on board an aircraft yielding 30 cm pixel resolution, observing: a) the different vineyard plots of Raimat (Lleida); 1) Pinot-noir (PN), 2) Chardonnay (CH), 3) Tempranillo (TMP) and 4) Syrah (SYR), b) the vineyard study sites used for field data collection, and c) detailed image of measured grapevines located with aluminium paper between rows.**

Estimation of leaf water potential from CWSI

Crop water stress index (CWSI) was calculated according with Eq.1 for each variety at different phenological stages using developed seasonal baselines. Curves were fitted to the empirical relationships between CWSI and Ψ_L for the following three manners: a) a general relationship made up by composite of all available data, b) relationships for each grapevine variety, and c) relationships for each phenological stage. For the three relationships, CWSI was determined using the developed baselines from our study. Estimation of Ψ_L was based on using the previous three relationships and its accuracy analyzed by comparing to the observed Ψ_L. To determine which of the three manners had the best fit and prediction, estimated and observed Ψ_L measurements were plotted against each other.

Image processing methods were used to extract canopy temperature (T_c) from pixels of those vines where Ψ_L was measured. We manually selected the pixels in each vine to ensure that only pure crown vegetative pixels were taken. The same selected pixels in each vine were used to extract T_c in each of the six thermal images.

Validation measurements

The methodology proposed to estimate Ψ_L was validated during 2013 in different vineyards from those of 2011. The new vineyards were located in the same region of Raimat (Lleida, Spain). Three different vineyards of Chardonnay ageing thirteen years old and one of Tempranillo ageing fourteen were used for the validation. Areas of Chardonnay vineyards were 44.2, 19.0 and 17.8 ha, respectively, and Tempranillo vineyard area was 5.9 ha. The spacing between vines and between rows in Chardonnay vineyards was 2 and 3 m, respectively, and with a north-south orientation. Tempranillo vineyard spacing was 3.2 m between rows and 1.6 m within rows, and with a east-west orientation. Canopies of all vineyards were cordon-trained to an espalier system at a height of 0.9 m, and their width ranged from 25 to 80 cm. All vineyards were under drip irrigation and irrigation was managed by each grower.

Two and three flights were carried out during stages II and III of each variety, respectively. During each flight, twenty and eight Ψ_L measurements were made respectively for each Tempranillo and Chardonnay vineyard. Location of measured vines within each vineyard was randomly selected at each flight. The same methodology described in 2011 for obtaining T_c was also used in 2013. Aluminum paper was also used between rows to mark the exact location where Ψ_L was measured and the considered canopy temperature (T_c) pixels. CWSI of each measured vine was calculated by using the respective phenological baselines developed in this study (Table 3.3).

Statistical data analysis

Non-watered-stressed baselines (NWSB) were transformed to a linear regression model with the proposal to analyze differences between varieties and phenological stages. A covariance analysis (ANCOVA) was performed to analyze these differences using the SAS statistical package (version 9.2; SAS Institute, Cary, NC, USA). Specific differences among varieties and phenological stages in the slopes and intercept of the lines were subsequently tested by orthogonal contrasts.

Data from the six thermal images were analyzed by phenological stages. Stage I corresponded with the thermal image from 9 June (Cumulative degree-day since budbreak, CDD=577). Stage II was the averaged data obtained in 27 June (CDD=866) and 8 July (CDD=1051). Stage III for Pinot-noir and Syrah was assessed using the averaged data of 4 (CDD=1467) and 24 August (CDD=1835). Chardonnay was harvested at the beginning of August, and only data of 4 August was used for Stage III. For Tempranillo, we used the data averaged for 4 and 24 August, and 12 September (CDD=2144). The post-harvest period was studied in Chardonnay and Pinot-noir. Thermal images acquired on 24 August and 12 September referred to 15 and 35 days after harvest for Chardonnay. The 12 September image corresponded to 20 days after Pinot-noir harvest.

Results

Crop water stress index

The calculation of CWSI relies on the relationship between T_c-T_a and VPD of well-watered grapevines for obtaining a 'non-water-stressed baseline'. Encompassing all collected data from six grapevine varieties, a significant relationship between T_c-T_a and VPD was detected (Fig.3.2). There was, however, a wide range of variability in this relationship which recommended analyzing data separately by phenological stages and varieties.
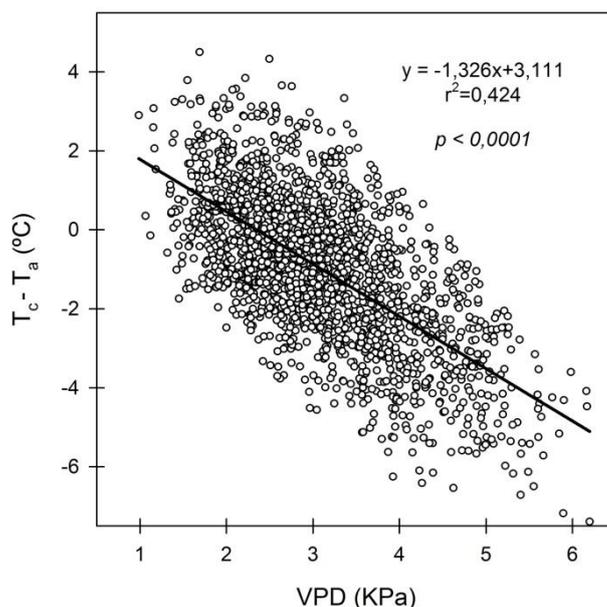
Figure 3.2. Relationship between difference of canopy and air temperature (T_c-T_a) and vapour pressure deficit (VPD) of all available days of the season in the well-irrigated grapevine varieties of Pinot-noir, Chardonnay, Syrah and Tempranillo. Relationship was obtained using data from 11:00 to 16:00 hours.

The relationships between T_c-T_a and VPD presented a significant phenological response, which mainly indicated differences between stage I and further stages (Figs.3.3, 3.4). Variety also interacted with the seasonal effect. In fact, the covariance analysis performed by each phenological stage indicated a distinctive variety effect with VPD on T_c-T_a (Table 3.1; Fig.3.3). Coefficients of determination (r^2) ranged from 0.401 to 0.667. The slopes of the relationship T_c-T_a vs. VPD were significantly different between varieties during stages I and II (Table 3.1). During stage I in Chardonnay and Syrah in stage II, their slopes were significantly gentler than in other varieties. The variety parameter of the covariance analysis was significant (p < 0.0001) during stage III and postharvest stage (Table 3.1). The varieties that were significantly different during stage III were Chardonnay and Tempranillo. Both varieties had a low intercept during stage III (Fig.3.3c),

104

although Tempranillo had the lowest T_c-T_a values in response to VPD in stage III. During postharvest stage, intercept of Chardonnay was much lower than Pinot-noir. In fact, T_c-T_a mean was -1.62 and -0.03 ºC for Chardonnay and Pinot-noir, respectively (Fig.3.3d).
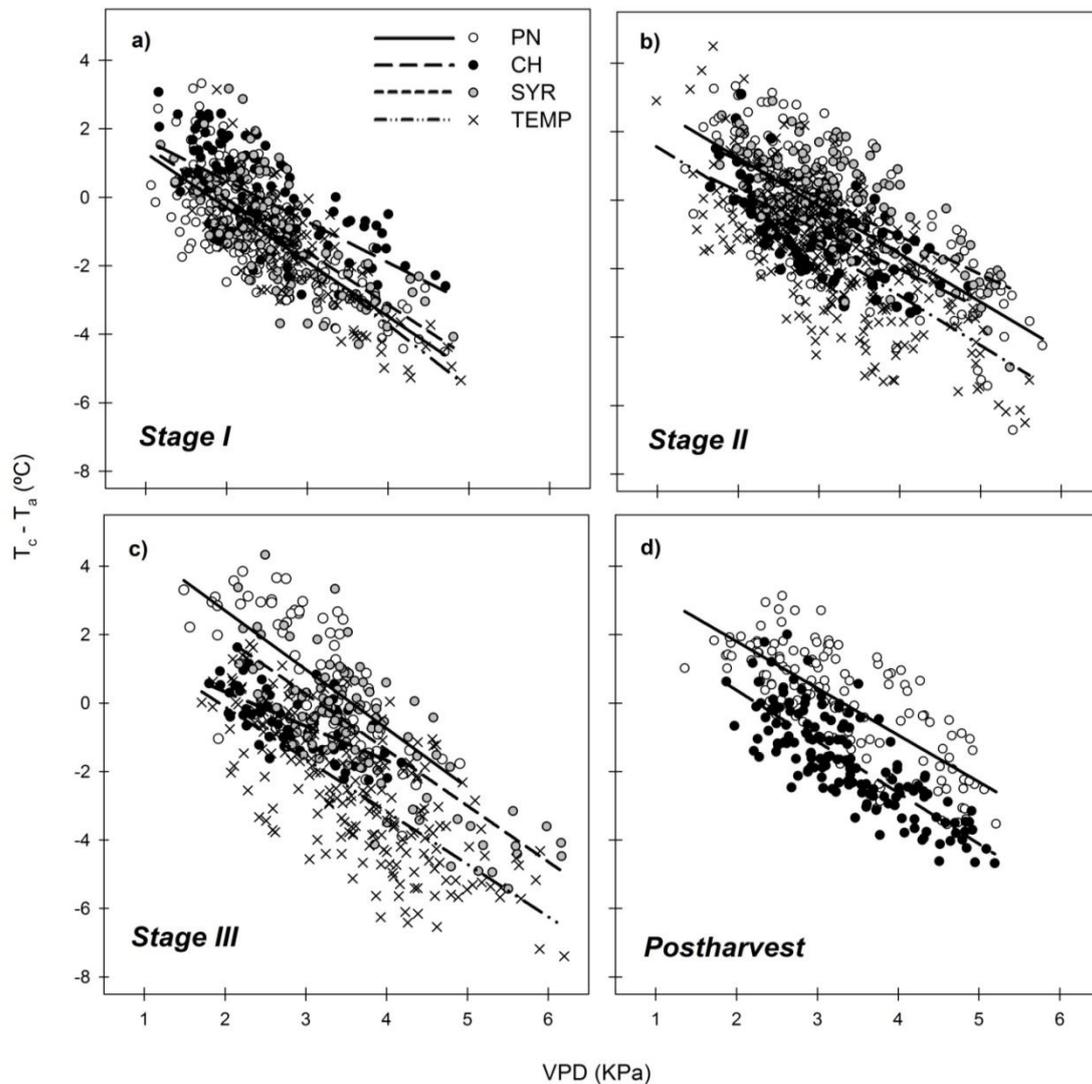
Figure 3.3. Differences between varietiesPinot-noir (PN), Chardonnay (CH), Syrah (SYR) and Tempranillo (TMP) in therelationship between difference of canopy and air temperature (T_c-T_a) and vapour pressure deficit (VPD) at different phenological stages (Stage I, II, III and post-harvest). Equations and coefficients of determination (r^2) are: Stage I; PN: y = -1.592x+2.885, r^2=0.553; CH: y = -1.194x+2.869, r^2=0.437; SYR: y = -1.542x+3.027, r^2=0.521; TMP: y = -1.848x+3.675, r^2=0.649. Stage II; PN: y = -1.403x+4.043, r^2=0.524; CH: y = -1.138x+2.529, r^2=0.401; SYR: y = -1.026x+3.066, r^2=0.457; TMP: y = -1.479x+3.107, r^2=0.489. Stage III; PN: y = -1.722x+6.146, r^2=0.469; CH: y = -1.004x+2.335, r^2=0.426; SYR: y = -1.576x+4.929, r^2=0.565; TMP: y = -1.449x+2.685, r^2=0.515. Post-harvest; PN: y = -1.367x+4.536, r^2=0.575; CH: y = -1.540x+3.535, r^2=0.667. All relationships were significant (p< 0.0001).

Taula 3.1. ANCOVA analysis of T_c-T_a for grapevine varieties at different phenological stages, and probabilities tested by orthogonal contrasts of slopes (VPD*Variety) and intercepts (Variety).

ANCOVA	Stage I	Stage II	Stage III	Post-harvest
VPD	< 0.0001	<0.0001	<0.0001	<0.0001
Variety	0.4203	0.1368	<0.0001	0.0120
VPD*Variety	0.0073	0.0034	0.1180	0.3415

Contrast	VPD*Variety		Variety	
	Stage I	Stage II	Stage III	Post-harvest
CH vs. PN	0.0310[*]	0.2831	0.0003[*]	0.0122[*]
PN vs. SYR	0.8991	0.0192[*]	0.1408	-
PN vs. TEMP	0.1122	0.2991	<0.0001[*]	-
CH vs. SYR	0.0562	0.5592	0.0065[*]	-
CH vs. TEMP	0.0010[*]	0.0690	0.9999	-
SYR vs. TEMP	0.1094	0.0004[*]	<0.0001[*]	-

*Significant at P<0.05 (SAS, 2002).

Phenological responses in the relationship between T_c-T_a and VPD were analyzed for each variety (Fig.3.4). Relationship between T_c-T_a and VPD for all seasonal data showed that Pinot-noir and Syrah presented a higher variability in comparison with those of Tempranillo and Syrah. Phenological variations in the T_c-T_a response to VPD for Pinot noir and Syrah during stage I explained this variability (Fig.3.4a,c). In fact, the covariance analysis indicated that the stage parameter (intercept) was significant for varieties Pinot-noir and Syrah (Table 3.2), and T_c-T_a values for both varieties were clearly lower during stage I than those of stages II-III. No significant differences were found in Pinot-noir between stage II-III and postharvest (Fig.3.4a). In Chardonnay, the covariance analysis showed that the interaction between stage and VPD (slope) changed significantly with the phenological stage, with the postharvest stage slope significantly steeper than that in the preharvest stages (Fig.3.4b, Table 3.2). However, non significant differences were found for the slope of Chardonnaybetween stages I and II-III. Phenology did not affect the relationship between T_c-T_a and VPD in well-watered vines of Tempranillo (Fig.3.4d, Table 3.2). The T_c-T_a vs. VPD relationships of stages II and III were not significantly different (p=0.698) and data presented in Fig. 3.4 for both stages was joined obtaining a unique baseline (stage II-III).
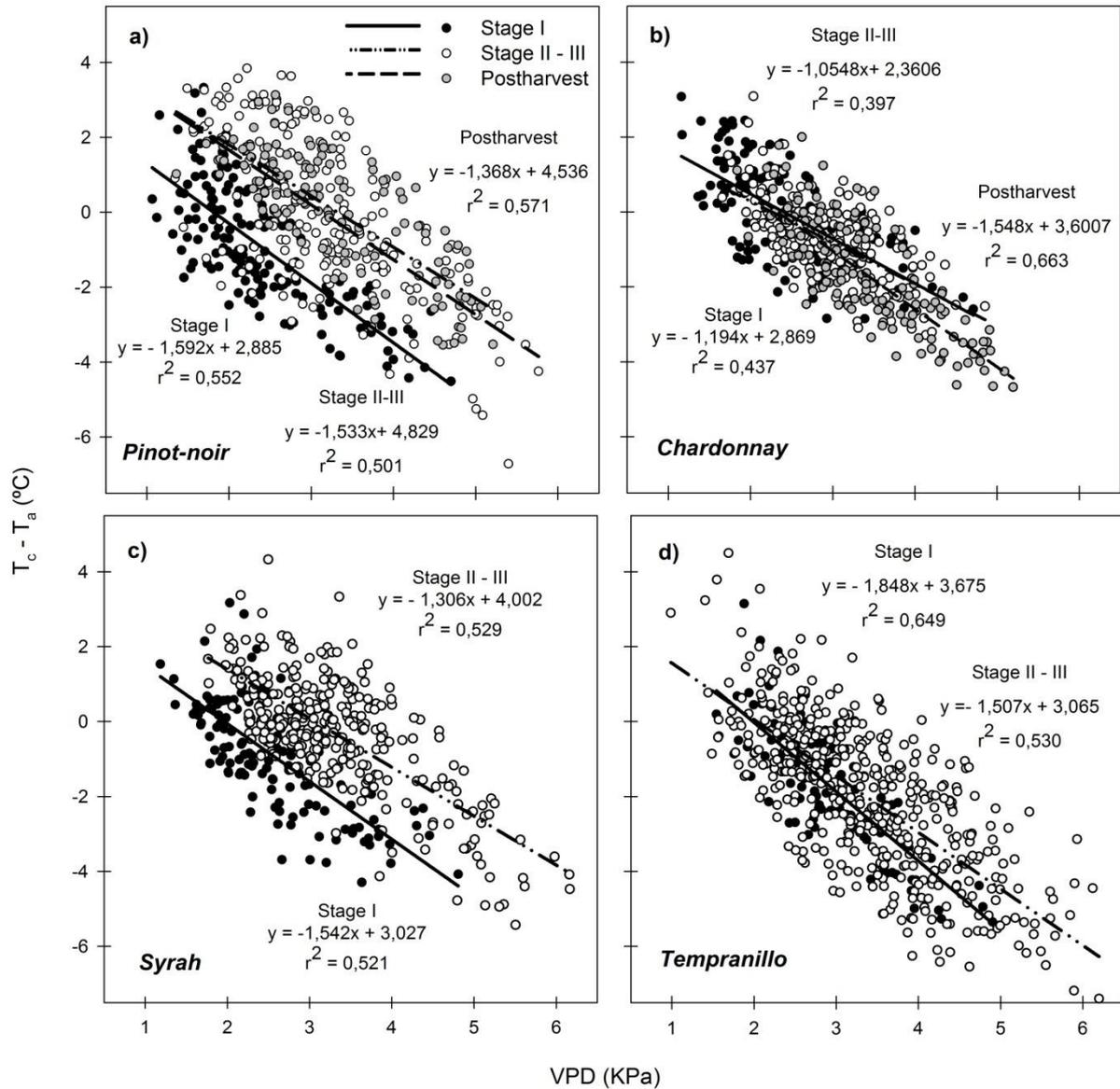
**Figure 3.4. Seasonal response of difference between canopyand air temperature (T_c-T_a) to vapour pressure deficit (VPD) for Pinot-noir (PN), Chardonnay (CH), Syrah (SYR) and Tempranillo (TMP). Regression lines are plotted for each phenological stage. Data from stages II and III was joined in this analysis obtaining a unique baseline of stage II-III. All relationships were significant (p< 0.0001).**

Taula 3.2. ANCOVA analysis of T_c-T_a for phenological stages, and probabilitiestested by orthogonal contrasts of slopes (VPD*Stage) and intercepts (Stage).

ANCOVA	Chardonnay	Pinot-noir	Syrah	Tempranillo
VPD	< 0.0001	<0.0001	<0.0001	<0.0001
Stage	0.0551	0.0003	0.0192	0.2855
VPD*Stage	0.0037	0.4543	0.1055	0.0657

Contrast	VPD*Stage	Stage		
	Chardonnay	Pinot-noir	Syrah	
I vs. II-III	0.5723	0.0002[*]	0.019[*]	-
I vs. PH	0.0142[*]	0.0021[*]	-	-
II-III vs. PH	0.0018[*]	0.9284	-	-

*Significant at P<0.05 (SAS, 2002).

   Equations of the baselines (lower and upper limits, LL and UL) are shown in Table 3.3. The baselines followed a lineal regression model. During stage I, Chardonnay had the maximum intercept of the upper limit (UL) by reaching at 6.61 ºC when vapour pressure deficit was zero (Fig.3.5a). At this stage, the upper limit of Pinot-noir and Syrah were similar, but Tempranillo had the lowest intercept. The UL during stages II-III also showed differences between varieties (Fig.3.5b). Chardonnay had the maximum intercept, reaching 6.45 ºC when vapour pressure was zero. On the other hand, Syrah was the variety that had a UL with lower T_c-T_a values. Tempranillo and Pinot-noir had a similar upper limit during stages II-III. Postharvest period showed differences in the baselines between Pinot-noir and Chardonnay (Fig.3.5c). The maximum intercept of the UL corresponded to Pinot-noir, by reaching 5.38 ºC when vapour pressure deficit was zero. Analyzing differences between the baselines among phenological stages, it seemed that the UL did not varied between stage I and II-III, with the exception of Tempranillo, that had a higher intercept during stages II-III than in stage I. During postharvest, the UL of Chardonnayappeared shifted down compared to preharvest stages. The lower limits (LL) showed that during stages II-III, Tempranillo was the variety that presented more transpirational cooling for a given increase in the air vapour pressure deficit. During postharvest, the lower limit of Chardonnay had a slope and intercept lower than Pinot-noir.
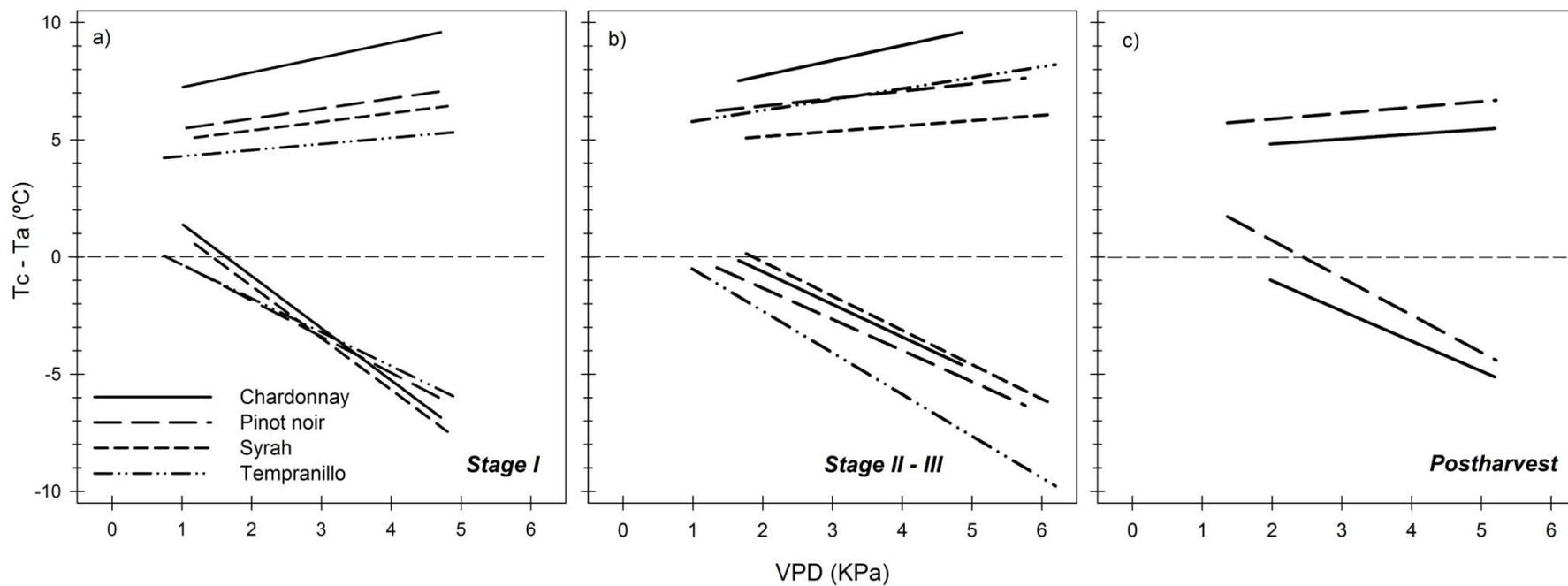
Figure 3.5. Lower and Upper limits of the relationships between (T_c-T_a) and VPD for determination of crop water stress index (CWSI) in Chardonnay, Pinot-noir, Syrah and Tempranillo, at phenological stages: a) stage Stage I, b) Stage II-III, and c) Postharvest. Equations are shown in Table 3.3.

Table 3.3. Equations of lower and upper limits for each phenological stage of the grapevine varieties Pinot-noir, Chardonnay, Syrah and Tempranillo. *y* corresponds with difference of canopyand air temperature (T_c-T_a), and *x* represents vapour pressure deficit (VPD).

	Lower limits			Upper limits		
	Stage I	Stage II-III	Post-harvest	Stage I	Stage II-III	Post-harvest
Pinot-noir	y = -1.544x+1.226	y = -1.331x+1.332	y = -1.593x+3.887	y = 0.429x+5.043	y = 0.316x+5.808	y = 0.250x+5.383
Chardonnay	y= -2.226x+3.638	y = -1.393x+2.157	y = -1.285x+1.551	y = 0.632x+6.609	y = 0.635x+6.451	y = 0.205x+4.415
Syrah	y= -2.213x+3.176	y= -1.465x+2.729	-	y= 0.371x+4.653	y= 0.228x+4.673	-
Tempranillo	y= -1.438x+1.098	y= -1.780x+1.253	-	y= 0.261x+3.977	y= 0.466x+5.3167	-

Relationships between remotely sensed CWSI and midday Ψ_L

Midday Ψ_L measurements correlated significantly with remotely sensed CWSI for our four varieties (Fig.3.6). However, the relationship found by using all data indicated a high variability (Fig.3.6a), which suggested separate data analysis by variety and phenological stage.

All relationships had a curvilinear shape, indicating a clearly signal of water stress with only after a threshold value in CWSI. Maximum CWSI corresponded with Ψ_L values around -1.6 MPa, with the partial exception of Tempranillo which seemed to be around -1.4 MPa (Fig.3.6b). This point was associated with complete stomatal closure and zero transpiration. Sensitivity of CWSI to changes in Ψ_L was different between varieties. In Chardonnay, for a given decrease of Ψ_L changes in CWSI were lower than in the other three varieties. On the contrary, it seems that Tempranillo was the variety which presented the highest changes of CWSI as Ψ_L values decreased. Phenological effects were also evident; it seems that for a determinate level of CWSI, the values of Ψ_L were more negative as crop developed (Fig.3.6c). Therefore, stage III was related with lower Ψ_L which implied a higher water uptake from soil in comparison with early stages. It seemed that postharvest period was similar to stage III.

These results suggested both a varietal and seasonal different response in the relationship between CWSI and Ψ_L. With the purpose to identify which one of the effects had strongest influence on CWSI vs. Ψ_L, Ψ_L was estimated by three different manners and related with observed Ψ_L by linear regression. Ψ_L was first estimated from a general relationship between CWSI and observed Ψ_L, and successively for each varietal and phenological relationship. The one-to-one relationships between estimated and observed Ψ_L were significant ($p<0.0001$), but differences in their slopes and intercepts were found depending on the method used for estimating Ψ_L (Fig.3.7). The linear regression from a general relationship showed the lowest coefficient of determination (r^2) (Fig.3.7a). This regression also had the lowest slope and intercept. The linear regression for estimating Ψ_L considering the variety had a higher r^2 (Fig.3.7b). The slope and intercept of the regression were also higher in comparison with the general method. Finally, it seems that the best fit was obtained when each phenological stage was considered (Fig.3.7c). This relationship presented the highest r^2, and an equation with the closest slope to one and intercept to zero.

Discussion

The developed non-water-stressed baselines and the relationships between CWSI and leaf water potential (Ψ_L) differed with respect to variety and phenological stage. Accordingly we will discuss first the CWSI baselines and their relationships with Ψ_L, and subsequently the effect of variety and phenological stage.

Crop water stress index baselines

For the four studied varieties, T_c-T_a values for well-watered grapevines decreased as vapour pressure deficit increased (Fig. 3.3, 3.4). However, differences in the slopes and intercepts of the relationship between T_c-T_a and VPD were found between varieties and phenological stages. For instance, in stage I of Chardonnay and stage II of Syrah, the relationships presented a gentler slope in comparison to other varieties (Table 3.1). This implied that, for a given increase in VPD, Tempranillo and Pinot-noir had more transpirational cooling than Chardonnay and Syrah in their respective stages. It should be considered that stage III was longer for the two red varieties (Syrah and Tempranillo) and this could have provided better opportunities for finding differences between varieties. The intercept of the T_c-T_a vs. VPD relationship was significant for Tempranillo during stage III, indicating a higher evaporative cooling than Syrah and Pinot-noir (Fig. 3.3c). Stomatal density, size of stomata and the degree of opening of the pore could modulate stomatal conductance (Weyers and Meidner, 1990). Costa et al. (2012) reported a higher leaf stomatal conductance (g_s) and stomatal density in Tempranillo than in Syrah, which could explain, in part, the lower T_c-T_a values found in Tempranillo. Chardonnay was harvested around fifteen days before Pinot-noir. Then, most of T_c data measured in Chardonnay during this period corresponded with leaves fifteen days younger than those of Pinot-noir, and could have a higher transpiration capacity. Significant differences found in the intercept of Chardonnay and Pinot-noir during postharvest, could be related with a leaf age effect (Field 1987).

Different phenological responses in the relationship between T_c-T_a and VPD were also shown in Fig.3.4 for some grapevine varieties. Differences between phenological stages may be explained in part by the energy balance of a crop canopy, zenith solar angle or leaf orientation. The intercept of the relationship between T_c-T_a and VPD is a function of aerodynamic resistance to water vapour transfer (r_a) and net radiation (R_n), according with the theoretical equation provided by Jackson et al. (1981). Thus, the intercept is expected to increase with solar radiation. Testi et al. (2008) demonstrated that the intercept of the relationship between T_c-T_a and VPD for well-watered pistachio trees (NWSB) increases with zenith solar angle, and probably acts on the targeted canopy temperature area by changing the fraction of shaded leaves. For this reason, as the season advances we identified a shift in the intercept of the relationship between T_c-T_a and VPD in Pinot-noir and Syrah (Fig.3.4, Table 3.2). In these two varieties, the intercept increased as crop developed. This could be explained assuming that during early stages both R_n and zenith

solar angle are lower. However, this phenological shift was not detected in Chardonnay and Tempranillo and the reason for this is unknown. The linear relationship between T_c-T_a versus VPD in Pinot-noir was also reported by Bellvert et al. (2013) for two year previous to the present study, corresponding with T_c-T_a= -1.925 VPD + 4.738. This equation fitted well the relationship of stage II-III from our study (Fig.3.4). Despite slight differences in the slopes, the intercepts of both were very similar (T_c-T_a = -1.533x + 4.829). This agreement gives consistency to the CWSI approach.

The developed baselines indicated that Chardonnay was the variety that could reach the highest leaf temperatures in the UL during preharvest stages (Table 3.3, Fig.3.4). Morphological considerations of leaves and canopy light distribution effects may explain part of the leaf heating differences between varieties at stomatal closure. When stomata are closed, leaf temperature becomes more dependent on the ability of a leaf to exchange sensible heat with the air. The heat exchange ability depends in part on the width of the leaf, related boundary layer development (Gates and Papian 1971; Nobel 2009). Entire leaves, such as those of Chardonnay may have limited sensible heat exchange and heat up significantly when stomates close in sunny conditions. Moreover, the studied Chardonnay vines had very thin vertical canopies. Compressing large entire flat leaves with high radiative heat loads may have contributed to leaf heating. In contrast, lacinated Tempranillo and Syrah leaves contained more canopy gaps, which could produce a wider range of light levels within the canopy due to a more porous exterior canopy. With more radiation penetrating into less exposed leaves may have reduced the intensity of radiation and leaf heating in the most exposed leaves. Pinot-noir leaves tend to be smaller than others and probably leaf heating in relation with stomatal closure could be less than in Chardonnay.

Relationship between CWSI and leaf water potential

The established method for quantifying plant water status in grapevines is the measurement of leaf water potential (Ψ_L) (Williams and Araujo 2002). In our work, the relationship between Ψ_L and CWSI had a curvilinear shape and indicated that transpiration rate must have been reduced progressively from a specific Ψ_L threshold until reaching complete stomatal closure (CWSI=1) (Fig.3.6). The high variability found in this relationship by using all data (Fig.3.6a), suggested that there might be variety and/or seasonal effects. Stomatal conductance is the physiological parameter that affects leaf water vapour exchange and therefore canopy temperature. Osmotic adjustment can influence stomatal closure in response to water deficits, as it has been shown to occur in the grapevine and to be different among varieties (Costa et al. 2012) and phenological stages (Alsina et al. 2007).
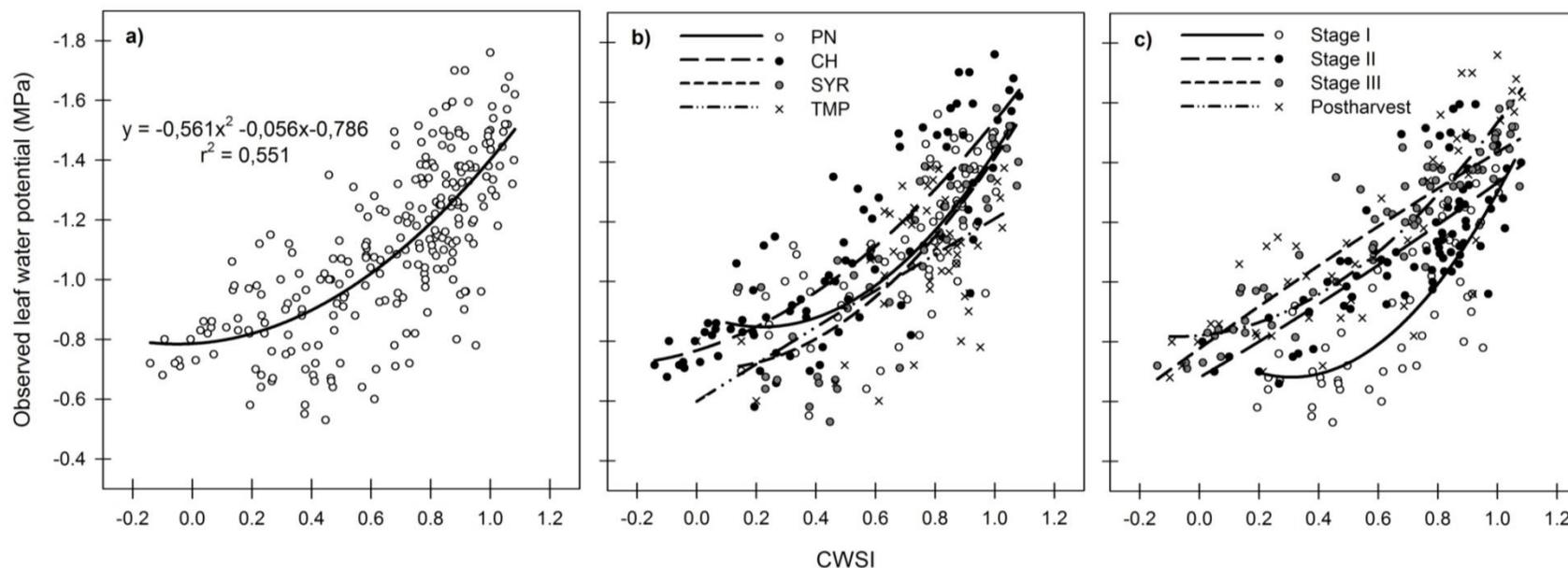
Figure 3.6. Relationships between CWSI and observed leaf water potential (Ψ_L), showing in: a) a general relationship with all data, b) relationships for grapevine varieties, and c) relationships for phenological stages. Equations and coefficients of determination (r^2) of the relationships shown in b and c, were: (b) PN: $y = -0.963x^2+0.425x-0.895$, $r^2=0.571$, CH: $y = -0.464x^2-0.303x-0.769$, $r^2=0.724$, SYR: $y = -0.762x^2+0.058x-0.709$, $r^2=0.752$, TMP: $y = 0.016x^2-0.628x-0.598$, $r^2=0.561$. (c) Stage I: $y = -1.294x^2+0.798x-0.805$, $r^2=0.647$, Stage II: $y = -0.063x^2-0.589x-0.681$, $r^2=0.605$, Stage III: $y = 0.061x^2-0.718x-0.778$, $r^2=0.861$, Postharvest: $y = -0.616x^2-0.096x-0.821$, $r^2=0.715$.

Analyzing the relationships among varieties, it seemed that different responses in the relationship between Ψ_L and CWSI could be related with their different ability to regulate stomatal aperture. Changes in CWSI were less per unit change of Ψ_L in Chardonnay in comparison with the other three varieties (Fig.3.6b). By contrast, Tempranillo had the greatest change in CWSI per unit change of Ψ_L. Chardonnay is characterized for a lower control over stomatal closure under water stress (Schultz, 2003; Pou et al. 2012). This may explain the reason why Chardonnay had lower CWSI values in comparison with other varieties. While vine water status can regulate stomatal conductance, stomatal control over transpiration also involves chemical and/or hydraulic messages (Tardieu and Davies 1993). Thus, differences in hydraulic conductance between varieties may be also related to Ψ_L responses to CWSI. Considerations about this aspect may deserve more attention in further studies. Phenological responses detected in the relationship between CWSI and Ψ_L may depend on osmotic potential and leaf turgor seasonal changes (Fig.3.6c). These changes must be associated with fluctuations in leaf transpiration. Alsina et al. (2007) reported differences between varieties and phenological stages inosmotic potential values at full turgor and at the turgor loss point. In most cases, osmotic potential decreased as crop developed. Girona et al. (2006) also reported in Pinot-noir that Ψ_L values indicative of stress were higher during stage I than in further stages. Therefore, this hypothesis could explain the seasonal relationships shown in Fig.3.6c, where for a specific CWSI value, midday Ψ_L was higher at early stages than at full development.

According to these results, it seems that both parameters variety and phenology affected the relationship between Ψ_L and CWSI. In fact, the high variability of the general relationship between observed and estimated Ψ_L (Fig.3.7a), also emphasized that variety and/or phenological stage should be taken into account. Although the linear regression of estimated Ψ_L for considering each variety had a slightly improvement of r^2, slope and intercept (Fig.3.7b), it seems that phenology was the parameter that mostly affected on the relationship between CWSI and Ψ_L (Fig.3.7c). To carry out an irrigation schedule based on CWSI successfully, we recommend taking into account the differences due to phenological stage as well as the specific influence of Ψ_L for each variety.
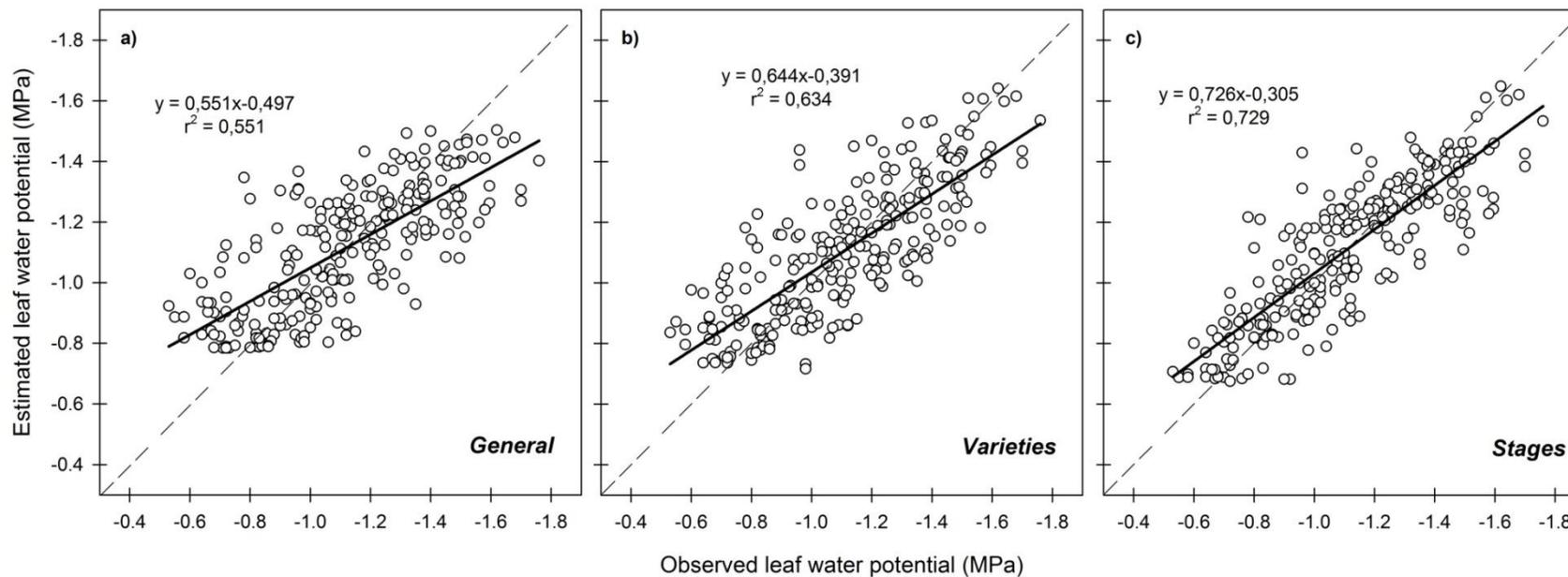
Figure 3.7. Simulation of the relationships between observed and estimated Ψ_L, where the latterwas calculated from:a) the general relationship between CWSI and Ψ_L, b) the relationships between CWSI and Ψ_L for each variety, and c) the relationships between CWSI and Ψ_L for each phenological stage.

Validation measurements

The robustness of the developed seasonal baselines in 2011 for calculating CWSI was tested by evaluating their accuracy on a validation data set during 2013. Estimated CWSI values in 2013 agreed with those of 2011 which were significantly related with Ψ_L for both Chardonnay and Tempranillo (Fig.3.8). In agreement with Fig.6c, the intercept of the relationship CWSI vs. Ψ_L was lower in stage II than stage III. Despite all Ψ_L values for Tempranillo during stage II of 2013 indicated that vines were well-watered, it follows the same tendency that data from 2011 (Fig.3.8a). The confirmatory data for two different seasons and different vineyards confirm that the developed seasonal baselines could be implemented in different years with irrigation management purposes. However, it is known that the empirical approach to determine CWSI has some degree of site specificity (Hipps et al. 1985). Thus, the extrapolation of our results to other growing conditions should be done with caution.
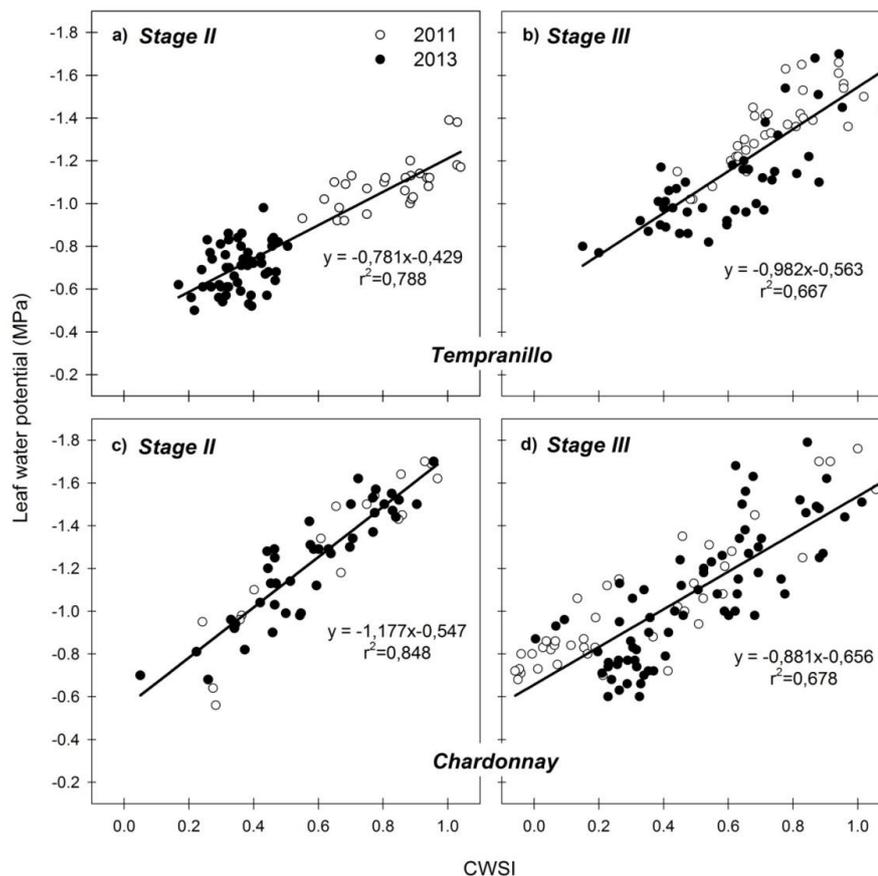
**Figura 3.8. Validation of the relationships between CWSI and observed leaf water potential (Ψ_L) for varieties Chardonnay and Tempranillo. Validations were obtained separately for the phenological stage II (a,c) and stage III (b,d). Relationships corresponded with data obtained during 2011 (○), and validation was made with data from 2013 (●). All relationships were significant (p< 0.0001).**

CWSI baselines for this study were well adjusted for each variety and correlated well with Ψ_L. The results in Pinot-noir were consistent with those developed in previous studies for the same variety. Our results demonstrated the necessity to develop seasonal baselines for each of the four varieties studied to reduce uncertainty in the calculation of CWSI. The developed baselines (lower and upper limits) showed significant differences among phenological stage and varieties. We suggest that for monitoring efficiently CWSI, the most appropriate procedure would be to establish the baselines and relationships with Ψ_L taking into account first the effect of phenology and secondly the variety.

References

Alsina, M.M., Herralde, de F., Aranda, X., Savé, R., Biel, C (2007) Water relations and vulnerability to embolism are not related: Experiments with eight grapevine cultivars. Vitis. 46, 1-6.

Bellvert, J., Zarco-Tejada, P.J., Girona, J., Fereres, E (2013) Mapping crop water stress index in a `Pinot-noir´ vineyard: comparing ground measurements with thermal remote sensing imagery from an unmanned aerial vehicle.Precision agriculture. Submitted.

Berni, J.J., Zarco-Tejada, P.J., Sepulcre - Cantó, G., Fereres, E., Villalobos, F (2009a) Mapping canopy conductance and CWSI in olive orchards using high resolution thermal remote sensing imagery. Remote sensing of Environment. 113, 2380-2388.

Berni, J.A., Zarco-Tejada, P.J., Suarez, L., & Fereres, E (2009b) Thermal and narrow-band multispectral remote sensing for vegetation monitoring from an unmanned aerial vehicle. IEEE Transactions on Geoscience and Remote Sensing. 47, 722-738.

Costa, J.M., Ortuño, M.F., Lopes, C.M., Chaves, M.M (2012) Grapevine varieties exhibiting differences in stomatal response to water deficit. CSIRO Publishing. Functional Plant Biology.39, (3) 179-189.

Clawson, K.L., Jackson, R.D, Pinter, P.J (1989) Evaluating plant water stress with canopy temperature differences. Agronomy Journal. 81, 858-863.

Field, C.B (1987) Leaf-age effects on stomatal conductance. In 'Stomatal Function'. (Eds E. Zeiger, G.D. Farquhar and I.R. Cowan.) (Stanford Univ. Press: Stanford, California.). 367-384.

Gates, D.M., Papian, L.E (1971) Atlas of Energy Budgets of Plant Leaves. Academic Press, New York.

Girona, J., Mata, M., del Campo, J., Arbonés, A., Bartra, E., Marsal, J (2006) The use of midday leaf water potential for scheduling deficit irrigation in vineyards. Irrigation Science 24, 115-127.

Hipps, L., Asrar, G., kanemasu, E (1985) A theoretically-based normalization of environmental effects on foliage temperature. Agricultural and Forest Meteorology. 35, 113-122.

Idso, S.B., Jackson, R.D., Pinter, P.J., Reginato, R.J., Hatfield, J.L (1981) Normalizing the stress-degree day parameter for environmental variability. Agricultural Meteorology. 24, 45-55.

Jackson, R.D., Idso, S.B., Reginato, R., Pinter, P.J (1981) Canopy temperature as a drought stress indicator. Water Resources Research. 17, 1133-1138.

Jackson, R.D., Kustas, W.P., Choudhury, B.J (1988) A re-examination of the crop water stress index. Irrigation Science. 9, 309–317.

Leinonen, I., H.G., Jones (2004) Combining thermal and visible imagery for estimating canopy temperature and identifying plant stress. J. Exp. Bot. 55, 1243-1231.

Marsal, J., Girona, J (1997) Relatioship betweenleaf water potential and gas exchange activity at different phenological stages and fruit loads in peach trees. J. Amer. Soc. Hort. Sci. 122, 415-421.

McCutchan, H., Shackel, K (1992) Stem-water potential as a sensitive indicator of water stress in prune trees (Prunus domestica L. cv. French). J. Amer. Soc. Hort. Sci. 117, 607-611.

Meron, M., Tsipris, J., Charitt, D (2003) Remote mapping crop water status to assess spatial variability of crop stress. In: Stafford J, Werner A, eds. Precision agriculture. Proceedings of the 4th European Conference on Precision Agriculture, Berlin, Germany. Wageningen: Academic Publishers, 405-410.

Möller, M., Alchanatis, V., Cohen, Y., Meron, M., Tsipris, J., Naor, A., Ostrovsky, V., Sprintsin, M., Cohen, S (2007) Use of thermal and visible imagery for estimating crop water status of irrigated grapevine. J. Exp. Bot. 58, 827-838.

Nobel, P.S (2009) Physiochemical and environmental plant physiology. 4th ed. Academic press, Amsterdam, Boston. p. 582.

Olivo, N., Girona, J., Marsal, J (2009) Seasonal sensitivity of stem water potential to vapour pressure deficit in grapevine. Irrigation Science. 27, 175-182.

Pou, A., Medrano, H., Tomàs, M., Martorell, S., Ribas-Carbó, M., Flexas, J (2012) Anisohydric behaviour in grapevines results in better performance under moderate wáter stress and recovery tan isohydric behaviour. Plant Soil. 359, 335-349.

Poni, S., Bernizzonia, F., Civardia, S., Gattia, M., Porro, D., Caminc, F (2009) Performance and water-use efficiency (single-leaf vs. whole-canopy) of well-watered and half-stressed split-root Lambrusco grapevines grown in Po Valley (Italy). Agriculture, Ecosystems & Environment. 129, 97–106.

Rogiers, S.Y Greer, D.H., Hatfield, J.M., Hutton, R.J., Clarke, S.J., Hutchinson, P.A., Somers, A., (2012) Stomatal response of an anisohydric grapevine cultivar to evaporative demand, available soil moisture and abscisic acid. Tree physiology. 32, 249-261.

SAS (2002) Enterprise Guide version 4.2 (SAS Institute Inc. Cary, NC, USA).

Schultz, H.R (2003) Differences in hydraulic architecture account for near-isohydric and anisohydric behavior of two field-grown Vitis vinifera L. cultivars during drought. Plant, Cell and Environment. 26, 1393-1405.

Schultz, H.R., Stoll, M (2010) Some critical issues in environmental physiology of grapevines: future challenges and current limitations. Australian Journal of Grape and Wine Research. 16, 4-24.

Soar, C.J., Dry, P.R., Loveys, B.R (2006a) Scion photosynthesis and leaf gas exchange in Vitis vinifera L. cv. Shiraz: Mediation of rootstock effects via xylem sap ABA. Australian Journal of Grape and Wine Research, 12, 82-96.

Soar, C.J., Speirs, J., Maffei, S.M., Penrose, A.B., Mc Carthy, Loveys, B.R (2006b) Grape vine varieties Shiraz and Grenache differ in their stomatal response to VPD: apparent links with ABA physiology and gene expression in leaf tissue. Australian Journal of Grape and Wine Research. 12, 2-12.

Tardieu, F., Davies, W.J (1993) Integration of hydraulic and chemical signalling in the control of stomatal conductance and water status of droughted plants. Plant, Cell and Environment. 16, 341-349.

Testi, L., Goldhamer, D.A., Iniesta, F., Salinas, M., (2008) Crop water stress index is a sensitive water stress indicator in pistachio trees. Irrigation Science. 26, 395-405.

Turner, N.C., Long, M.J (1980) Errors arising from rapid water loss in the measurement of leaf water potential by pressure chamber technique. Austr. J. Plant. Physiol. 7, 527-537.

Weathon, A.D., Cooley, N.C., Dunn, G.M (2011) Use of Thermal Imagery to Detect Water Stress during Berry Ripening in Vitis vinifera L. 'Cabernet sauvignon'. 6th IS on Irrigation of Hort. Crops.Acta Hort. 889, 123-130.

Weyers, J.D.B., Meidner, H (1990) Methods in Stomatal Research. Longman Scientific & Technical, Harlow, England.

Williams, L.E., Araujo, F.J (2002) Correlations among predawn leaf, midday leaf and midday stem water potential and their correlations with other measures of soil and plant water status in vitis vinifera. J Am Soc Hort Sci. 127, 448-454.

Yuan, G., Luo, Y., Sun, X., Tang, D (2004) Evaluation of a crop water stress index for detecting water stress in winter wheat in the North China Plain. Agricultural Water Management. 64, 29-40.

Discusión general

La variabilidad espacial de los viñedos es actualmente una de las principales preocupaciones del sector vitivinícola, ya que afecta la heterogeneidad productiva y de la calidad de la uva. Realizar un manejo diferencial del riego en viñedos ha demostrado ser una herramienta útil para obtener producciones más uniformes. A lo largo de esta tesis doctoral se ha presentado una novedosa herramienta basada en la teledetección, la cual permite identificar el estado hídrico de la vid y tomar decisiones de riego a nivel de toda la parcela.

El primer paso para poder realizar un manejo del riego eficiente es disponer de un diseño de los sectores de riego acorde con la variabilidad del viñedo. Los métodos más extendidos para re-sectorizar los sectores de riego se basan en el conocimiento del viñedo por parte del viticultor, las propiedades del suelo, diferencias productivas o crecimiento vegetativo. Sin embargo, el elevado número de medidas que requieren muchos de estos métodos hace que sean sistemas poco económicos. En el ***Capítulo 1*** de esta tesis doctoral se ha estudiado la influencia sobre la variabilidad productiva de re-sectorizar un viñedo comparando dos metodologías distintas: i) potencial hídrico de hoja (Ψ_L) y, ii) índice de vegetación Plant Cell Density (PCD). Se determinaron diferencias entre los años en que se adoptó una estrategia de riego deficitario controlado (RDC) y aquellos que se regaron en la totalidad de sus necesidades hídricas. Así, la variabilidad productiva intra-parcelaria de un viñedo regado al 100% de sus necesidades hídricas fue menor que cuando se adoptaron estrategias de RDC. Teniendo en cuenta que la adopción de estrategias de RDC en variedades tintas de viña es común, los resultados del presente estudio recomendaron que cuando se adopta una estrategia de RDC, la mejor metodología para definir unos nuevos sectores de riego sea mediante el método del Ψ_L, el cual está más relacionado con los parámetros fisiológicos de la viña. Así, el método del Ψ_L disminuyó la heterogeneidad productiva en un 26.4%, mientras que el método PCD solamente la disminuyó en un 16.7%.

Los índices estructurales de vegetación se basan en determinar la vegetación activa densa a partir del contraste entre la reflectividad en el rojo y en el infrarrojo cercano. Sin embargo, actualmente su aplicación más extensa se basa en identificar subzonas con características similares dentro de los viñedos e incluso para re-sectorizar en función de las diferencias de vegetación. Sin embargo, el Capítulo 1 de esta tesis ha demostrado que si se pretende obtener viñedos productivamente más uniformes, ésta no parece ser la metodología más adecuada para re-sectorizar, ya que estos índices no están estrictamente relacionados con los parámetros fisiológicos del cultivo y no siempre tienen porqué presentar una relación con la producción o calidad de la uva. Algunos de los problemas más significativos de éstos índices se presentan a continuación:

-      Algunos estudios han demostrado que no presentan una relación lineal con el índice de área foliar (LAI) y fracción de radiación interceptada (FIR), saturándose a partir de un cierto nivel (Haboudane et al. 2004; Guillén-Climent et al. 2012). Por lo tanto, al ser estos índices indicadores de densidad de vegetación por píxel y no estrictamente de vigor vegetativo, en determinadas circunstancias podemos encontrarnos viñas con una alta FIR que presenten un mismo valor o incluso menor de PCD, en comparación con cepas con una

baja FIR. Cabe mencionar que el PCD también es sensible al sistema de conducción utilizado en la viña.

- Son índices altamente sensibles a cualquier parámetro que afecte la coloración de las hojas (enfermedades, tratamientos fitosanitarios, deficiencias cloróticas, etc.), ya que modifica la reflectividad del infrarrojo cercano y por lo tanto, disminuye el valor del índice.

- El Ψ_L está íntimamente ligado con los parámetros fisiológicos del cultivo y por lo tanto, está relacionado con el crecimiento vegetativo, producción y composición de la uva. Sin embargo, en determinadas circunstancias, el PCD y Ψ_L no presentan una buena relación, ya que un exceso de vegetación puede hacer disminuir el Ψ_L si el agua aportada no abastece la totalidad de la demanda hídrica del cultivo. En esos casos, identificaremos viñas con altos PCD y bajos valores de Ψ_L.

Por otro lado, una de las posibles desventajas de la utilización del Ψ_L para re-sectorizar los viñedos ha sido hasta hoy, el elevado número de medidas manuales que se requieren. Sin embargo, la implementación de la tecnología y teledetección en la agricultura y el desarrollo de plataformas aéreas capaces de sobrevolar a bajas altitudes han permitido que actualmente se pueda estimar el estado hídrico de grandes extensiones mediante la adquisición de imágenes térmicas. Esta tecnología por lo tanto, abre un abanico de oportunidades en distintas aplicaciones de la agricultura.

En el *Capítulo 2* de la tesis se ha desarrollado el índice Crop Water Stress Index (CWSI) como indicador del estado hídrico en viña. El método se ha desglosado para la variedad 'Pinot-noir' siguiendo el modelo empírico desarrollado por Idso et al. (1981). Para ello, durante los años 2009 y 2010 se determinaron las líneas base (non-water stressed baseline, NWSB) midiendo en continuo la temperatura de la hoja (T_c) de viñas que transpiraban a pleno, con los estomas completamente abiertos y sin déficit hídrico, utilizando sensores de temperatura infrarrojo (IRT). Ambos años, las NWSB mostraron una buena relación entre la diferencia de temperatura de la hoja y del aire (T_c-T_a) y el déficit de presión de vapor (DPV). Sin embargo, se observó que esta relación solamente fue significativa en el intervalo horario de las 10:00-16:00 hora solar, ya que fuera de este intervalo horario podía existir un efecto de la radiación solar. El distinto ángulo cenital solar a lo largo del día, afecta sobre la radiación total incidente en el dosel vegetativo y también en que haya una mayor proporción de hojas sombreadas a primeras y últimas horas del día. Por lo tanto, esta es una de las limitaciones del método a tener en cuenta y que algunos autores habían ya citado con anterioridad (Hipps et al. 1985).

Las validaciones del CWSI con el Ψ_L fueron consistentes tanto en las viñas individuales dónde se midió T_c con los sensores de temperatura infrarrojo (R^2=0.83), como en el viñedo entero a partir de la adquisición de imágenes térmicas de alta resolución (R^2=0.71). Con anterioridad, algunos autores también habían presentado relaciones significativas entre el CWSI y el Ψ_L, por ejemplo en la variedad 'Merlot' (Möller et al. 2007) o 'Cabernet Sauvignon' (Wheaton et al. 2011), desarrollando el CWSI bajo otras metodologías. Sin

126

embargo, todos los estudios previos consistían en realizar medidas a nivel de suelo en viñas individuales utilizando sensores de temperatura infrarrojo o cámaras termográficas manuales. El valor añadido de este estudio es que por primera vez se ha demostrado la posibilidad de detectar remotamente el estado hídrico de un viñedo mediante la adquisición de imágenes térmicas de alta resolución, además de poder validarlo con el Ψ_L.

Aspectos de operatividad del sistema de detección del estado hídrico mediante imágenes térmicas aéreas también se han estudiado en este capítulo. Se concluyó que operativamente, el momento idóneo para detectar el estado hídrico mediante imágenes térmicas debe de ser alrededor del mediodía, ya que por la mañana y tarde, el ángulo cenital solar es inferior y existe un efecto del sombreo en el dosel vegetativo, que hace disminuir la temperatura de la hoja. La validación realizada entre T_c-T_a y Ψ_L a las 7:30, 9:30 y 12:30 hora solar certificaron esta teoría, ya que en el vuelo de las 7:30 h no se pudo distinguir la diferencia de temperatura entre vegetación y suelo, y a las 9:30 h hubo un efecto de hojas sombreadas (R^2=0.46), obteniendo la mejor relación a las 12:30 horas (R^2=0.71).

La evaluación de la influencia del tamaño del píxel sobre la relación entre T_c-T_a y Ψ_L mostró que el tamaño de píxel mínimo en el cultivo de la vid debe ser de 30 cm, ya que es necesario aislar los elementos vegetativos del resto de componentes, como el suelo. Algunos sistemas de conducción del dosel vegetativo más recientes se basan en optimizar la intercepción de luz y facilitar la mecanización (ej. espaldera). Para ello, en estos sistemas es habitual el levantamiento de alambres para generar una cubierta vegetativa con una intercepción de radiación máxima, pero a la vez implica que tenga poca anchura. Es en estos casos cuando es importante disponer de imágenes térmicas de alta resolución, ya que un mínimo efecto del suelo puede hacer aumentar el valor del píxel objeto considerablemente y producir un error en el cálculo del CWSI. Esta necesidad de trabajar con altas resoluciones implica a la vez, una limitación en el sistema, ya los sensores térmicos disponibles actualmente (Miricle 307K o FLIR SC655) presentan una resolución espacial de 640 x 480 píxeles, y por lo tanto es necesario sobrevolar a bajas altitudes. Esto implica que la superficie sobrevolada por día, para detectar el estado hídrico (3 horas al mediodía) pueda ser como máximo alrededor de unas 2500 ha. Se espera que en un futuro próximo, nuevos sensores térmicos de mayor resolución espacial permitan obtener imágenes a una mayor altitud de vuelo, y con ello poder abastecer a una mayor superficie.

En este mismo sentido, otro tema a tener en cuenta es la idoneidad de la plataforma aérea. Por un lado, la utilización de vehículos aéreos no tripulados presentan claramente la ventaja de poder ser operados con alta frecuencia temporal y juntamente con los sensores térmicos actuales, ser una buena plataforma para adquirir imágenes térmicas de alta resolución. Sin embargo, la aplicación de estas plataformas para uso civil precisa superar ciertos aspectos técnicos y legislativos, que en el momento actual difieren según el país, siendo en algunos países muy restrictivos. Por otro lado, las avionetas tripuladas disponen de un espacio aéreo común y la legislación permite sobrevolar a bajas altitudes en determinadas circunstancias. La principal ventaja de utilizar estas plataformas es la mayor autonomía de vuelo y la facilidad para poder desplazarse de una zona estudio a otra más

rápidamente. La instalación de cámaras térmicas en avionetas tripuladas ha permitido que esta tecnología pueda ya ser aplicada comercialmente de forma rentable.

En el *Capítulo 3* de la tesis se estudió el efecto de la variedad y fenología sobre el CWSI y su relación con el Ψ_L. Se desarrollaron las líneas base (NWSB) para las variedades de viña 'Chardonnay', 'Pinot-noir', 'Tempranillo' y 'Syrah' en las distintas fases fenológicas (fase I, II, III y postcosecha). La relación entre T_c-T_a y DPV presentó diferencias significativas entre fases fenológicas, principalmente en las fases iniciales. Esas diferencias entre fases fenológicas pueden ser debidas al balance de energía del dosel vegetativo, al ángulo solar cenital o a la orientación de las hojas. Por ejemplo, la radiación solar en las fases iniciales de desarrollo vegetativo es menor en comparación con las fases posteriores. Estas diferencias afectan sobre la relación T_c-T_a vs. DPV, aumentando la intercepción de la función a medida que aumenta la radiación solar. El efecto varietal también debe de tenerse en cuenta para determinar el estado hídrico a partir del CWSI. Para un determinado déficit de presión de vapor, las variedades 'Tempranillo' y 'Pinot-noir' presentaron una mayor capacidad de refrigeración de las hojas (menor T_c-T_a) en comparación con 'Chardonnay' y 'Syrah'. Estas diferencias suelen ir ligadas a los parámetros que afectan la distinta capacidad estomática de las variedades, tales como la densidad, el tamaño o la capacidad de obertura de los estomas.

La validación del CWSI con el Ψ_L también mostró diferencias significativas entre variedades y fases fenológicas. Estas diferencias pudieron ser debidas a la distinta capacidad de las variedades a regular el cierre estomático bajo condiciones de déficit hídrico. Por ejemplo, la variedad Chardonnay se caracteriza por tener un menor control sobre el cierre estomático en comparación con otras variedades (Schultz, 2003; Pou et al. 2012), y por ello los cambios de CWSI a medida que disminuía el Ψ_L, fueron menores. La fase fenológica también afectó sobre dicha relación, de tal modo que un mismo valor de CWSI, se correspondió con valores más negativos de Ψ_L a medida que avanzó la fenología. El distinto potencial de turgencia de las hojas en las distintas fases fenológicas se planteó como una posible causa de la evolución estacional en la relación CWSI vs. Ψ_L. Aunque se demostró que la variedad debe de tenerse en cuenta, los resultados determinaron que es la fenología el parámetro que mayormente afectó a la relación de CWSI vs. Ψ_L, siendo la función lineal entre el Ψ_L estimado y observado la que menos ruido presentó, con un coeficiente de determinación (R^2) de 0.729.

Los resultados aportados en este capítulo permiten avanzar un paso más para que la teledetección pueda ser aplicable como herramienta para programar el riego. Hasta el momento nunca se había validado el Ψ_L con el CWSI, en distintos momentos fenológicos a partir de imágenes térmicas de alta resolución. En este capítulo se ha demostrado la robustez del método, validándolo para las variedades Tempranillo y Chardonnay en un segundo año de estudio (2013) y en unos viñedos distintos. Por lo tanto, para que programar el riego en base a valores estimados de Ψ_L sea una realidad, se recomienda no solamente conocer la variedad, sino lo que es aún más importante, considerar el momento fenológico, para que en cada caso pueda aplicarse la relación más adecuada.

En esta tesis se ha desarrollado el CWSI en viña de acuerdo con el método empírico (Idso et al. 1981). En esta decisión se han supesado los pros y contras de los distintos métodos para el cálculo del CWSI. La implementación del método empírico en zonas áridas y semiáridas (Raimat, Lleida) ha presentado unos resultados atractivos para aplicaciones comerciales. Sin embargo, parece ser que éste método puede presentar ciertas limitaciones en zonas húmedas y con una baja radiación solar (Hipps et al. 1985). En aquellas zonas dónde el método empírico pueda presentar ciertas limitaciones, puede ser aconsejable combinarlo con el método de superficies de referencia (Jones 1999), para así obtener una mayor precisión en las medidas. Sin embargo, el uso del método de referencias ya precisa de medidas puntuales en campo durante el vuelo, lo que hace el sistema más caro y con pocas posibilidades de ser utilizado continuadamente como herramienta para programar el riego. Por otro lado, existe también la posibilidad de utilizar el método teórico desarrollado por Jackson et al. (1981). El inconveniente de este método es que requiere del uso de variables que son difíciles de obtener (radiación neta y resistencia aerodinámica de la cubierta vegetativa a la transferencia de vapor de agua) en cultivos heterogéneos. Monteith (1973) desarrolló empíricamente para cultivos homogéneos dos de los parámetros necesarios para el cálculo de la resistencia aerodinámica, como son la rugosidad de la cubierta vegetativa (z_0) y altura de desplazamiento (d). Sin embargo, la dificultad está en obtener éstos parámetros para cultivos heterogéneos. Además, en el caso que esto fuera posible, cabe tener en cuenta que estos parámetros pueden variar en función de la anchura de la cubierta vegetativa, densidad foliar, y a la vez son sensibles al manejo del cultivo. Para ello, actualmente es necesario realizar medidas en cada parcela, lo que hace que a nivel comercial también sea un método de difícil implementación. Por todo ello, consideramos que el método empírico es el que actualmente tiene un mayor recorrido para ser implementado como herramienta para programar el riego, aunque es necesario tener en cuenta sus limitaciones.

A día de hoy, podemos decir que existe y está disponible la tecnología para programar el riego en viña mediante la teledetección del estado hídrico. Empresas del sector vitivinícola, tales como Codorniu han mostrado un enorme interés en la implementación de esta tecnología en sus fincas. Sin embargo, es necesario seguir investigando y mejorar la metodología para que pueda extenderse su uso. Para ello, es necesario mejorar aspectos tales como el desarrollo de algoritmos y correspondientes validaciones para nuevas variedades de viña, determinar la frecuencia necesaria de adquisición de imágenes para tomar decisiones de riego, validar el método en distintas condiciones climáticas, etc. Aunque las ventajas técnicas parecen bastante claras, también es necesario hacerlo económicamente factible. Para que pueda ser útil al viticultor es necesario que el tiempo transcurrido desde la adquisición de las imágenes, hasta que el usuario final pueda acceder a la información sea menor a 48 horas. Solamente de esta forma, el viticultor o técnico de la finca podrá programar el siguiente riego individualmente para cada sector de riego, en función de su estado hídrico. Este escenario le permitirá poder adoptar la estrategia de riego más oportuna en cada caso, además de hacer un uso sostenible del agua de riego.

Referencias

Guillén-Climent, M. L., Zarco-Tejada, P. J., Berni, J. A. J., North, P. R. J., & Villalobos, F. J (2012). Mapping radiation interception in row-structured orchards using 3D simulation and high resolution airborne imagery acquired from a UAV. Precision Agriculture, 13, 473–500.

Haboudane, D., Miller, J.R., Pattey, E., Zarco-Tejada, P.J., Strachan, I (2004) Hyperspectral vegetation indices and novel algorithms for predicting green LAI of crop canopies: Modeling and validation in the context of precision agriculture. Remote Sensing of Environment 90, 337 – 352.

Hipps, L.E., Ashrar, G., Kanemasu, E.T. (1985) A theoretically-based normalization of the environmental effects on foliage temperature. Agricultural and Forest Meteorology 35, 113–122.

Idso, S.B., Jackson, R.D., Pinter, P.J., Reginato, R.J., Hatfield, J.L (1981) Normalizing the stress-degree day parameter for environmental variability. Agricultural Meteorology. 24, 45-55.

Jackson R.D., Idso, S.B., Reginato, R.J., Pinter, P.J. Jr. (1981) Canopy temperature as a crop water stress indicator. Water Resour Res, 17, 1133.

Jones, H.G (1999) Use of infrared thermometry for estimation of stomatal conductance as a possible aid to irrigation scheduling. Agricultural Forest Meteorology. 95(3):139–149.

Monteith J.L. (1973) Principles of environmental physics. Arnold, London.

Möller, M., Alchanatis, V., Cohen, Y., Meron, M., Tsipris, J., Naor, A., Ostrovsky, V., Sprintsin, M., Cohen, S (2007) Use of thermal and visible imagery for estimating crop water status of irrigated grapevine. J. Exp. Bot. 58, 827-838.

Weathon, A.D., Cooley, N.C., Dunn, G.M (2011) Use of Thermal Imagery to Detect Water Stress during Berry Ripening in Vitis vinifera L. 'Cabernet sauvignon'. 6th IS on Irrigation of Hort. Crops.Acta Hort. 889, 123-130.

Conclusiones

A modo de resumen, las conclusiones y consideraciones finales que pueden establecerse de la presente tesis doctoral son las siguientes:

- La variabilidad espacial del estado hídrico en un viñedo parece seguir un mismo patrón a lo largo de los años y dicho patrón se atribuye a diferencias en las propiedades del suelo. Disponer de un diseño de los sectores de riego acorde con la variabilidad intraparcelaria permite reducir la heterogeneidad productiva. Se determinó que re-sectorizar en función de mapas de potencial hídrico de hoja (Ψ_L) redujo significativamente el coeficiente de variación (C_v) de la producción en un 26.4 %, en aquellos años donde se adoptaron estrategias de riego deficitario controlado (RDC), mientras que re-sectorizar en función de mapas de Plant Cell Density index (PCD=infrarrojo cercano/rojo) solamente se redujo en un 16.7 %. En cambio, en años donde se regó en la totalidad de las necesidades hídricas del viñedo, ninguno de los dos métodos fue capaz de reducir significativamente el C_v de la producción.

- Se ha demostrado la viabilidad de obtener mapas de *Crop Water Stress Index* (CWSI) en viñedos mediante la adquisición de imágenes térmicas de alta resolución, utilizando dos tipos de plataformas aéreas (tripuladas y no tripuladas). Se ha determinado que el tamaño de píxel mínimo necesario para detectar el estado hídrico en viña es de 30 cm, ya que menores resoluciones de píxel se ven afectadas por la influencia de la temperatura del suelo. El intervalo horario óptimo para detectar el estado hídrico mediante imágenes térmicas fue alrededor del mediodía.

- Se determinó que las líneas base desarrolladas para el cálculo del CWSI son dependientes de la variedad y de la fenología. Las relaciones entre CWSI y el Ψ_L también dependen de la variedad y de la fenología, aunque fue el último el parámetro que mayormente afectó en la relación. Por ello, para realizar recomendaciones de riego en base al CWSI se requiere de calibraciones en función de estos dos parámetros. Actualmente, en esta tesis se presentan las ecuaciones de las variedades de viña Pinot-noir, Chardonnay, Tempranillo y Syrah.

- El desarrollo de esta tecnología, permitirá que pueda realizarse un manejo del riego intraparcelario más eficiente en función de la detección del estado hídrico a lo largo del ciclo fenológico. En base a ello podrán adoptarse las estrategias de riego más adecuadas para cada variedad en cuestión y con ello mejorar los parámetros productivos, de calidad de la uva, además de ahorrar cantidades de agua significativas.